Wilfrid Laurier University

Scholars Commons @ Laurier

Theses and Dissertations (Comprehensive)

2009

Laboratory Studies in Chemically Mediated Phosphorus Removal

Rebecca L. Gilmore
Wilfrid Laurier University

Follow this and additional works at: https://scholars.wlu.ca/etd

 Part of the Environmental Sciences Commons

Recommended Citation

Gilmore, Rebecca L., "Laboratory Studies in Chemically Mediated Phosphorus Removal" (2009). *Theses and Dissertations (Comprehensive)*. 933.
https://scholars.wlu.ca/etd/933

This Thesis is brought to you for free and open access by Scholars Commons @ Laurier. It has been accepted for inclusion in Theses and Dissertations (Comprehensive) by an authorized administrator of Scholars Commons @ Laurier. For more information, please contact scholarscommons@wlu.ca.

Library and Archives Canada
Published Heritage Branch
395 Wellington Street
Ottawa ON K1A 0N4
Canada

Bibliothèque et Archives Canada
Direction du Patrimoine de l'édition
395, rue Wellington
Ottawa ON K1A 0N4
Canada

Your file Votre référence
ISBN: 978-0-494-54228-6
Our file Notre référence
ISBN: 978-0-494-54228-6

NOTICE:

The author has granted a non-exclusive license allowing Library and Archives Canada to reproduce, publish, archive, preserve, conserve, communicate to the public by telecommunication or on the Internet, loan, distribute and sell theses worldwide, for commercial or non-commercial purposes, in microform, paper, electronic and/or any other formats.

The author retains copyright ownership and moral rights in this thesis. Neither the thesis nor substantial extracts from it may be printed or otherwise reproduced without the author's permission.

AVIS:

L'auteur a accordé une licence non exclusive permettant à la Bibliothèque et Archives Canada de reproduire, publier, archiver, sauvegarder, conserver, transmettre au public par télécommunication ou par l'Internet, prêter, distribuer et vendre des thèses partout dans le monde, à des fins commerciales ou autres, sur support microforme, papier, électronique et/ou autres formats.

L'auteur conserve la propriété du droit d'auteur et des droits moraux qui protège cette thèse. Ni la thèse ni des extraits substantiels de celle-ci ne doivent être imprimés ou autrement reproduits sans son autorisation.

In compliance with the Canadian Privacy Act some supporting forms may have been removed from this thesis.

While these forms may be included in the document page count, their removal does not represent any loss of content from the thesis.

Conformément à la loi canadienne sur la protection de la vie privée, quelques formulaires secondaires ont été enlevés de cette thèse.

Bien que ces formulaires aient inclus dans la pagination, il n'y aura aucun contenu manquant.

Canada

Laboratory Studies in Chemically Mediated Phosphorus Removal

By

Rebecca L. Gilmore

Bachelors of Science, Honours Chemistry, Wilfrid Laurier University, 2007

THESIS

Submitted to the Department of Geography and Environmental Science
in partial fulfillment of the requirements
for the Masters of Environmental Science degree
Wilfrid Laurier University
May 2009

©Rebecca L. Gilmore 2009

Abstract

Chemically mediated phosphorus removal, done during wastewater treatment, is an effective means of reducing nutrient loads to sensitive environments. Although this method of treatment is widely used, the mechanism of removal is poorly understood. Moreover, phosphorus regulations for wastewater effluents are moving to concentration ranges of 10-100 μg P/L (total phosphorus). This is much lower than current regulations (~0.1 -0.2 mg P/L as TP) required by municipalities (Takács et al., 2006a; Murthy et al., 2005). The analytical methods for low level phosphate analysis need to be optimized to perform reliably and accurately at these low levels. To accomplish this, absorbance measurements with long path lengths of 10 cm and 1 m were performed. The ascorbic acid method (Standard Methods 4500-P. E.) was modified for a 10 cm path length by using a colour-forming reagent volume that was 30% of the volume recommended by Standard Methods (4500-P. E.) and a colour development time of 1 hour. The same reagent volume is recommended for a 1 m path length with colour development overnight (24 hours). Additionally, a filtration protocol was found to be necessary to better define the "dissolved" fraction in synthetic iron and phosphate solutions used to model chemically mediated phosphorus removal. It was found that a 0.45 μm syringe filter gave variable results, likely due to a build-up of iron hydroxide colloids (less than 450 nm) on the filter. Phosphorus is associated with the iron hydroxide and remains on the surface of the filter as the colloids build-up and block the pores of the filter. This resulted in less phosphorus passing through the filter to be measured as dissolved. For jar tests designed to evaluate chemically mediated phosphorus removal, the recommended protocol to achieve the lowest reproducible orthophosphate concentration employs a 47 mm diameter Millipore filter, filtration at a rate of 250 mL/hour and a filtered volume of 10 mL.

To improve the understanding of the chemically mediated phosphorus removal process and integrate modeling of phosphorus removal into computerized plant models such as BioWin™ (EnviroSim Inc.), laboratory tests employing a factorial design were conducted. A 2^4 factorial design allowed two extremes of four significant factors in the nutrient removal process to be considered simultaneously. The four factors (with the

high and low values in brackets) were solution pH (pH 6 and 8), iron dose (5 mg Fe/L and 10 mg Fe/L), mixing intensity (G = 23.5 s^{-1} and 376 s^{-1}), and water hardness (~44 mg/L as $CaCO_3$ and ~170 mg/L as $CaCO_3$). The 16 experiments required by the 2^4 factorial design were each performed over a 24-hour period, monitoring the residual orthophosphate concentration as a measure of effective P removal. The results confirmed factors of the process that were thought to affect phosphorus removal: faster mixing resulted in better initial removal and higher dose (5 compared to 2.5 in terms of molar Fe:P dose) resulted in an order of magnitude difference in residual orthophosphate concentration. Statistical analysis revealed that the most significant factors ($p<0.05$) in phosphorus removal are the two-way interactions of dose by mixing and dose by pH. These two-way interactions indicate that modeling the phosphorus removal process should consider these factors simultaneously, not as individual variables. Additionally, residual phosphorus measurements versus time were fit to a simultaneous precipitation dissolution model assuming first order kinetics. The results suggest that the kinetics of the Fe-H-PO_4 system are highly variable and depend on the factors of dose, pH, mixing, and water hardness.

Acknowledgements

First and foremost, I would like to thank my supervisor, Dr. Scott Smith, for your support, encouragement and feedback for the past couple of years. I am grateful for the opportunities you have given me to travel, publish, and present my work at various big-deal conferences. I am continually learning from you both academically and socially (the importance of getting in with the "movers and shakers"). You kept me uplifted and constantly reassured when I thought I was getting off track, and I am confident my future endeavors will be successful because of you.

My gratitude is extended to the members of my thesis committee, Dr. Merrin Macrae, Dr. Wayne Parker and Dr. Mike English, for your guidance and suggestions. Also my gratitude goes out to Merrin and Wayne and all who helped collect samples for analysis. For funding and feedback on the project, I would like to acknowledge Sudhir Murthy and DCWASA as well as Imre Takács and EviroSim Associates Ltd. Ontario Centre of Excellence is also acknowledged for funding. Thank you to Sarah Goertzen and Monique Robichaud for your help with laboratory work.

Thank you to my family and friends for putting up with me. Sarah, thank you for being my gym buddy and teaching me all your PowerPoint and Linux "tricks". I have enjoyed working beside you. Mom and Dad, your love and support keep me motivated. Dad, thank you for reading my thesis and taking time and interest in understanding my project. You do a wonderful job explaining my research simply and concisely. Meghan, your e-mails, phone calls, cards, and msn conversations always leave me on the floor laughing. Thanks for keeping my spirits high. Pat, your no-stress attitude and calmness are invaluable. I love you.

Table of Contents

List of Figures

List of Tables

Chapter 1
Introduction

Phosphorus is an essential nutrient found in fertilizers, human waste, and commercial cleaning products (Neethling, 2007; vanLoon and Duffy, 2000). Excess phosphorus in natural systems such as lakes, rivers, and streams causes eutrophication. Phosphorus enters lakes and rivers through urban and rural runoff, discharges from factories and municipal wastewater effluent (vanLoon and Duffy, 2000). In most cases, municipal wastewater is the largest source of phosphorus (vanLoon and Duffy, 2000). Due to the environmental impacts of surplus nutrient loads, there is a need for efficient wastewater treatment to clean contaminated waters. This thesis deals with chemical phosphorus removal during wastewater treatment.

Chemical phosphorus (P) removal, during wastewater treatment, is performed with the addition of metal (Al^{3+}, Fe^{3+}, F^{2+}) salts to precipitate the soluble phosphorus. Orthophosphate is the most reactive phosphorus species and the one removed most efficiently in the precipitation process. Although chemical phosphorus removal has been used in the treatment process for years, the mechanism of phosphorus removal is poorly understood (section 2.4). There is significant similarity between metal oxide and phosphorus interactions in wastewater and sediment phosphorus interactions and nutrient cycling in the natural environment. For this reason, the understandings of phosphorus interactions in natural environments are often used to better understand and model the nutrient removal process in wastewater treatment. Excess phosphorus entering sensitive natural environments affects the balance and natural cycle of P (transient uptake of P by

soils and sediments) and to avoid eutrophication (growth of aquatic microorganisms such as algae (van Loon and Duffy, 2000)) there must be stringent limits on effluent P.

To protect pristine environments from eutrophication, wastewater effluent regulations are moving to lower levels. Treated effluent often flows directly into sensitive environments, therefore regulation for allowable loading rates are determined based on the receiving water body and the volume of effluent (Sedlak, 1991). Regulations in North America and around the world require total phosphorus (TP) in effluents to be less than 0.1 mg P/L (Takács et al., 2006a). The District of Colombia Water and Sewage Authority (DCWASA) Advanced Wastewater Treatment Plant in Washington, DC strives for dissolved orthophosphate concentrations around 0.01 mg P/L to ensure they meet the regulations on total phosphorus (Murthy et al., 2005). This treatment plant is the largest of its kind in the world and performs chemically mediated phosphorus removal with ferric iron to reach these low effluent concentrations. However, effluent regulations could be moving lower, down to 10 and 50 μg/L (total phosphorus) in sensitive receiving water areas of the United States (Neethling et al., 2007). In order to reach these low effluent regulations, the treatment process for phosphorus removal needs to be optimized. The analytical methods for laboratory analysis of phosphate, specifically low levels of orthophosphate, need to be tested and optimized to work towards achieving optimal phosphorus removal during wastewater treatment.

Currently, the accepted method (Standard Method 4500-P.) for orthophosphate determination (Standard Methods. 1998) is designed for samples in the range of 0.01 to 0.25 mg P/L (orthophosphate). This colorimetric method involves adding a colour-forming reagent to a sample containing phosphate and measuring the absorbance of the coloured sample after a set colour development time. Theoretically, the same method can be used with a longer path length for absorbance (as long as 1 m) to measure samples with lower orthophosphate concentrations (as low as 0.0001 mg P/L). Testing this theory and optimizing the method for low level analysis is still needed. Furthermore, there is a demand for low level analysis in wastewater effluents and natural aquatic environments as phosphorus concentrations are regulated at lower and lower levels.

An additional limitation to low level orthophosphate analysis is the error associated with filtration of samples containing iron and phosphate. Soluble orthophosphate determination is operationally defined as filtration through a 0.45 μm filter to separate the dissolved and particulate fractions. This conventional definition of dissolved does not consider the colloidal fraction of samples containing iron that can clog a membrane filter (Morrison and Benoit, 2001). Colloidal particles range in size from 1 nm to 1 μm and iron oxyhydroxides can be classified as inorganic colloids (Morrison and Benoit, 2001). The iron particles that interact to removal phosphorus are on the order of 50 nm, as determined from SEM and TEM images (Smith et al., 2008a), will theoretically pass through the 450 nm pores of a membrane filter. However, aggregation of the iron particles on the surface of the filter can clog the pores and reduce the phosphate passing through the filter to be measured as dissolved.

Synthetic samples of phosphorus and iron were prepared in ultra-pure water to study chemically mediated phosphorus removal in the lab. In these special systems filtration through a 0.45 μm filter shows volume dependence with respect to orthophosphate in the filtrate. The cause of this volume dependence was likely the iron colloids that are found aggregating on the surface of the filter. To reduce the error associated with filtration of the synthetic samples, different filters will be examined for effective dissolved particulate separations. With an appropriate protocol for filtration and an optimized method for low level orthophosphate determination laboratory studies focusing on the mechanism of chemical P removal can be performed.

Research is still needed on understanding chemically mediated phosphorus removal in more complex matrices of the natural environment and wastewater streams. Specifically, the interaction of other anions and cations to the phosphorus removal process are not well studied. Cations, such as calcium and magnesium are present in both natural systems and wastewater environments and are known to form precipitates with phosphate under specific conditions (Jenkins et al., 1971; WEF, 1998). Performing experiments which incorporate these cations in the removal process on a lab scale is of primary importance. Additionally, the current equilibrium based models for chemical phosphorus removal need to be updated to include the effects of variable water chemistry.

Further understanding chemically mediated phosphorus removal on a molecular level and in terms of kinetics (rate of removal) is needed in order to model chemical P removal within the entire wastewater treatment process. The rate of phosphorus removal in an important consideration from both an engineering and a modeling perspective. The rate of removal is thought to be variable depending on conditions such as metal dose and mixing. There are limited temporal studies on the rate of removal (kinetics), as previous work has focused on equilibrium systems. Currently, the software BioWin™ provides full plant modeling capabilities to assist treatment plant designers and operators. However, chemical phosphorus removal is calculated in BioWin based on semi-empirical models and not mechanistic models (Takács et al. 2006a). An equilibrium based model for chemical P removal, the Surface Complexation Model (SCM) is a mechanistic based model that more accurately defines phosphorus iron interactions in chemical P removal.

The surface complexation model (SCM) proposed by Smith et al. (2008a) (described in section 2.4.3.2) uses a more realistic approach to model chemical phosphorus removal by considering the surface reactions that take place on the hydrous ferric oxide. The SCM identifies mixing as a potential key factor in modeling this process. Refining this model must quantitatively take mixing intensity into account. A significant gap in chemical phosphorus removal research and therefore modeling is an understanding of the combined effect of some of these key variables. Iron dose, pH, mixing intensity and water chemistry, for example, are known to be significant factors in chemical phosphorus removal and have been individually studied. By better understanding the combined effect of the keys factors in this process a more complete understanding of the process and an improved model can be created.

1.1 Research Goals and Objectives

There is a need to protect sensitive environments, through effective nutrient removal in the wastewater treatment process. To do this, a detailed understanding of chemically mediated phosphorus removal is needed in order to optimize and model the process. To study chemically mediated phosphorus removal in the laboratory requires that the analytical methods be accurate and reliable, specifically for low level phosphorus analysis. The goals of this research project are therefore to optimize the Standard

Method for low level orthophosphate determination and minimize the interference of filter clogging artifacts by designing a filtration protocol acceptable for dissolved particulate separation. With the analytical methods for low level orthophosphate measurements optimized, experiments to test key factors affecting chemically mediated phosphorus removal can be designed. These experiments will systematically consider key variables needed to move forward in terms of understanding and modeling the process. The main objectives are to identify the research areas that require more attention due to their significant effect on the removal process, and gain insight into improving the model for nutrient removal.

1.2 Research Questions

To satisfy the objectives outline in section 1.1 a few detailed research questions are presented:

1. In an effort to measure increasingly lower levels of phosphorus, can the Standard Method for orthophosphate determination be optimized for longer path lengths to determine levels as low as 0.1 μg P/L?
2. To minimize the error associated with dissolved particulate separations two important questions arise:
    a. How significant are filter clogging artifacts for different sample types?
    b. Can we design a reproducible protocol to correct for the artifacts?
3. To improve the understanding of chemically mediated phosphorus removal from a modeling perspective. Previous research indicates iron dose, mixing intensity, solution pH and water hardness are factors that affect the removal process, but have not been systematically studied.
    a. How and to what extent do these factors affect chemical phosphorus removal?
    b. What is the combined effect of these factors on chemical phosphorus removal?

The research goals and answers to these questions will be addressed in the thesis project presented in the subsequent chapters.

1.3 Thesis Organization

The objectives and research questions will be addressed in Chapters 4, 5 and 6, each written as a manuscript for publication. Relevant background material pertaining to the thesis project is reviewed in Chapter 2. Chapter 3 gives an overview of the methodology used throughout the thesis project with a focus on experimental details common to the three main projects (addressed in chapters 4 to 6), with more detailed methods sections included in each chapter. Chapter 4 focuses on optimizing the standard method for low level orthophosphate determination. Chapter 5, also address the analytical issues associated with low level determination, by examining a filtration protocol suitable for dissolved particulate separations that minimize the error associated with filter clogging artifacts. Chapter 6 addresses the third and final project of this thesis, by outlining the experimental design that considers key factors poorly understood in terms of the chemically mediated phosphorus removal process. Chapter 7 summarizes the thesis by unify the three main projects and outlining areas for future work. Appendices contain supplemental material to expand understanding all aspects of this project.

Chapter 2
Literature Review

2.1 Introduction

Phosphorus in natural and wastewater environments exists in different forms (species) as will be discussed in section 2.2. The interactions between phosphorus and metal oxide surfaces are similar in soils and in wastewater where metal salts are added to remove soluble phosphorus. In the natural environment P interacts with metal oxide surfaces in soils and sediments to be transported and cycled through aquatic systems. Some types of phosphorus interactions possible in natural aquatic environment resemble those occurring in engineered systems used to understand chemical phosphorus removal in wastewater treatment. The following sections examine P in more detail, specifically how P is classified and analyzed (section 2.2) and how it is removed during the wastewater treatment process (sections 2.3 and 2.4).

2.2 P Species and Analysis

Phosphorus can exist in many forms, as illustrated in Figure 2-1. The sum of all the species (all forms) is referred to as total phosphorus (TP).

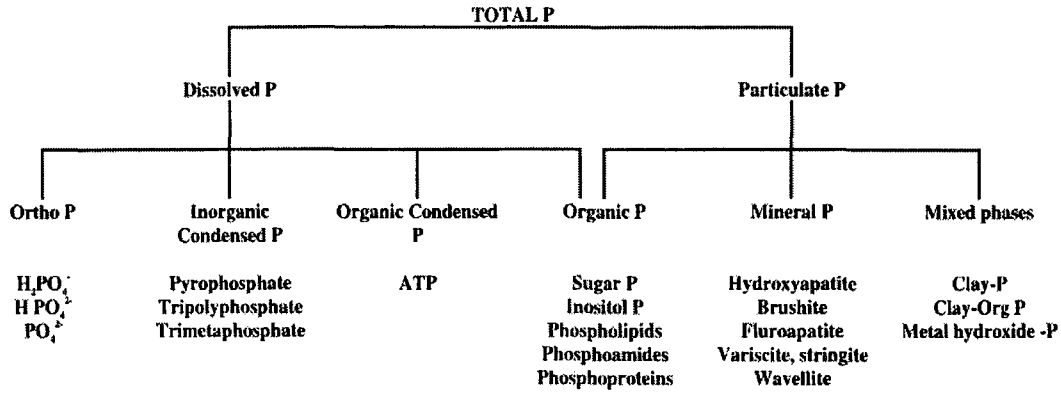

Figure 2-1: Examples of dissolved and particulate species of phosphorus (Maher and Woo, 1998)

The breakdown of P species shown in Figure 2-1 shows dissolved and particulate P species. Dissolved species includes orthophosphates, inorganic condensed phosphates (polyphosphates) such as pyrophosphates, tripolyphosphates and trimetaphosphates and organic phosphates such as sugar phosphates, phospholipids and nucleotides (Maher and Woo, 1998; Sedlak, 1991). The sources of these phosphorus species vary from fertilizers (orthophosphates) to cleaning products (condensed phosphate) and from the breakdown of organic material such as bacterial cells (organic phosphorus) (Neethling et al., 2007; Maher and Woo, 1998).

In natural systems and in wastewater, particulate and soluble phosphorus forms are also present. Particulate phosphorus can be the product of weathered material, incorporated into plant, animal or bacterial material or direct precipitation of inorganic phosphorus. Insoluble phosphorus is found adsorbed to particles or incorporated into amorphous and crystalline material. Additionally, soils and sediments contain P bound to iron or aluminum (Maher and Woo, 1998; Richardson, 1985; Spivakov, 1999). Struvite ($MgNH_4PO_4 \cdot 6H_2O$) and Vivianite ($Fe(PO_4)_2 \cdot 8H_2O$) are two examples of specific minerals containing phosphorus. Polyphosphate accumulating organisms (PAOs) are used in wastewater treatment to hydrolyze and store poly-P and orthophosphate under anaerobic and aerobic conditions respectively (Mino et al., 1998).

The P species outlined in Figure 2-1 can be grouped into four operationally defined fractions shown in Figure 2-2.

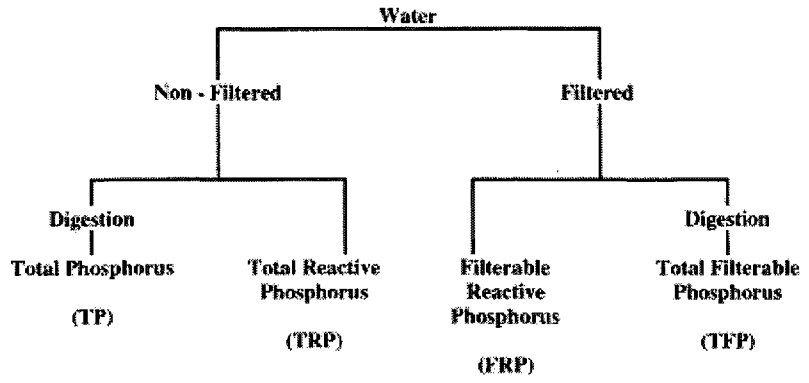

Figure 2-2: Operationally defined phosphorus fractions defined in natural waters (Maher and Woo, 1998)

Figure 2-2 shows four generalized fractions which can be grouped under 'filtered' and 'non-filtered' fractions. Since TP incorporates all fractions, it is typically used for wastewater effluent regulations. However, filterable reactive phosphorus (FRP) and total filterable phosphorus (TFP) are thought to be better indicators for algal growth rates since they are the fractions available for consumption (bioavailability) (Bradford and Peters, 1987).

Orthophosphate fits into the FRP fraction outlined in Figure 2-2. Orthophosphates are the most frequently found soluble form and are also referred to as reactive phosphorus (Spivakov, 1999). Phosphoric acid is a triprotic acid with pKa values of 2.13, 7.21 and 12.02. Based on the pKa values, the dominant forms of orthophosphate (H_3PO_4) at circumneutral pH are $H_2PO_4^-$ and HPO_4^{2-} (pKa values from NIST, 2001). Reactive phosphorus forms are analyzed using colorimetric methods. Acid hydrolysis converts dissolved and particulate condensed phosphate forms to orthophosphate. Organically bound phosphates require digestion to remove the organic matter before being converted to orthophosphate, for colorimetric determinations (Standard Methods 4500- P). Orthophosphate is the focus of this study because it is the predominant form of P in wastewater and being the most reactive form it is most readily removed in the chemical phosphorus removal process (Murthy et al., 2005).

2.2.1 Colorimetric P Determination

Colorimetric phosphorus determination can measure orthophosphate in a water sample. All phosphorus forms (Figure 2-2) are converted by pre-treatment to orthophosphate for analysis. Thus, all phosphorus speciation analysis is dependent on the quality of orthophosphate determination. The concentration of phosphate in the water is determined by spectrophotometric methods according to Beer's law. According to Beer's law, the measured absorbance (A) of a coloured complex is proportional to the concentration (c) of orthophosphate as shown in Equation (1).

$$A = c\varepsilon\ell \qquad (1)$$

Where

ε = molar absorptivity ($M^{-1}cm^{-1}$)

ℓ = path length (cm)

c =concentration of a substance in a sample (M)

The coloured complex is formed by combining phosphoric acid with ammonium molybdate. The complex is then reduced with either ascorbic acid or stannous chloride in the presence of potassium antimonyl tartrate (Spivakov et al., 1999). The reduction of phosphomolybdic acid forms molybdenum blue whose absorbance can be measured at 650 nm or 880 nm (Standard Methods, 1998).

Performing the method involves adding accurate volumes of reagents to a sample containing phosphorus then allowing the colour to develop before measuring the absorbance with a spectrometer. There are a number of colorimetric methods acceptable for orthophosphate determination. Standard Methods (1998) and the Environmental Protection Agency (EPA, 1978) outline methods for manual determination of phosphorus and the use of an auto-sampler with various reducing agents. For example, the stannous chloride method, vanadomolybdophosphoric acid method, and ascorbic acid method can all be used for colorimetric orthophosphate determination. Stannous chloride method is thought to be the most sensitive of the methods. Standard Methods (1998) reports the minimum detectable concentration for the stannous chloride (4500-P. D.) method is 3 μgP/L compared to 10 μg P/L for the ascorbic acid method (4500-P.E.). All of these methods were designed for path lengths of absorbance between 1 and 5 cm.

The time allotted for full color development varies between methodologies (EPA method 365.3; Standard Methods, 1998; Towns, 1986), and there is some debate as to whether absorbance must be measured within a specific timeframe before the coloured complex becomes unstable, or whether there is a specific time after which the color should be fully developed and stable (Towns, 1986).

Presently, Standard Methods (Standard Methods, 1998) suggest a path length up to 5 cm can be used for the ascorbic acid method to measure concentration ranging from 0.01 to 0.25 mg P/L. Compared to a 1 cm cuvette, the use of a 10 cm or 1 m light path can measure concentrations 10 and 100 times lower according to Beer's Law (Equation ((28))). However, poor calibration and noisy data, from previous work, indicate the existing methods cannot be directly applied to low level orthophosphate measurements. To comply with updated regulations, the standard phosphorus analysis method needs to be optimized for low level analysis.

2.2.2 Separating Dissolved and Particulate

Analysis of orthophosphate involves filtration through a 0.45 μm filter to separate dissolved from particulate fractions. The dissolved fraction is defined as anything that cannot be removed by filtration, which is the fraction of interest to measure orthophosphate. Since the definition of dissolved is dependent on the filter technology there are numerous filtration factors to consider.

The traditional, operational definition of dissolved only specifies pore size but more needs to be considered with filtration (and therefore the definition of "dissolved"). Other parameters such as diameter of the filter, volume of sample processed, amount of suspended sediment, and type of filter will all affect the definition of dissolved (Horowitz, 1992). According to Horowitz et al. (1992), these factors are of concern when "dissolved" concentrations of Fe, and Al are being studied. The implications for phosphorus have not been explored.

2.2.2.1 Filtration Issues

The term "filtration artifacts" is used to describe the effect of a build up of colloids and colloidally associated material. The colloids are generally less than 450 nm in size, but the build up of material blocks the pores of the filter. A build-up of colloidal

hydrous ferric oxide (HFO) on the filter will aid in removing phosphorus from the sample during the filtration step. Phosphate associated with those colloids initially passing through the membrane will be interpreted as soluble phosphate. Although the particles are nanometer size (approximately 50 nm as determined from SEM images (Smith et al., 2008a)), a "mat" of these particles could block the 450 nm pores. Layers of HFO colloids on the surface of the filter continue to bind P to reduce the amount passing through the filter.

Inconsistencies in filtration affect many areas of study. For example, Horowitz et al., (1992) studied the effect of filtration on dissolved trace element concentrations in natural systems. Particularly, their concern was with the errors introduced by filtration on the seasonal trend of dissolved trace elements. The winter season is characteristic of low suspended sediment and the spring and summer have higher coarse sediment concentration, which can cause inconsistencies in dissolved trace element concentrations as a result of filtering these samples. Moreover, environmental studies often compare dissolved trace element data from a variety of sources such as local, national and global data and therefore require a more uniform definition of "dissolved" (Horowitz et al., 1996). Horowitz et al. (1996) comment that it is unlikely correction factors can be developed to eliminate the effect of filtration artifacts, but the effects could be reduced. Using large surface areas filters or performing pretreatments such as preliminary filtration or centrifugation could reduce the effect of filtration artifacts (Horowitz et al., 1996).

2.2.2.2 Alternative Methods of Separation

Separation of particulate solids from liquids through filtration involves passing the suspension through a permeable filter such as a membrane filter. Gravitational forces are the driving forces in most cases, but are often not enough to overcome the resistance associated with passing the sample through porous material (Raichenko et al., 1969). Syringe filtration physically forces the sample through the filter but is not the only method to separate the dissolved fraction. Suction filtration, such as vacuum filtration, act to pull the filtrate through the filter. The use of centrifugal forces through centrifuging the sample can also be used to separate dissolved and particulate samples.

Variations of the traditional membrane filtration have also been studied in an effort to reduce membrane clogging.

Hollow-fiber filters, commonly used in biotechnology, have been used to separate lake water with high particulate content. This technique is beneficial to ensure unchanging lake water composition with filtration and is gentle on fragile organisms (Jüttner et al., 1997). Tangential flow ultrafiltration (Morrison and Benoit, 2004) and electrofiltration using cross-flow filtration (Lin et al., 2007) minimize solid membrane contact to reduce clogging. Tangential flow ultrafiltration (TFU) is used for fractionation of colloids however, the exact size separation is poorly defined. Morrison and Benoit (2004) improved TFU size separation by combining TFU with membrane filtration for more actuate size separations. The compromise was that separations of natural water samples still showed some inconsistency in aluminum, iron and organic content in the filtrate when large colloids were present (Morrison and Benoit, 2004). Electrofiltration makes use of electrostatic forces to resist particles from interacting on the membrane surface. Lin et al. (2007) report that with increased electrostatic field strength applied to the filter membrane, the removal efficiency of naturally occurring colloids is increased. These techniques are beneficial for size separation and fractionation of colloids. However, for quick and easy on site sample filtration, to be used by plant operators, the ease and speed of syringe filtration is preferred.

2.2.2.3 Filtration Variables

Syringe filtration is the method of choice for researchers and wastewater engineers due to the ease of use and efficiency in dealing with large numbers of samples. Due to the widespread use of syringe filtration, filters come in a variety of types and sizes. The standard pore size for separating dissolved and particulate fractions is 0.45 μm, but other factors to consider include the diameter and thickness of the filter.

The two basic types of membrane filters are sieve and tortuous path. Sieve membrane filters are extremely thin (10-15 μm thick) and as a result, only trap particles on the surface of the filter. Tortuous path membrane filters are thicker (100-150μm thick) and sponge-like and are therefore able to trap particles within the filter as well as on the surface (Horowitz, 1992). Tortuous path filters, such as Millipore and Sartorius

filters are available in 0.45 μm pore size, and the sieve filters, such as Nuclepore and Poretics filters are 0.40 μm which is the real pore size, not woven like the tortuous path filters (Horowitz, 1992). Filter diameters range in size from 13 mm to as large as 142 mm. The large filter diameters are designed to filter larger sample volumes and are more expensive than the smaller diameter filters.

In addition to the type of membrane, the flow rate of the sample across the membrane can affect filtration results. According to Leppard (1992), the flow rate for filtration can provoke colloid aggregation. By reducing the flow rate in a series of experiments, filter-provoked aggregates should be reduced (in size and frequency) whereas natural aggregates will be unaffected.

In summary, many filtration variables need to be considered when dealing with samples containing iron or aluminum, since colloids can aggregate on the filter surface and phosphorus can associate with colloids. The key variables to consider are filter type and diameter, and the flow rate across the membrane.

2.3 P Removal during Wastewater Treatment

An overview of the wastewater treatment process is discussed below and shown in Figure 2-3. This is a general overview of how most plants operate, however there are many variations and the treatment process can differ from plant to plant. A preliminary treatment is usually done to remove the large grit and solids so they do not damage the mechanical equipment down the line. Primary treatment or primary clarification (labeled as "primaries" in Figure 2-3) is done by allowing large particles and organic matter to settle and move to the sludge digesters as well as removing scum from the surface.

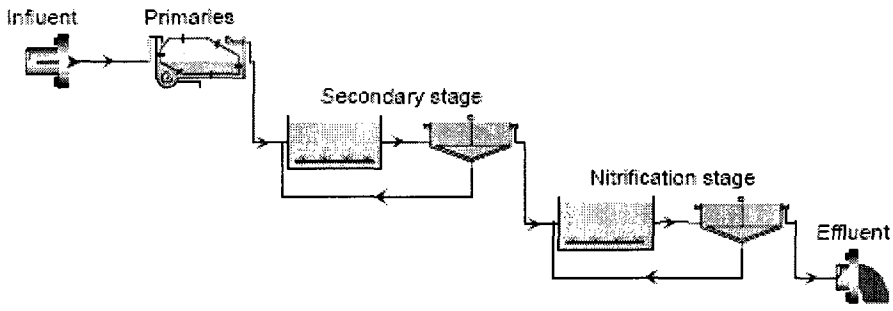

Figure 2-3: Wastewater treatment schematic (Takács et al., 2006a). Influent water is treated in the primaries before aeration in the secondary stage. Nitrification is part of the final treatment stage before the effluent is released to the environment.

Secondary treatment (see Figure 2-3) involves aeration forming an activated sludge (Hammer and Hammer, 2001). The activated sludge is biologically active, making use of small organisms working to disinfect the water. Sludge from the primary and secondary treatment passes though a sludge treatment before being taken to landfill. Tertiary treatment (shown as nitrification stage in Figure 2-3), also referred to as advanced treatment, is a broad term for any treatment following the traditional primary and secondary treatments (Hammer and Hammer, 2001). The final step is a disinfection stage before the treated effluent is released.

Phosphorus removal in wastewater treatment facilities involves chemical and biological treatment. Orthophosphates are removed from wastewater by forming precipitates with metal salt (chemical phosphorus removal), whereas polyphosphates (condensed phosphates) are removed through biological uptake by bacteria such as Accumulibacter (biological phosphorus removal) (Neethling et al., 2007, Spivakov, 1999). More details of the biological and chemical phosphorus removal process are discussed in the following sections.

2.3.1 Biological Phosphorus Removal

Biological phosphorus removal involves aerobic and anaerobic growth of bacterial populations capable of storing large amounts of phosphorus as polyphosphates (Sedlak, 1991). Typically, biological removal can achieve total phosphorus (TP) levels less than 1 mg P/L but chemical phosphorus removal is more stable and needed to meet more stringent regulations (Neethling et al., 2007). Often a plant will use chemical

phosphorus removal or a combination of biological and chemical phosphorus removal to meet low level regulations. Start up costs for biological P removal systems are higher than chemical P systems, however operation and maintenance costs are lower (de Haas, 2000). A disadvantage of the biological nutrient removal system is the sensitivity of the organisms and therefore lack of reliability (de Haas, 2000). For this reason, many plants opt to use chemical phosphorus removal or supplement biological P removal with chemical P removal (de Haas, 2000).

2.3.2 Chemical Phosphorus Removal

Chemical phosphorus removal involves the addition of metal salts, which precipitate the soluble phosphates to be removed with the sludge. Metal salts that are added to precipitate the phosphate are typically calcium in the form of lime ($Ca(OH)_2$), aluminum, as alum ($Al_2(SO_4)_3 \cdot 18H_2O$) or sodium aluminate ($NaAlO_2$) or iron salts (Sedlak, 1991). Some treatment plants add ferric chloride ($FeCl_3$) or ferric sulphate ($Fe_2(SO_4)_3$) while others add the ferrous form which is assumed to rapidly oxidize to the ferric form. The ferric (Fe^{3+}) form is thought to be the active form in removal, with the mechanism being a surface complex on hydrous ferric oxide (HFO). Freshly precipitated HFO are nanometer in size, and therefore have a large surface area for sorbing phosphate (Blaney et al., 2007). The ferrous form (Fe^{2+}) is very soluble but in an oxidizing environment will transform to the ferric form (Fe^{3+}) which is insoluble at circumneutral pH. Leckie and Stumm (1970) suggest this method of removal is better than adding Fe^{3+} directly, as P can be taken up inside the hydrous ferric oxide structure as it oxidizes. Similar interactions are observed in the natural aquatic environments where Fe(III) (oxidized form) forms surface complexes with P, but the reduced form (Fe(II)) releases P (Richardson, 1985). The ferrous forms typically added during wastewater treatment are ferrous sulphate ($Fe(SO_4)$), ferrous chloride ($FeCl_2$) or pickle liquor, a waste product of the steel industry in the form of $Fe(SO_4)$ (Sedlak, 1991).

Research has been done on the effectiveness of various iron (or aluminum) containing materials for the removal of phosphate. Work by Elliot et al. (2002) looked at water treatment residuals (Al-WTR, Fe-WTR and Ca-WTR), Oğuz et al. (2003) studied

gas concrete waste (2003) as well as blast furnace slag (2004), and Altundogan and Tümen (2001) used Bauxite, a raw material for alumina production.

The treatment process varies depending on the facility; therefore the metal salt dosing point for chemical phosphorus removal is not the same for each plant. The point of addition is determined by considering operation and the maintenance costs, the size of the facility, the degree of phosphorus removal required, and the reliability of the chemical supply (Sedlak, 1991). The metal salt can be dosed in either the primary or secondary stage of treatment, or dosed in both primary treatment and secondary treatment. Dosing the metal salt in three locations is also done at larger treatment plants to ensure low effluent P is achieved. Typically, the triple dosing method involves addition of the metal salt at each stage of the treatment (primary, secondary and tertiary). The metal salt addition during tertiary treatment has a significant cost increase compared to the other dosing points, but may be required to meet strict water quality standards (Sedlak, 1991). Moreover, the use of many dosing points or the addition of high doses of iron, results in increased sludge production contributing to the total cost of treatment.

Although the chemical P removal systems are able to achieve very low effluent levels, the disadvantages of high chemical costs and the need for solid separation facilities (de Haas, 2000) force operators to look at combining biological and chemical phosphorus removal. However, more research on each process and how the processes occur simultaneously is still needed. Preliminary findings on the combined process show that smaller to moderate chemical doses do not interfere with the biological processes of biological P removal (de Haas, 2000). The conflict between the two processes is largely that the organisms in the biological process require a minimum level of available nutrients to survive, so if the chemical process precipitates too much phosphorus, productivity in the biological process may be slowed (Murthy et al., 2005).

2.4 Mechanism of P Removal

Although chemical phosphorus removal is widely used, the mechanism of removal is poorly understood. Without knowledge of the mechanistic details for phosphorus removal, the required metal dose is determined experimentally and often results in overdosing the metal salt. To consistently and reliably meet the wastewater

regulations through efficient and cost effective means requires a detailed understanding and model for chemically mediated phosphorus removal. The coagulation reactions which remove soluble phosphorus are only partially understood, but seem to be a combination of adsorption and co-precipitation of phosphate and the metal cation (Hammer and Hammer, 2001; Smith et al., 2008a). The solid phase formations are thought to be very similar to those occurring in natural systems, such as the formation of ferric hydroxyl phosphate and surface complexation (Stumm and Morgan, 1970; deHaas et al., 2001). Many studies (Gunnars et al., 2002; Zanini, 1998; Richardson, 1985; Holliday and Gartner, 2007; Smeck, 1985; Froelich, 1988) have focused on phosphate binding with solids and minerals in natural systems and are often used as a starting point to better understand the interactions in a wastewater environment. The complex nature of the wastewater and the variable composition at each stage of treatment also needs to be considered in the mechanism of removal. There are numerous factors to consider such as the metal salt used, the amount of phosphorus in the influent, pH, alkalinity, mixing at dosing point, kinetic factors, and other colloidal material in the water. Iron is the metal salt that is the focus of this research due to its widespread use and effectiveness in P removal. Fe(III) is readily available and inexpensive, and the hydrated Fe(III) oxide (HFO) is chemically stable over a wide pH range. The current P removal methods using iron are effective but they need to be better understood in order to be optimized.

2.4.1 Rates of Removal

The mechanism of phosphorus removal with hydrous ferric oxides (HFO) is thought to be a combination of adsorption and surface precipitation. Szabó et al. (2008) describe an initial rapid removal, due to co-precipitation, followed by a slower removal process where the mechanism of removal is primarily adsorption (see Figure 2-4).

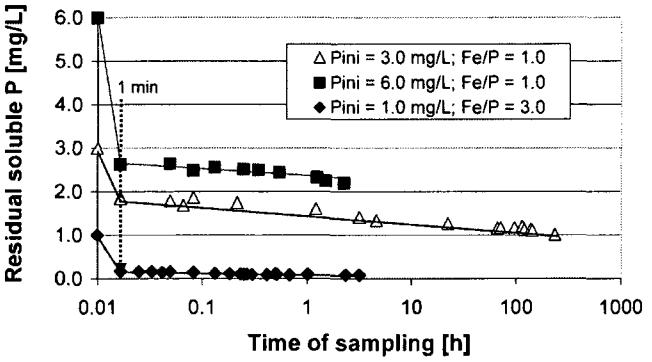

Figure 2-4: Kinetic of phosphorus removal. Initial rapid P removal (low residual soluble P) is due to co-precipitation (Szabó et al., 2008)

The International Union of Pure and Applied Chemistry (Research Triangle Park, North Carolina) (IUPAC) definition of co-precipitation is used here to avoid confusion in terminology. According to IUPAC the definition of co-precipitation is "the simultaneous precipitation of a normally soluble component with a macrocomponent from the same solution by the formation of mixed crystals, by adsorption, occlusion or mechanical entrapment" (McNaught and Wilkinson, 1997). The definition of Rapid, "instantaneous" removal occurs within the first minute of adding iron salts to a solution containing phosphate and the removal continues for hours or days (>100 hours in Figure 2-4) (Szabó et al., 2008). It is believed that the kinetics of the removal process are greatly affected by factors such as the Fe/P ratio, and mixing intensity. Aside from knowing there is initial rapid removal followed by slower processes, the kinetics have not been fully described. Determining rate constants is fundamental to understanding and being able to model the kinetic process. Kinetic studies have been done in other areas of wastewater treatment and even the removal of phosphorus by struvite precipitation. Rahaman et al. (2008) and Quintana et al., (2005) reviewed previous research as well as their findings on fitting a first order kinetic model for struvite precipitation. Their research was in agreement with others that the reactions fit a first order model, however kinetic constants appear to be higher in real wastewater compared to synthetic liquor. Also, they found that reaction rate constants change with mixing intensity (Rahaman et al., 2008).

2.4.2 Adsorption and Surface Complexation

The removal of phosphorus by metal salts is believed to be a combination of co-precipitation and absorption. The adsorption of anions to hydroxilated surfaces is termed surface complexation (Altundoğan and Tümen, 2001). Inner and outer sphere surface complexes form based on the degree of surface protonation or dissociation as shown in the following symbolic reaction:

$$\equiv SOH_{(s)} + H^{+}_{(aq)} \leftrightarrow \equiv SOH_2^{+}{}_{(s)} \quad (2)$$

$$\equiv SOH_{(s)} \leftrightarrow \equiv SO^{-}_{(s)} + H^{+}_{(aq)} \quad (3)$$

(Altundoğan and Tümen, 2001)

≡S is the mineral surface (≡Fe in this case). When the surface is positively charged anions such as PO_4^{3-} can adsorb creating outer-sphere or inner-sphere complexes as is the case with orthophosphate to hydoxylated mineral surfaces. Inner-sphere complexes form as chemical bonds, whereas outer-sphere complexes are the result of iron pairs between the cation and surface groups (Stumm, 1992). The inner-sphere complexes explaining phosphate adsorption can be further classified as binding in a mondentate or bidentate fashion (see Figure 2-5).

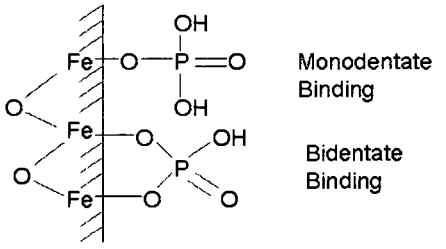

Figure 2-5: Formation of monodentate and bidentate inner sphere complexes between phosphate and HFO (adapted from: Blaney et al., 2007)

Monodentate binding of phosphate to iron hydroxide surface involves a single bond, whereas the stronger bidentate binding forms two covalent bonds. The binding of phosphate to the HFO is through the oxygen atom such that the bonding arrangement is Fe-O-P, resulting from the phosphate oxygen replacing hydroxyl oxygen (Li and Stanforth, 2000). It is still unknown which binding, mono- or bidentate, predominates.

Geelhoed et al. (1997) describe adsorption modeling in the Charge Distribution and Multi-Site Complexation (CD-MUSIC) model of Hiemstra and Van Riemsdijk (1996)

where both bidentate and monodentate surface complex formation of P are considered. The following set of equations shows the reactions for protonatation and formation of inner sphere complexes with phosphate on goethite with singly ($FeOH^{1/2-}$) and triply ($Fe_3O^{1/2-}$) coordinated surfaces. Fe_3O means the surface reactive oxygen is shared (bound to) by three Fe atoms with the oxide surface.

$$FeOH^{1/2-} + H^+ \leftrightarrow FeOH_2^{1/2+} \quad (4)$$

$$Fe_3OH^{1/2} + H^+ \leftrightarrow Fe_3OH^{1/2+} \quad (5)$$

$$2FeOH^{1/2-} + 2H^+ + PO_4^{3-} \leftrightarrow Fe_2O_2PO_2^{(2-)} + 2H_2O \quad (6)$$

$$2FeOH^{1/2-} + 3H^+ + PO_4^{3-} \leftrightarrow Fe_2O_2POOH^{(-)} + 2H_2O \quad (7)$$

$$FeOH^{1/2} + H^+ + PO_4^{3-} \leftrightarrow FeOPO_3^{(21/2-)} + H_2O \quad (8)$$

The protonation of the singly and triply coordinated surface groups is shown in Equations (4) and (5). Phosphate adsorption in a bidentate fashion is shown in Equations (6) and (7) and in a monodentate fashion in Equation (8). The Surface Complexation Model for chemical phosphorus removal developed by Smith et al. (2008a) assumes similar binding sites as discussed in section 2.4.3.3.

2.4.3 Modeling Chemical Phosphorus Removal

To improve the understanding of chemically mediated phosphorus removal in terms of mechanistic details, a few models have been developed that consider phosphorus removal on a molecular level. A semi-empirical model created by the Water Environment Federation (WEF, 1998) was recalibrated in Takács et al. (2006a) and a Surface Complexation Model (SCM) has been developed by Smith et al. (2008a) which builds on the chemical equilibrium reactions in the WEF model to include surface reactions on mineral oxides.

2.4.3.1 WEF Model

The WEF model is based on equilibrium reactions for the formation of iron hydroxide and iron phosphate precipitates to predict phosphorus removal from wastewater using aluminum and iron salts. Residual orthophosphate concentrations are calculated based on the iron dose as a function of pH (Smith et al., 2008a; WEF, 1998). To calculate residual soluble orthophosphate, the concentration of phosphorus and metal-phosphate complexes are determined and added according to Equation (9) (WEF, 1998)

$$C_{P\,res} = [H_3PO_4] + [H_2PO_4^-] + [HPO_4^{2-}] + [PO_4^{3-}] + [MeH_2PO_4^{2+}] \quad (9)$$

where $C_{P\,res}$ is total residual soluble orthophosphate

The concentration of each of the five species in Equation (9), can be determined from the equilibrium reactions. The reactions with iron (Fe^{3+}) and the associated equilibrium constants as reported in WEF (1998) are shown in the following system of equations.

$$Fe^{3+} + 3H_2O \leftrightarrow Fe(OH)_{3(s)} \qquad pK_{FeOH} = -0.5 \quad (10)$$

$$1.6Fe^{3+} + H_2PO_4^- + 3.8OH^- \leftrightarrow Fe_{1.6}(H_2PO_4)(OH)_{3.8(s)} \qquad pK_s = 67.1 \quad (11)$$

$$Fe^{3+} + H_2PO_4\text{-} \leftrightarrow FeH_2PO_4^{2+} \qquad pK_{FeP} = -21.3 \quad (12)$$

$$H_3PO_4 \leftrightarrow H^+ H_2PO_4^- \qquad pK_1 = 2.1 \quad (13)$$

$$H_2PO_4^- \leftrightarrow H^+ + HPO_4^{2-} \qquad pK_2 = 7.2 \quad (14)$$

$$HPO_4^{2-} \leftrightarrow H^+ + PO_4^{3-} \qquad pK_3 = 12.3 \quad (15)$$

The concentration of the metal species ($[Me^{3+}]$) is needed to calculate the concentration of the five species in Equation (9). The equilibrium constant, pK_{FeOH}, from Equation (10) is used to determine $[Fe^{3+}]$.

$$\log[Fe^{3+}] = pK_{FeOH} - 3pH \quad (16)$$

The phosphate species can be calculated from solubility product of metal phosphate (pK_s) and the acid dissociate values (pK_1, pK_2, and pK_3).

$$\log[H_2PO_4^-] = -pK_s - 1.6\log[Fe^{3+}] + 3.8(pK_w - pH) \quad (17)$$

$$\log[H_3PO_4] = \log[H_2PO_4^-] - pH + pK_1 \quad (18)$$

$$\log[HPO_4^{2-}] = \log[H_2PO_4^-] + pH - pK_2 \quad (19)$$

$$\log[PO_4^{3-}] = \log[HPO_4^{2-}] + pH - pK_3 \quad (20)$$

$$\log[FeH_2PO_4^{2+}] = \log[Fe3+] + \log[H_2PO_4^-] + pK_{FeP} \quad (21)$$

With the concentration of each of the five species determined from Equations (16) to (21) total residual orthophosphate concentration can be calculated according to Equation (9).

In addition to predicting residual orthophosphate, the model can be used to determine the required metal dose by assuming the ratio of metal dose to soluble orthophosphate removed is approximately equal to the overall precipitate concentrations.

This assumption is valid since the residual metal dose is negligible (WEF, 1998). The theoretical curves generated from calculating residual orthophosphate are shown in Figure 2-6 along with the recalibration WEF model presented by Takács et al. (2006a). The WEF model provides a narrow pH range at which low phosphate concentrations can be achieved. The lowest soluble phosphate concentration predicted by the model is 35 µg P/L, which is only achievable between pH of 6.8 and 7.1 (Takács et al., 2006a). Experience at treatment plants indicated that very low levels (0.01 mg P/L OP and lower) are frequently reached, and also indicate that a wider optimal pH range exists (Takács, et al., 2006a). By re-evaluating and empirically calibrating some of the chemical equilibria and constants used in the original WEF model, such as the solubility and dissociation constants, the enhanced WEF model was created by Takács et al., (2006a). The two WEF models are shown in Figure 2-6 where the broader pH range of removal determined by the enhanced (re-calibrated) model is clear.

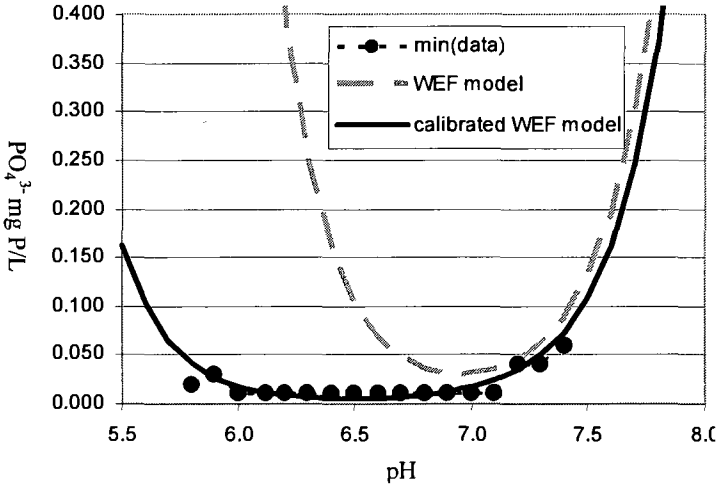

Figure 2-6: WEF model (dashed line) compared to the recalibrated (enhanced) model (solid line) (Takács, et al., 2006a)

The recalibrated model achieves a closer approximation of the removal process with Fe(III), and shows lower achievable phosphate concentrations over a wider pH range. This model was compared with plant data to best predict effluent phosphate concentrations. The new calibrated model shows optimal removal between pH 6.2-7 and

predicts a minimum orthophosphate concentration of 7 μg P/L at pH 6.5 (Takács et al., 2006a).

2.4.3.2 Geochemical Background for SCM

The WEF model provides a good foundation for modeling chemical phosphorus removal in wastewater however; it does not consider any of the surface reactions that are involved in phosphorus removal using iron. Additionally, a ferric phosphate ($FePO_{4(s)}$) species is assumed to precipitate in the WEF model but does not form above pH 3.5 under normal dosing conditions (Takács et al., 2006b). To improve the model for chemical phosphorus removal, the mechanism of removal involving surface reactions on precipitated hydrous ferric oxides needs to be considered. Studies on these precipitates and other iron oxides, give insight into the complex mechanism of phosphorus removal.

Hydrous ferric oxides (HFO) are formed from the rapid hydrolysis of ferric iron solutions, such as the addition of ferric chloride to wastewater. This solid is amorphous and is similar to the natural iron oxide ferrihydrite (Dzombak and Morel, 1990). The exact structure of HFO is unknown and usually described by the general formula $Fe_2O_3 \cdot nH_2O$ with n values between 1 and 3. The average density is 3.5 g/cm^3. Under conditions of high pH (>10) and high temperatures, HFO may eventually transform to a crystalline form such as goethite (α-FeOOH) (Dzombak and Morel, 1990; Lijklema, 1980).

Goethite is a crystalline iron oxide found in soils and sediments, which binds phosphate, in natural systems, through adsorption. It is often used in adsorption studies since it is stable and relatively easy to synthesize (Li and Stanforth, 2000; Daou et al., 2007). Phosphate binding to the surface of goethite is widely studied (Tribe and Barja, 2004; Li and Stanforth, 2000; Rietra et al., 2001; Geelhoed et al., 1997; Mikutta et al., 2006) and is useful since hydrous ferric oxide (HFO) has a similar chemical short range structure, although amorphous compared to the crystalline goethite (Smith and Ferris, 2001). As a crystal, goethite can be studied in ways amorphous HFO cannot, such as for surface charge or surface site calculations used in the CD-MUSIC model (Geelhoed et al., 1997).

2.4.3.3 Surface Complexation Model

Modeling the surface complexation reaction of phosphate on HFO is a two step process. The first step is to determine the amount of HFO precipitate then consider the amount of phosphate bound to the surface of the HFO. Modeling the surface complexation is based on the active phosphate binding sites. These are the oxygen atoms available for binding. Assuming that the amorphous HFO has a similar binding arrangement to the crystalline goethite, as discussed in Section 2.4.3.2, the oxygen atoms for binding are singly (FeO), doubly (Fe_2O) or triply (Fe_3O) coordinated to the iron atoms (Geelhoed et al., 1997). Since the doubly coordinated surface groups do not react in the normal pH range (Geelhoed et al., 1997), only the singly (site 1) and triply coordinated groups (site 2) are considered in the surface complexation model. The key modeling parameter is called the active site factor (ASF) and represents the oxygen groups available to bind with phosphate. The active site factor is thought to be a function of the amount iron in the system, the pH, the mixing intensity (G) and the age of the flocs as shown in Equation (22).

$$ASF = f(G, pH, dose, age\ of\ flocs) \quad (22)$$

The upper limit for the ASF, although not realistically achievable, is 6 (see Figure 2-7: Iron hexahydrate).

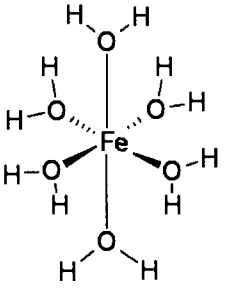

Figure 2-7: Iron hexahydrate

This means there are 6 oxygen atoms per iron atom available for binding (Smith et al., 2008a). The more realistic value for a well mixed system was determined by Smith et al. (2008a) to be 1.18 or 0.31 for a poorly mixed system since the HFO floc becomes larger and denser with age and poor mixing.

These values for the ASF were determined empirically. For the system being modeled the ASF is fixed (modeling parameter). The ASF relates the available binding sites to the total iron in the HFO precipitate where

$$S1T = S2T = ASF \times (Fe_T \text{ in HFO}) \quad (23)$$

S1T and S2T represent the total surface sites for singly and doubly coordinated oxygen atoms respectively.

An application of the surface complexation model is shown in Figure 2-8, where laboratory data from jar tests is compared to the SCM predicted residual P. The inputs into the SCM are iron dose (expressed as molar dose in Figure 2-8), solution pH and the ASF value (1.18 for the data in Figure 2-8).

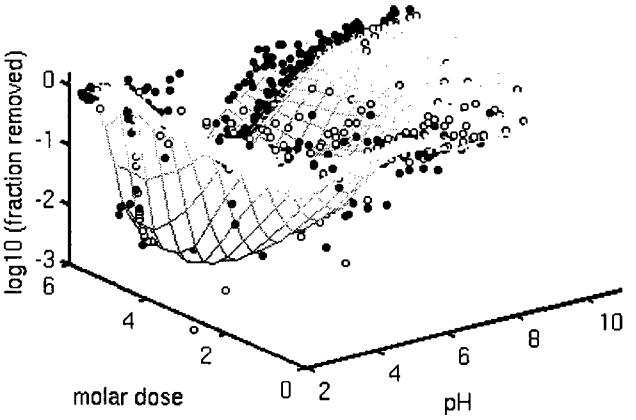

Figure 2-8: 3D plot showing the fraction of initial phosphorus remaining after removal with iron versus the molar dose of iron and final pH of the solution. The black dots are data and the open circles are model calculated fractions of P removed. The interpolated surface corresponds to the open circle model data to better illustrate the trends (Smith et al., 2008b)

In Figure 2-8, the measured phosphorus (expressed as fraction removed) is shown in black dots, and the model predicted P removal is shown in open circles. The interpolated surface corresponds to the open circle model points to better illustrate the trends. The lowest orthophosphate concentration predicted by the SCM is 5μg/L for a well mixed system (Smith et al., 2008a).

The WEF model, recalibrated WEF model, and the surface complexation model are all able to describe the chemical phosphorus removal process to a certain extent. Even with improvements to each model, there are key processes that are not adequately accounted for in the model. For example, the kinetics (rates of removal) are not represented since the three models discussed here are equilibrium based. Kinetic processes are not easily modeled, however. In a model of activated sludge developed by Briggs (1996) (as cited in deHaas et al., 2001) kinetics were incorporated as a variable,

however the precipitation reactions are still based on equilibrium and are therefore assume to be completely precipitated from the start (deHaas et al., 2001).

A summary of the models for chemical phosphorus removal discussed in the previous sections is given in Table 2-1.

Table 2-1: Comparison of three models for chemical phosphorus removal with iron

Model	Basis	Lowest achievable P	Assumptions
WEF	Predict residual OP as function of pH	35 µg P/L between pH 6.8-7.1	• $FePO_{4(s)}$ precipitation • Fixed residual concentrations • Ideal mixing • Instantaneous reactions
Enhanced WEF	Incorporates pH calculation to determine ions in solution	7 µg P/L (optimal pH range 6.2-7)	
SCM	• Models surface reactions on HFO as mechanism of P removal. • Modeling parameter, ASF, allows mixing and age of flocs to be considered as well.	5 µg P/L (lowest P pH 4 -6)	Instantaneous reactions

Table 2-1 summarizes the models in terms of their basis, such that the WEF model is the most basic of the three, able to predict residual orthophosphate as a function of pH and the enchanced WEF model builds on this by incorporating equilibrium pH calculations. The surface complexation model is the most sophisticated of the three models since it considers surface reactions on hydrous ferric oxide to more accurately describe the mechanism of P removal with iron. For each of the three models the lowest predicted P concentration is given, and it is clear as the models improve, minimum predicted P moves lower and the optimal range of removal becomes broader, more closely simulating experience at treatment plants. The last column in Table 2-1 summarizes some of the assumptions each of the models make.

From examining the existing models, it is clear there are key factors necessary for modeling the processes of chemical phosphorus removal. For example the pH dependence and dose dependence are recognized in all the models. Additionally, the limitations of the models indicate variables or factors that need more research before

being incorporated into the model. Mixing, for example, has been identified as a key factor by many researchers (Smith et al., 2008a; Szabó et al., 2008; Takács et al., 2006b) and is potentially incorporated into the surface complexation model through use of the active site factors (Equation (22)). However, the models currently assume ideal mixing to theoretically determine values for ASF (Szabó et al., 2008; Smith et al., 2008a). Mixing intensity still needs to be better accounted for in chemical phosphorus modeling. Another factor that is thought to be significant to the process and is not considered in any of the models discussed here is the effect of water chemistry. Various cations and anions, such as calcium, magnesium, organic matter and sulphates for example, are present in wastewater and also interact with phosphorus in natural environments. A discussion of some of the potentially significant constituents in wastewater (and natural environments) is presented in section 2.4.7.

2.4.4 Dose Dependence on P Removal

Metal dose is a main factor influencing chemical phosphorus removal (Szabó et al., 2008; Takács et al., 2006a). The metal dose is often referred to in terms of the molar ratio of metal to phosphorus (Me/P). Generally, a higher metal dose results in lower residual phosphate (in terms of soluble orthophosphate) (Szabó et al., 2008). According to Szabó et al. (2008) ratios of 1.5-2 Me/P (molar metal dose to initial P concentration) are needed to achieve 80 to 98% removal when initial P concentrations are around 0.5 to 0.6 mg P/L and even higher doses are needed to reach residual levels below 0.1 mg P/L. To get down to residual P concentrations of 0.01 mg P/L, excess metal dose is needed. Szabó et al. (2008) used a Me/P ratio up to 5.0 in their tap water samples to reach these low levels. At the District of Columbia Water and Sewage Authority (DCWASA) treatment plant, iron is dosed at 8 mg Fe/L which is a Me/P ratio of 3.5 (Murthy et al., 2005). With their system of multiple dosing points, this iron dose achieves effluent orthophosphate concentration around 0.01 mg P/L (from ~1 mg P/L as orthophosphate)

The modeling with respect to dose dependence is better considered in the SCM than the WEF model (both models were discussed in section 2.4.3). In the WEF model, varying Me/P ratios are not considered. Moreover, the hydrous ferric phosphate precipitate is assumed to be in equilibrium with the solution which is not realistic since

this precipitate will only form at acidic pH (Smith et al., 2008b). The SCM considers varying dose as well as initial phosphorus concentration which the WEF model did not do.

2.4.5 Effects of pH on P Removal

The study of phosphorus and chemically mediated phosphorus removal, should consider a range of pH values since the chemical species in the system change with pH. According to the WEF model the pH of optimal removal is between 6.5 and 7.3 (discussed in section 2.4.3.1). The SCM, with more realistic equilibrium chemistry, indicates good removal (down to 1% of input P) is possible between pH 4-6 where hydrous ferric phosphate species predominate (Smith et al., 2008a). This is in agreement with laboratory scale data as well. Determining different ranges for optimal P removal depends on what species and factors are considered. For example, the SCM considers more chemical species involved in the P removal process than the WEF model and this contributes to the variability in determining the optimal pH.

In the whole scheme of water treatment, a delicate balance of optimal pH values is needed since different processes may have different optimal ranges. For example, biological P removal has slightly higher optimal pH than chemical P removal. The optimal pH range for biological P removal is around 6.8-8 (deHaas, 2000a). Treatment plants typically operate near neutral pH, but have shown that achieving low effluent P is possible over a range of pH. Plant data from two different treatment plants shows effluent soluble P concentration less than 0.05 mg P/L are possible from pH 6 to 7.5 (Szabó et al., 2008). Outside of this neutral pH range where the minimum residual P can be achieved, the equilibrium chemistry for complex formation and proton competition for binding sites on the oxide surface limits P removal. At low pH soluble phosphate complexes form, and metal hydroxide precipitation is limited. On the other end, at high pH, metal hydroxides form but interactions with phosphate are poor near the point of zero charge of the metal oxide. High pH may allow for P removal with calcium and magnesium, which is further discussed in section 2.4.7.1.

The pH of zero proton charge for HFO is also something to consider in determining an optimal pH of removal. Above the point of zero net charge adsorption is

reduced due to electrostatic repulsion (negative solid and negatively charged phosphate) (Daou et al., 2007), however, adsorption interactions are present since the covalent bond between phosphate and the HFO surface forms inner sphere complexes as opposed to outer sphere interactions which are directly pH dependent. These surface electrostatic interactions will also play a significant role in the binding of other anions and cations to the surface of HFO. For HFO, the pH_{zpc} is 7.9 to 8.2 (Dzombak and Morel, 1990), however this value can decrease as phosphate is adsorbed to the surface. Li and Stanforth (2000) describe this decrease in pH_{zpc} for goethite (pH_{zpc} 7.2 to 9.7) as phosphate is bound to the surface, since phosphate hydroxyl groups are more acidic than the surface hydroxyl groups on goethite. Approaching the pH_{zpc} will also affect floc formation, which is a consideration in the treatment process since efficient P removal requires P to associate with particles, but also that those particles can be separated from solution.

2.4.6 Effect of Mixing on Iron Phosphorus Interactions

Mixing is a significant factor for phosphorus interactions both in wastewater treatment and the natural environment. P loading, related to eutrophication, varies between lakes largely due to mixing in the body of water along with other factors, such as water temperature and sediment biochemistry (Carpenter and Lathrop, 2008). In terms of phosphorus removal efficiency, mixing along with reaction times and age of flocs are key factors studied in laboratory and modeling studies (Szabó et al., 2008). As was described in section 2.4.3.2 on the surface complexation model, the key modeling parameter, the active site factor, is a function of how well the system is mixed. A well mixed system will have a high ASF value and therefore better phosphorus removal than a poorly mixed system. Szabó et al. (2008) performed laboratory jar tests varying mixing and observed a relationship between mixing intensity (G) and residual soluble P. Figure 2-9 shows this relationship.

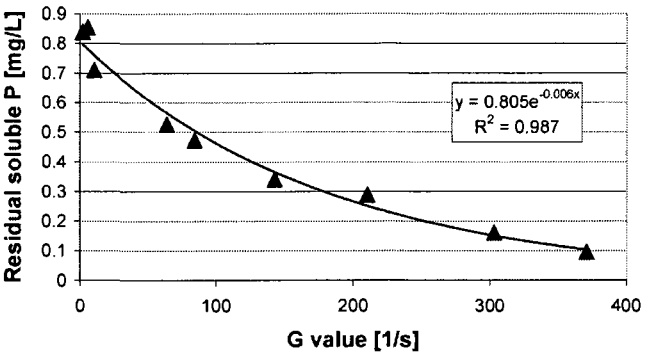

Figure 2-9: Effect of G (mixing intensity) on phosphorus removal (Szabó et al., 2008)

Szabó et al. (2008) also show an equation, shown in Figure 2-9, that fits the relationship between residual soluble P and mixing intensity (G). In a well mixed system, 300 s^{-1} for example, the equation in Figure 2-9, predicts residual soluble phosphate to be ~0.1 mg P/L, and for a poorly mixed system, ~20 s^{-1} residual P is expected to be ~0.7 mg P/L. Mixing also plays a major role in floc formation with respect to hydrous ferric oxides that interact with phosphate.

2.4.6.1 Floc Formation and Age

The size and shape of the HFO flocs plays a significant role in the phosphate interactions. As the HFO floc ages it becomes denser and the sorption capacity decreases. The decrease in sorption sites begins within minutes of the floc forming, such that the sorption capacity is decreased by 25% when the floc is aged for 30 minutes (Szabó et al., 2008) and only half the sorption capacity remains after aging for one day (Lijklema, 1980).

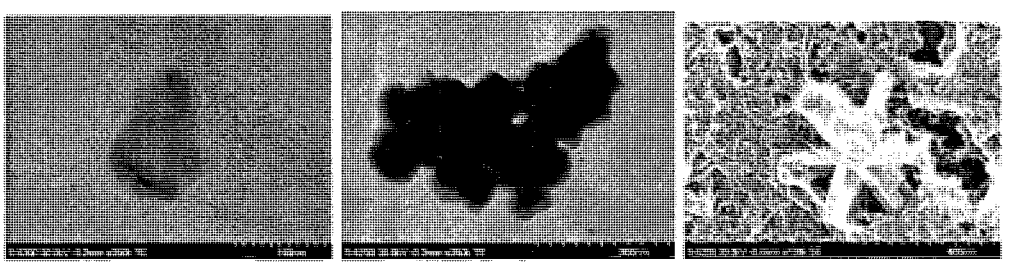

1 day 4 days 2 years

Figure 2-10: TEM and SEM images of HFO after 1 day, 4 days and 2 years of aging (Smith et al., 2008a).

Figure 2-10 show the HFO floc growing larger and denser with age. After 2 years of aging the floc is beginning to show crystallization.

In addition to the iron colloids changing with age, adsorption of phosphate alters the colloid formation. Magnuson et al. (2001) used sedimentation field flow fractionation with multiangle laser light scattering detection to compare iron-phosphate colloids to iron-hydroxide colloids (no phosphate scenario). Since hydroxyl ions are smaller than phosphate ions, iron colloids formed in the absence of phosphate are denser than iron-phosphate colloids. Moreover, phosphate may interfere with the iron oxide particle growth.

2.4.7 Water Chemistry

To continue expanding the model for chemical phosphorus removal, experiments to investigate the effects of more complex water chemistries are needed. Particularly focusing on constituents of wastewater that are present at the metal salt dosing point and that would interact with phosphorus or iron. Due to the consistent presence of calcium, magnesium and organic matter both in wastewater and natural systems, and their ability to form complexes with both phosphorus and iron, these factors need to be considered in expanding the SCM. Despite research and experimentation on the effect of calcium and magnesium on the precipitation of phosphorus, the mechanism of the effect is poorly understood.

2.4.7.1 Calcium and Magnesium

The effect of calcium on chemical phosphorus removal could be beneficial for achieving low effluent concentrations since phosphate precipitation with lime is a method of chemical P removal along with Al and Fe. Due to the high lime dose required (1.5 times the total alkalinity of the solution) for P removal with calcium, this metal salt is less commonly used. Moreover, significant removal is only achieved at high pH (>10) (WEF, 1998). The calcium phosphate precipitates that form include tricalcium phosphate ($Ca_3(PO_4)_2$), hydroxyapatite ($Ca_5(OH)(PO_4)_2$), dicalcium phosphate ($CaHPO_4$) and calcium carbonate ($CaCO_3$) (WEF, 1998). It is believed to be the hydroxyapatite precipitation that removes the bulk of the phosphate; however, it is also in competition

with calcium carbonate precipitation (Jenkins et al., 1971). Alternatively, soluble calcium phosphate species can also form. Many of the soluble calcium phosphate species form from polyphosphates at high pH (Jenkins et al., 1971). The breakdown of polyphosphates to orthophosphates (process is called reversion) is affected by pH, temperature and cations such as calcium (Lytle and Snoeyink, 2002).

More research on the effects of calcium on phosphorus precipitation has continued to show that the presence of calcium will aid in P removal under the right conditions. Diamadopoulos and Benedek (1984) studied the effect of precipitating phosphorus with calcium when no other coagulants were added and also in the presence of an aluminum coagulant (the aluminum coagulant would be expected to behave similarly to an iron coagulant). The results showed that the addition of the coagulant lowered the pH to a range where phosphorus was released into solution along with calcium. A study done by Carlsson et al. (1997) also showed redissolution of P and Ca is pH dependent, but also affected by the P concentration. They also concluded that calcium phosphate precipitation only occurs at sufficiently high concentrations of both calcium and phosphate. Alternatively, Hsu (1973) found when a small amount of calcium (2 mmol/L) was added to the chemical precipitation process with aluminum or iron a broader pH range of optimal removal could be achieved. Small amount of calcium may aid in P removal by affecting aluminum or iron floc morphology (Fettig et al., 1990).

According to Rietra et al. (2001) the adsorption of Ca^{2+} on goethite is limited to pH values near or above the pH_{pzc}. It was also found that in a system of phosphate, calcium and goethite, more calcium is adsorbed with low goethite concentrations where there is more phosphate bound to the surface (compared to higher goethite concentration). With more P bound to the surface of the precipitate, a decrease in repulsive potential is achieved since PO_4^{3-} makes the surface more negative for positive Ca^{2+} to bind (Rietra et al., 2007). Fettig et al. (1990) found similar results where below pH 5 a mixed phosphate, Fe(III) and calcium precipitate forms, and above pH 6.8 calcium phosphate alone precipitates (when ortho-P concentrations are greater than 0.5 mol/L). For wastewater treatment this indicates the presence of calcium could aid in achieving lower residual phosphorus in the effluent.

Magnesium in wastewater can precipitate phosphate as struvite ($MgHN_4PO_4 \cdot 6H_2O$) when ammonium ions are also present (WEF, 1998). The precipitation of struvite is regarded as a problem in the anaerobic stage of wastewater treatment since it clogs the pipes (Rahaman et al., 2008). However, these 'problems' are also considered for recovery of phosphorus through struvite crystallization. This form of P removal is advantageous since it reduced sludge volumes compared to P precipitation with aluminum and iron salts (Quintana et al., 2005).

The presence of magnesium also affects calcium phosphate precipitations. Jenkins et al. (1971) reported that in the presence of magnesium, beta-tricalcium phosphate will precipitate instead of apatite. Also, according to Peng et al. (2007) magnesium and organic acids may inhibit Ca-P precipitation.

The effects of water hardness (i.e. the presence of calcium and magnesium) on P removal systems cannot be generalized. The literature reviewed is inconsistent where some researchers report calcium may improve phosphorus removal and some say it may decrease removal. Small changes in calcium, magnesium and pH will affect precipitation (nucleation) formation and therefore, the residual phosphate level achieved (Jenkins et al., 1971). Additionally, water hardness levels can vary tremendously based on location (Waterloo Region is known to have very hard water). More research is still needed on the effects of water hardness under specific conditions characteristic of wastewater treatment. Moreover, combined effects of pH, metal salt dose, mixing at the dosing point, and water hardness need to be investigated simultaneously.

2.4.7.2 Organic Matter

Organic matter affects P interactions in both wastewater and natural systems. Experiments done on municipal wastewater by Szabó et al. (2008) found that organic matter significantly influences P removal efficiency. More specifically, high chemical oxygen demand (COD) and total suspended solids (TSS) (both indirect measures of organic matter content) in the water result in higher residual P levels than when low COD and TSS are present. These trends are shown in Figure 2-11.

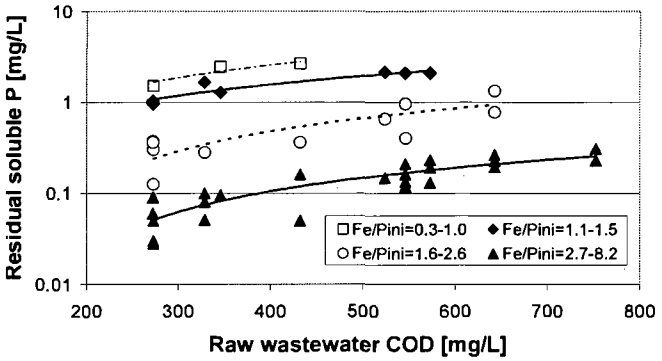

Figure 2-11: Residual soluble P concentration in terms of raw wastewater COD. Four different Fe dosed: initial P molar ratios are shown (Szabó et al., 2008).

For the experiments performed at high COD (and therefore high organic matter concentrations) less efficient P removal is observed (high residual soluble P) compared to water with lower COD. Szabó et al. (2008) have only observed this phenomenon but have not separated the effects from COD and TSS. With the knowledge of organic matter interferences, metal salts are added during wastewater treatment at the outlet of the aeration, to reduce these interferences.

Studies have been done on the effect of organic matter to metal P interactions using organic matter-like compounds. Kreller (2000) used tannic acid as a surrogate for organic matter and found it blocked the bidentate binding of orthophosphate to colloid surfaces. Moreover, it has been suggested that natural organic matter (NOM) may act as a complexing agent to alter Fe particles (Lytle and Snoeyink, 2002), or that is competes with P for binding sites on HFO (Mikutta et al., 2006). Research by Togesayi et al. (2008) does not reject these ideas, but suggests pH changes make organic matter interact differently. Togesayi et al. (2008) specifically studied the adsorption of fulvic acid and phosphate on Fe_2O_3. Their findings show that fulvic acid displaced phosphate from surface sites on Fe_2O_3 at pH 5.30 and 6.30 but at pH 8.30 fulvic acids and phosphate both adsorbed to the surface. This trend is observed with pH since at lower pH, FA^- forms stronger bonds (stronger base) than $H_2PO_4^-$ or HPO_4^{2-} but at high pH (>8) the high charge density from HPO_4^{2-} or PO_4^{3-} compete with FA^- for adsorption on the surface, and may bind to the phosphate instead of the iron oxide surface (Togesayi et al., 2008). At the pH of wastewater (~7), the presence of fulvic acid may reduce the amount of phosphorus bound by the HFO.

In addition to direct competition, humic acid can interfere with P removal by stabilizing particles to reduce P adsorption. In a study on phosphate precipitation with aluminum, Fettig et al. (1990) found that the interference of humus causes increased particle stability and therefore additional metal dose was required for particle destabilization to bind P. Fettig et al. (1990) also found that the effect was more pronounced in hard water (high calcium and magnesium concentrations). Since P removal with iron follows a very similar mechanism to aluminum, it can be assumed that a similar interaction is observed when iron is used as the metal salt.

From this overview, it can be seen that organic matter needs to be considered in phosphorus interactions. As with calcium and magnesium, a generalization of the organic matter impacts cannot be made. To be complete on future P removal studies, organic matter from various sources, at various concentrations and pH's needs to be considered. Experiments performed with organic matter are not done in this thesis.

The literature review has provided the background necessary to reach objectives of the thesis project. Ultimately a better understanding of chemically mediated phosphorus removal is desired in order to reduce the impacts of eutrophication on pristine environments. From the review of the literature and previous experiments, it is clear there are analytical issues to overcome related to orthophosphate measurements. This thesis project, will first address optimizing the standard method for low level orthophosphate determination, and designing a filtration protocol to reduce inconsistency in filtering the synthetic samples used to mimic chemically mediated phosphorus removal in the lab. Finally, a better understanding of the removal process including iron dosing, solution pH, mixing intensity and water hardness will provide insight to improve the model for chemically mediated phosphorus removal.

Chapter 3
Methodology

3.1 Introduction

Accurate and reliable methods are essential for testing and analysis. Standard Methods (1998) outline colorimetric orthophosphate determination and suggests 0.45 μm pore size filters for separating dissolved and particulate fractions. For this project, an optimized method for low level orthophosphate determination is developed. Additionally, a filtration protocol that outlines more than simply pore size is needed, as the colloidal iron used in these studies affects filtration by blocking the pores of the filter. Developing a method for low-level orthophosphate determination and a filtration protocol are presented in Chapters 4 and 5, respectively. This Chapter outlines the methodology, used throughout the project, in detail. Only the final methods and protocols are presented here since the details of the method developments can be found in subsequent chapters.

3.2 Synthetic Sample Preparation

All experiments were performed in an analytical laboratory. All glassware and containers were acid washed in 10% nitric acid solution overnight. All standards and samples were prepared with ultra pure water (Milli-Q, 18MΩ). All chemicals were analytical grade or better.

Synthetic lab samples containing phosphorus and iron were prepared in one of two ways. One approach was to add stock phosphate solution and stock iron solution in a volumetric flask and dilute with Milli-Q water. The second approach, used in Chapter 6, was to prepare synthetic fresh water spiked with phosphate in a volumetric flask, then

transfer to a beaker where iron was dosed while the solution was mixed with a propeller mixer. The stock phosphate solution (1000 mg P/L) was prepared from tribasic sodium phosphate (Fischer Scientific, New Jersey, USA) and stored in a high density polypropylene container in the fridge (~4°C). Dilutions of the stock were prepared daily to minimize the error due to sorption of P to the container walls. 1 mg P/L was used for all synthetic lab samples.

Stock iron solutions were prepared from $FeCl_3 \cdot 6H_2O$ (Fluka, Switzerland) and stored in a high density polypropylene container at 4°C. 10 mg Fe/L or 5 mg Fe/L were added to 1 mg P/L phosphate solution (Fe:P molar ratio of 5.5 or 2.5). The pH of the samples was adjusted with 0.1 M NaOH (Sigma Aldrich, St. Louis, MO, USA) or H_2SO_4 (concentrations up to 0.2M, 95-98% pure, Sigma Aldrich, St. Louis, MO, USA). The prepared sample of phosphate and iron were mixed for 24 hours, since this is considered the time to reach equilibrium (Li and Stanforth, 2000).

Mixing the sample was done one of two ways. One method was in a polypropylene container on an Eberbach reciprocal shaker (Eberbach 6000, USA). This method is rather aggressive and does not allow different mixing intensities to be tested. The alternative method of mixing is with a propeller mixer. This top down approach to mixing more closely resembles the mixing in a treatment plant. The three bladed propeller was attached to a motor (Talboys Instruments Corp., Bodine Motor, model 102) which was attached to a variable autotransformer (Power Stat 3PN116B) to adjust the speed of rotation. RPM measurements were determined manually and used to calculate mixing intensity (G). The mean velocity gradient (G) was calculated following equation by Camp and Stein (1943), Equation (24).

$$G = \sqrt{\frac{P}{V \cdot \mu}} \tag{24}$$

where P is power dissipated in the water, V is the volume of the suspension and μ is the dynamic viscosity. The calculation for P is adapted from Svarovsky (2000) and shown as an expanded expression for mean velocity gradient in Equation (25).

$$G = \sqrt{\frac{C_D A_p \rho (V_p - V)^3}{2V\mu}} \tag{25}$$

In this expression (Equation (25)), C_D is a drag coefficient, A_p is the projected area of the paddles, ρ is density, and (V_p-V) is the relative velocity between the paddle (V_p) and the fluid. C_D is assumed to be 1.2 (based on the length to width ratio of the paddle (Svarosky, 2000)) and viscosity and density of pure water were used (detailed calculations are shown in the Appendix).

pH Measurement and Control

For many experiments, pH was adjusted manually with the addition of sodium hydroxide or hydrochloric acid. The pH was measured on a TANANGER Scientific Systems Inc. dual pH meter and titrimeter (model 9501) with Orion double junction reference electrode (90-20) and pH electrode (8003) from Thermo Electron Corporation, USA). The reported pH is the pH after equilibration (24 hours of mixing). For the experiments detailed in Chapter 6, pH was held constant for the full duration of each experiment. pH was controlled with pH stat using the Tanager pH unit connected to a computer as well as a buret. A schematic for the set up is shown in Figure 3-1.

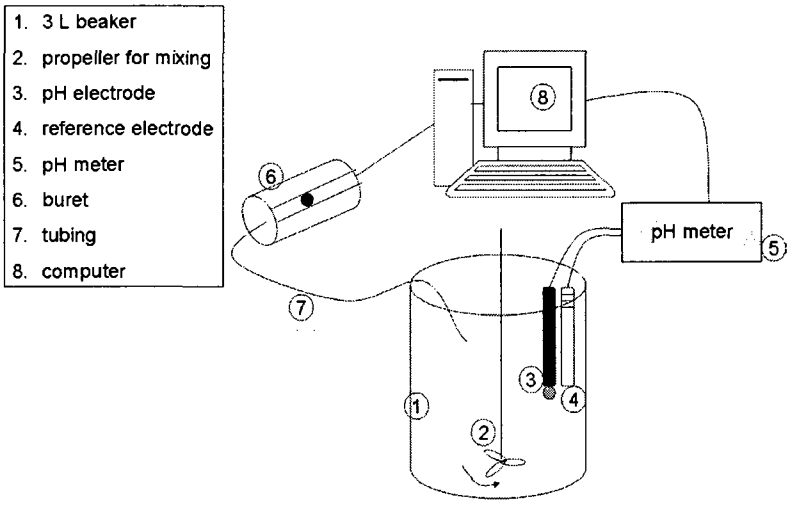

Figure 3-1: Schematic for pH controlled experiments.

The buret could hold either acid or base (not both). 0.1 M NaOH or 0.2 M H_2SO_4 were used with the buret depending on the desired pH. The software was developed to run in DOS and is designed to add acid or base from the buret to maintain a desired pH. Inputs into the program include volume of the sample, type of acid or base, concentration of

OPTION 1	BURET 1	REACTOR 1	
PH STAT PARAMETER		VALUE	#
TIME FRAME (sec)		30.000	1
RESPONSE (sec)		2.00	2
PRECISION (pH)		0.01	3
REPLICATES		4.000	4
TITRANT CONCENTRATION (M)		0.1	5
CONSTANT VALUE (pH)		8.000	6
MAXIMUM ADDITION (ml)		0.1	7
INITIAL ADDITION (ml)		0.005	8
TYPE (A,B,M+, M-)		B NaOH	9
TOTAL BURET VOLUME (ml)		25.00	11
MAXIMUM TITRANT ADDED (ml)		20.00	12

TASK (S,M)	S	13
FILENAME	One.dat	
DURATION [0]		
ELECTRODE	1	15
CALIBRATION FILE	Z	16
BURCAL (STEPS/ml)	800	18
UNITS (pH, mV)	pH	19
BURET VOLUME (ml)		20
EVENT NUMBER		
READING (pH)		
DEVIATION (pH)		
TITRANT ADDED (ml)		
STATUS	| | | |	

Figure 3-2: DOS window for pH stat set up. Required input values are in grey for a sample experiment.

acid or base and various parameter inputs for how precise and how quickly pH should be adjusted or maintained. An example of the inputs is shown in Figure 3-2. For the sample experimental inputs illustrated in Figure 3-2, a constant pH of 8 was desired, and 0.1M of NaOH was in the buret to achieve this. For each experiment, pH, acid or base concentration and file name would differ. The other parameters (precision and replicates for example) dictate how fast, how often, or how much, titrant to add to maintain the pH. The decision to titrate with acid or base depends on the experiment. The pH would drift depending largely on the hardness of the water, but mixing, and dose of iron affected how the pH changed. Depending on the natural drift of the pH for the experimental conditions and the desired pH, either acid (0.2M H_2SO_4) or base (0.1M NaOH) were used as the titrant.

The experiments performed with the pH stat were time sensitive, where the addition of iron signaled time zero and sub-samples were taken over a 24 hour period of

analysis. The addition of acidic iron caused the pH to drop and it was difficult for the pH stat to maintain the desired pH within the desired 0.1 range over the whole period. To accommodate this, manual adjustments were often performed for the first 30 minutes of the experiment to get and keep the pH at the desire level within 0.1 (i.e. 5.9 to 6.1). After the pH was more stable the stat was able to maintain the pH by adding acid or base over the 24 hour period. Occasionally, restarting the program was needed after manual adjustments were complete.

3.2.1 Synthetic Fresh Water

Synthetic fresh water was prepared following guidelines from Environment Canada (1990). Both synthetic hard water and soft water were prepared such that the hard water would have a final hardness between 160 and 180 mg/L as $CaCO_3$ and the soft water between 40-48 mg/L as $CaCO_3$. Sodium Bicarbonate, $NaHCO_3$ was obtained from EMD Chemicals Inc., Gibbstown, N.J. USA and calcium sulfate dehydrate, $CaSO_4 \cdot 2H_2O$, magnesium sulfate heptahydrate, $MgSO_4 \cdot 7H_2O$ and potassium chloride, KCl were obtained from Sigma Aldrich, St. Louis Mo., USA. 1000 mg/L stocks solutions of each of the four reagents were prepared by dissolving appropriate quantities of the salt in Milli-Q water (18.2 MΩ, Milli-Q). Table 3-1 shows the concentrations of each salt used to obtain the desire water hardness.

Table 3-1: Preparation of synthetic water of a desired hardness. Adapted from Environment Canada (1990)

Water Type	$NaHCO_3$ (mg/L)	$CaSO_4$ (mg/L)	$MgSO_4$ (mg/L)	KCl (mg/L)
Soft (40-48 mg/L as $CaCO_3$)	48	30	30	2
Hard (160-180 mg/L as $CaCO_3$)	192	120	120	8

Appropriate volumes of each salt were added to a volumetric flask along with 1 mg P/L and diluted to the mark.

3.3 Sampling Sites

In addition to synthetic samples, natural samples were collected for analysis and to test the developed methods. Samples were collected near the effluent of a treatment

plant in Cambridge, Ontario, Canada. These natural samples were used to confirm the methods and protocols that were developed to ensure they hold true for natural water samples. The treatment plant is located in Preston, a division of Cambridge, Ontario, Canada, and has a variety of wastewater influent from industrial and residential areas nearby. Industrial inputs, including that from the nearby Toyota and Hostess plant force the plant to deal with a large organic load. For this reason, the maximum operating load is less than what the plant has been designed for. The maximum load with the high organic input is 16,820 m^3/d (Earth Tech Canada Inc, 2007). The effluent is released through a storm ditch into the Grand River. Total phosphorus concentration in the effluent averages 0.7 mg P/L (Earth Tech Canada Inc., 2007).

Sampling from this location was chosen because it is a treatment plant close to Wilfrid Laurier University and the near by park allows easy access to the effluent and Grand River. Samples were collected at three sites as shown in Figure 3-3.

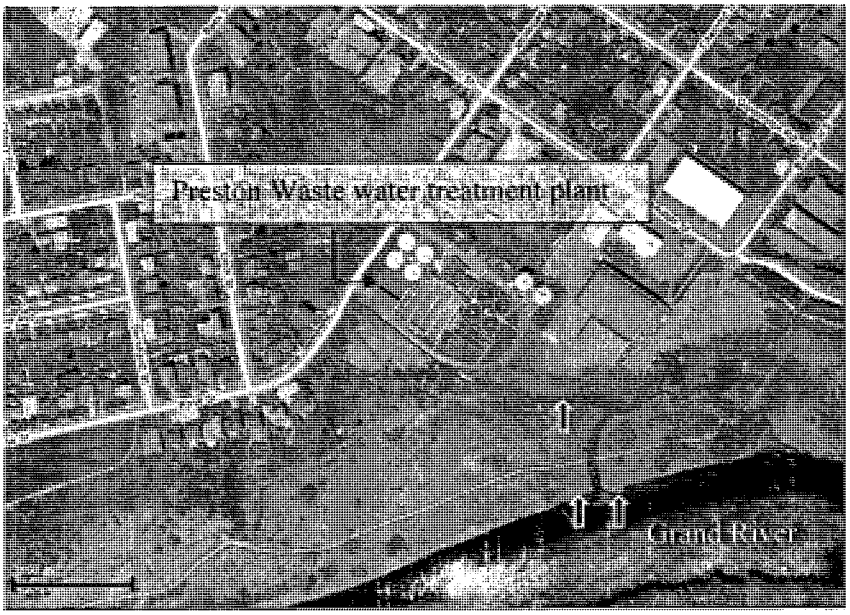

Figure 3-3: Preston Wastewater Treatment Plant in Cambridge Ontario Canada. Sampling sites are shown with black and white arrows. Image adapted from ©2009 Google.

One sample was taken from the storm water ditch the effluent is released into, a second sample from the Grand River, upstream from where the effluent stream reaches the river and a third sample down stream from where the effluent stream meets the Grand River.

Additionally, samples of groundwater were obtained to test for matrix effects and confirm the methods developed for synthetic samples are applicable to natural samples as well. The groundwater samples were collected from shallow wells in the riparian zone of the Beverly Swamp, at the John Mount field site, near Valens, Ontario, Canada. The sample was collected by drawing water from the well into a plastic bottle with a peristaltic pump and silicone tubing.

Raw wastewater influent is the final sample type used for analysis. Samples were obtained from a pilot treatment plant near New Hamburg, Ontario, Canada. The pilot plant branches off the New Hamburg Wastewater treatment plant in the Township of Wilmot, and is used for wastewater research purposes.

3.4 Sample Collection

Samples were collected in high density polypropylene containers cleaned with acid (10% nitric acid bath) and rinsed with Milli-Q water. The containers were rinsed three times with the sample water to be collected then filled and capped underwater to reduce the air headspace. pH and water temperature were recorded at the time of sampling using an Accumet® Portable Laboratory kit from Fisher Scientific (model: AP61. Mississauga, Ont., Canada). Samples were used immediately upon returning to the lab, with the remaining samples stored at 4°C for future reference.

3.5 Filtration

All samples, prepared in the lab or collected, were filtered before measuring the orthophosphate concentration. No filter pretreatments were performed as previous tests and work from Horowitz et al. (1996) and Hall et al. (1996) indicate there is no interference from filter material associated with the artifacts. Aside from testing various filters, as reported in Chapter 5, the filters used were a Whatman Millipore filter with pore size of 0.45 μm and diameter of 47 mm. The filters were housed in a reusable filter casing from Whatman-"pop-top and swin-lok". Samples were drawn into a syringe (50 mL or 20 mL sterile syringe from NORM-JECT®, Germany) and filtered with a syringe pump to control the flow rate. The set up for filtration is shown in Figure 3-4.

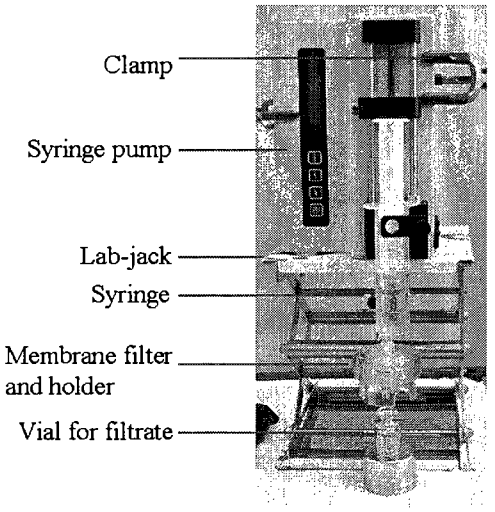

Figure 3-4: Set up for filtration using a syringe pump. The syringe pump is mounted on the lab jack, with a clamp on a retort stand. The syringe is placed on the syringe pump and the sample is filtered into a vial for orthophosphate determination.

The syringe pump (KD Scientific 100, USA) is mounted on a lab-jack with clamps for stability. The diameter of the syringe is programmed and calibrated for accurate volume outputs. Figure 3-3 shows the sample being filtered directly into the vial used for color-development before analyzing the orthophosphate concentration. This reduced loss of P in transferring the sample. Additionally, the mixed reagent added to measure the amount of orthophosphate, contains acid which will ensure P sorption to the glassware is minimized.

3.6 Sample Analysis

3.6.1 Spectroscopic Determination of Orthophosphate

Standard Methods (1998) outlines spectroscopic orthophosphate determination using ascorbic acid and stannous chloride as reducing agents. A comparison of the two methods is provided in Chapter 4. All other orthophosphate determinations are performed using ascorbic acid. For determination of orthophosphate at concentrations greater than 0.01 mg P/L Standard Method 4500 P.E is followed using a 1 cm path length. The following reagents are used.

Reagents

a. Sulfuric acid, H_2SO_4, 95-98% pure, Sigma Aldrich, St. Louis, MO, USA
b. Potassium antimonyl tartrate, $K(SbO)C_4H_4O_6 \cdot \frac{1}{2}H_2O$, 99% pure, Sigma Aldrich, St. Louis, MO, USA
c. Ammonium molybdate, $(NH_4)_6Mo_7O_{24} \cdot 4H_2O$, Fluka, Germany
d. Ascorbic acid, 99% pure, Aldrich, St. Louis, MO, USA

A 100 mL mixed reagent was prepared daily (stable for 4 hours) following the method (Standard Methods 4500 P.E). In a 100 mL volumetric flask, 50 mL 5N H2SO4, 5 mL, potassium antimonyl tartrate and 15 mL ammonium molybdate were added and diluted to the mark with ascorbic acid. For samples with lower concentrations of orthophosphate (<0.01 mg P/L) a modified method was used with a 10 cm or 1 m light path. The development of this modified method is outlined in Chapter 4. The same mixed reagent is used for these measurements, however, less mixed reagent is added to the sample and the colour is allowed to develop for a longer period of time. Table 3-2 summarizes orthophosphate determination with various path lengths for different concentrations.

Table 3-2: Summary of methods for different path lengths for orthophosphate determination

	1 cm	10 cm	1 m
Volume mixed reagent for 10 mL sample	1.6 mL	500 µl	500 µl
Colour development time	10 min (max. 30 min)	1 to 1.5 hours	24 hours
Detection Limit (approx.)	0.01 mg P/L	0.001 mg P/L	0.0001 mg P/L

The volume, colour development time and detection limit outline in Table 3-2 for the 1 cm path length are from the Standard Method 4500 P.E. The parameters for the 10 cm and 1 m path length are the result of the method development described in Chapter 4.

Absorbance measurements were performed with an Ocean Optics (Sarasota, FL, USA) fiber optic spectrometer and the absorbance was measured at 650 nm. Light was passed from a tungsten halogen light source (Ocean Optics LS-1) through an optical fiber to a cuvette (1 cm or 10 cm) containing the sample. A second optical fiber transmitted

the light signal to the detector (Ocean Optics QE5000). The 1 m light path was obtained from World Precision Instrument Liquid Waveguide Capillary Cell (LWCC-2100, Sarasota, FL, USA), in which the sample was pumped by a syringe pump (KD Scientific 100, USA). The 1 m light path had to be frequently flushed with water and cleaned with acid. Repeated measurements of just Milli-Q water were performed between samples to ensure signal stability (reproducible signal for Milli-Q water). The syringe pump was set to pump at speeds between 2 mL/hour up to 10 mL/hour; the signal was read after the sample had stopped pumping. A few minutes (up to 5 minutes) between stopping the pump and taking a reading were needed to ensure the sample is not moving within the tubing and the signal is at its maximum. The signal reading needs to be taken when the sample is not moving and due to the surface tension in the small capillary tubing the sample continues to move for a few minutes after the pump has been turned off.

A calibration curve was prepared daily, including a blank sample (Milli-Q water and mixed reagent) and three or four calibration standards (0.1 mg P/L, 0.25 mg P/L, 0.5 mg P/L and 1 mg P/L for a 1 cm calibration curve for example; 10 and 100 times lower for a 10 cm or 1 m calibration respectively). Calibration standards were measured three times, recording three signal readings each time. Sample signals were also recorded three times and the average of the signal was used to calculate P (in mg P/L).

Signal readings were recorded in intensity and converted to absorbance following equation (27).

$$A = -\log(\frac{I}{I_o}) \tag{27}$$

where A is absorbance, I is the intensity of the sample and I_0 is the intensity of the blank. If multiple samples were being measured, multiple blanks were prepared, such that a new blank reading was taken between four or five samples.

3.6.2 Atomic Adsorption Spectroscopy for Iron Determination

Determination of iron was performed on a Perkin Elmer Atomic Absorption spectrometer (3100). The wavelength was set to 248.3 (a unique Fe analytical line). Calibration standards were prepared from the 1000 mg Fe/L stock solution. Standards and samples were acidified with a drop of concentrated nitric acid. Standards were

measured three times, recording three or four signal readings for manual calibration. Due to the volume of samples available, samples were only read once, recording multiple absorbance signals. Flushing with acidified Milli-Q water was performed between readings.

Chapter 4
Chemically Mediated Phosphorus Removal: Optimization of Analytical Methods

4.1 Introduction

Eutrophication in natural systems is the result of excess nutrients (primarily phosphorus and nitrogen) reaching sensitive water bodies, often from treated wastewater effluent flowing directly into these environments. Regulations for allowable discharge levels are determined based on the volume of effluent and the sensitivity of the receiving water body. Currently, effluents are regulated by regions or municipalities, but the Canadian Council of Ministers of the Environment (CCME) are working towards developing a Canada-wide strategy for Municipal Wastewater Effluent (MWWE) (Marbek Resource Consultants, 2005). Regulations in certain jurisdictions in North America require total phosphorus (TP) in effluents to be less than 0.1 mg P/L which suggests orthophosphate levels need to be below 0.01 mg P/L (Takács et al., 2006a). Effluent concentrations, as low as 10 and 50 μg/L TP, are being considered in Florida and Washington State (Neethling et al., 2007). To ensure treatment plants are meeting these low effluent regulations, the analytical methods for measuring phosphorus need to be optimized for trace level phosphorus determination.

Chemical phosphorus removal is achieved with the addition of metal (Fe and Al) salts, which precipitate, co-precipitate or adsorb the soluble phosphates to be removed with the sludge. Although chemical phosphorus removal is widely used, the mechanism of removal is poorly understood. Without knowledge of the mechanistic details for phosphorus removal, the required metal dose is difficult to determine and might result in overdosing the metal salt. The consequences of overdosing include a high cost of

chemicals and sludge processing. Recent publications by Smith et al. (2008a) and Szabó et al. (2008) introduce a Surface Complexation Model (SCM) to describe the phosphorus removal process with Fe(III). This chemical equilibrium based model is supported with laboratory data where simple abiotic samples containing phosphorus and iron are mixed for different times, filtered and residual phosphate is determined colorimetrically. The data in Smith et al. (2008a) provides good proof of concept that SCM methods can model chemically mediated phosphorus removal, but the measured data shows poor reproducibility. The noise is likely due to the analytical issues with the standard colorimetric method for phosphorus determination not being optimized for low level analysis.

4.2 Phosphate Determination: Colorimetry

In wastewater, orthophosphates make up the phosphorus species that are reactive (Spivakov et al., 1999). For phosphorus determination, all forms of phosphorus are converted by pre-treatment to orthophosphate for analysis via hydrolysis, oxidation or other methods (Spivakov et al., 1999). Thus, all phosphorus speciation analysis is dependent on the quality of orthophosphate determination. The concentration of phosphate in the water is determined by spectrophotometric methods. The measured absorbance (A) of a coloured complex is proportional to the concentration (c) of orthophosphate according to Beer's Law (Equation (28)).

$$A = \varepsilon bc \qquad (28)$$

Where

ε = molar absorptivity ($M^{-1}cm^{-1}$)

b = path length (cm)

c =concentration of a substance in a sample (M)

The coloured complex is formed by combining phosphoric acid with ammonium molybdate. The complex is then reduced with either ascorbic acid or stannous chloride in the presence of potassium antimonyl tartrate (Spivakov et al., 1999). The reduction of phosphomolybdic acid forms molybdenum blue whose absorbance can be measured

(Standard Methods, 1998). The reducing agent is the most significant difference between the two standard methods commonly used for phosphorus determination.

One main concern is that the time allotted for full colour development varies between methodologies proposed for the ascorbic acid method (EPA Method 365.3; Standard Methods, 1998; Towns, 1986). There is some debate as to whether absorbance must be measured within a specific time frame before the coloured complex becomes unstable, or whether there is a specific time after which the colour should be fully developed and stable, if not indefinitely, then at least for an hour or two (Towns, 1986). In the work presented here, the two main colorimetric methods for phosphate determination, the ascorbic acid method and the stannous chloride method are optimized. Additionally, experiments are applied to low level phosphate concentrations for which there are limited previous studies. Presently, Standard Methods (Standard Methods, 1998) suggest a path length up to 5 cm can be used for the ascorbic acid method to measure concentration ranging from 0.01 to 0.25 mg P/L. Concentration measurements 10 and 100 times lower than with a 1 cm cuvette are possible with a 10 cm and 1 m light paths, respectively. However, potential poor calibration and noisy data indicate the existing methods cannot be directly applied to low level orthophosphate measurements. To comply with updated regulations, the standard phosphorus analysis method needs to be optimized for low level analysis.

4.3 Experimental

4.3.1 Principle of Colorimetric Phosphate Determination

The two different colorimetric methods, used in this project for the determination of phosphate in wastewater, are the Standard Method using ascorbic acid (4500-P E.), and the Standard Method using stannous chloride (4500-P D.). A basic schematic of colorimetric phosphate determination for either method is outlined in Figure 4-1.

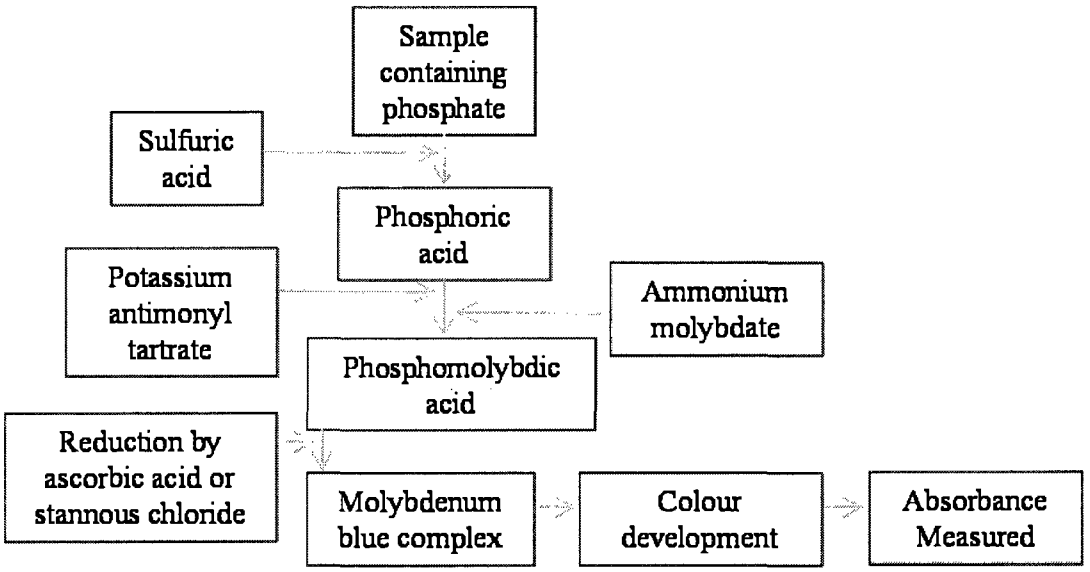

Figure 4-1: Schematic for coloured complex formation and measurement

Both methods involved acidifying a sample containing phosphate, followed by adding potassium antimonyl tartrate and ammonium molybdate before being reduced. Depending on the method, the reduction is done by ascorbic acid or stannous chloride to form a molybdenum blue complex which is allowed to develop for a period of time before the absorbance is measured.

4.3.2 Apparatus

A Varian Cary 50 UV-Vis Spectrophotometer (Varian Canada, Mississauga, ON, Canada) was used for samples above 0.01 mg P/L with a 1 cm light path. Measurements using 10 cm and 1 m path lengths were done with an Ocean Optics (Sarasota, FL, USA) fiber optic spectrometer and the absorbance was measured at 650 nm. In the case of the 10 cm light path, which has a detection limit of approximately 0.001 mg P/L, light was passed from a tungsten halogen light source (Ocean Optics LS-1) through an optical fiber to a 10 cm cuvette containing the sample. A second optical fiber transmitted the light signal to the detector (Ocean Optics QE5000). The 1 m light path was obtained from World Precision Instrument Liquid Waveguide Capillary Cell (LWCC-2100, Sarasota, FL, USA), in which the sample was pumped by a syringe pump (KD Scientific 100, USA). The 1 m light path has a detection limit of approximately 0.0001 mg P/L.

4.3.3 Reagents

a. Sulfuric acid, H_2SO_4, 95-98% pure, Sigma Aldrich, St. Louis, MO, USA
b. Potassium antimonyl tartrate, $K(SbO)C_4H_4O_6 \cdot \frac{1}{2}H_2O$, 99% pure, Sigma Aldrich, St. Louis, MO, USA
c. Ammonium molybdate, $(NH_4)_6Mo_7O_{24} \cdot 4H_2O$, Fluka, Germany
d. Ascorbic acid, 99% pure, Aldrich, St. Louis, MO, USA
e. Stannous chloride, $SnCl_2 \cdot 2H_2O$, 98%, Sigma Aldrich, St. Louis, MO, USA
f. Glycerol, Sigma Aldrich, St. Louis, MO, USA
g. Stock phosphate solution for ascorbic acid method, 1000 mg P/L, $Na_3PO_4 \cdot 12H_2O$, Fischer Scientific, New Jersey, USA
h. Stock phosphate solution for stannous chloride method, 50.0 mg P/L anhydrous KH_2PO_4, 99% pure, Sigma, St. Louis, MO, USA

All solutions were prepared with Milli-Q water (18.2MΩ, Milli-Q)

4.3.4 Procedure

4.3.4.1 Ascorbic acid (4500-P. E.)

In the ascorbic acid method, a mixed reagent was added to the standards and samples. The mixed reagent contained sulfuric acid, potassium antimonyl tartrate, ammonium molybdate and ascorbic acid. The volume of this mixed reagent suggested by the Standard Method was 1.6 mL per 10 mL sample and the colour development time of 10 to 30 minutes. The absorbance of the coloured complex was measured at one of two points; 880 nm or 650 nm (corresponding to the peaks in the UV-Vis spectra of molybdenum blue (Standard Methods 4500-P E; EPA 365.3).

4.3.4.2 Stannous Chloride Method (4500-P. D.)

The stannous chloride reagent was prepared by dissolving stannous chloride in glycerol and heating in a water bath. The ammonium molybdate reagent and the stannous chloride reagent were thoroughly mixed. The samples, standards and reagents were held within 2°C of each other, between 20 and 30°C to keep the rate and intensity of colour development controlled. The absorbance was measured according to the Standard

Method between 10 and 12 minutes at 690 nm with 0.4 mL ammonium molybdate reagent and 1 drop of stannous chloride reagent for a 10 mL sample.

4.3.4.3 Optimization of Standard Method

To optimize the colorimetric method for phosphorus determination two variables were addressed, time for colour development and volume of colour forming reagent. These two variables were varied to optimize the absorbance of a fixed concentration of phosphate. The objective of the optimization was to maximize sensitivity as a function of time and volume. Altering one variable at a time to determine optimal conditions is a sequential "one-factor-at-a-time" approach (Morgan et al., 1974). This method has its limitations, as interactions between the factors are not taken into account. It also does not maximize efficiency, as do methods that alter multiple factors at a time. This project, therefore, made use of the experimental design outlined below rather than the traditional method. A heuristic design was used which involved solving a problem based on previous knowledge (Clancey, 1985). In this case, that meant that the experimentalist could use logic to choose new points to be measured based on the results from the ones already completed.

This heuristic technique to determine which time and volume points to measure maximizes the efficiency of experiments, while identifying the optimal conditions, maximum absorbance in this case. The results obtained from optimization of the ascorbic acid method were compared to the optimization of the stannous chloride method to determine whether reproducible results can be obtained using both methods, or whether one is superior to the other in reproducibility, based on relative standard deviation. Once the methods were optimized, they were tested with natural water samples. For the stannous chloride method, the varied volume was of the mixed colour forming reagent. The reducing agent (stannous chloride) volume was fixed.

4.4 Results and Discussion

4.4.1 Optimization of Ascorbic Acid Method: 10 cm Light Path

To optimize absorbance, and therefore sensitivity, of the ascorbic acid method, the volume of the mixed reagent and the colour development time were varied.

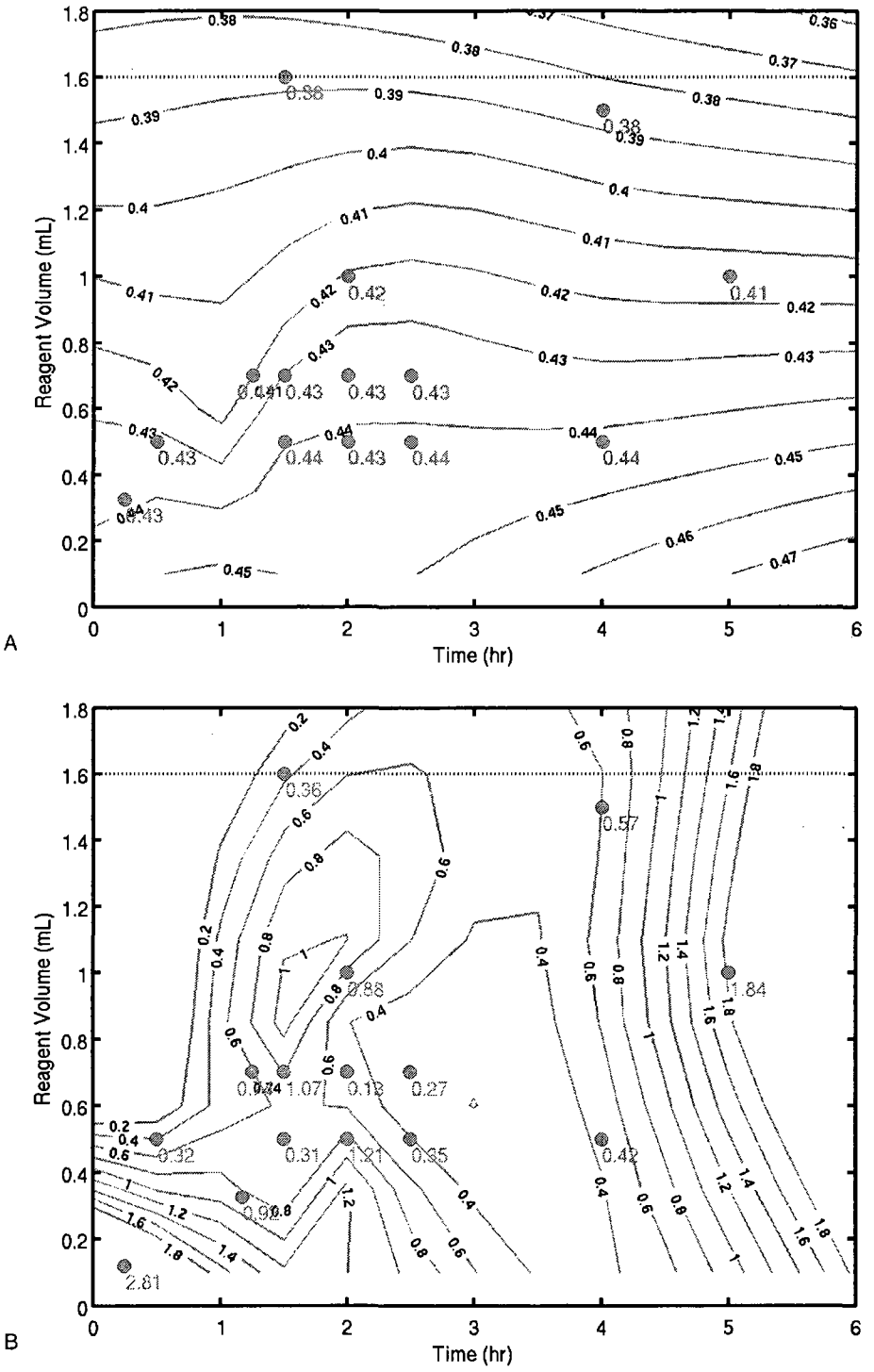

Figure 4-2: Contour plot of absorbance (A) and relative (%) standard deviation (B) by the ascorbic acid method with 10 cm light path. Each point represents one measurement (no replicates).

A 10 mL standard with a concentration of 0.08 mg P/L was used for all measurements with the 10 cm light path. The results; illustrated in Figure 4-2, are shown in contour plots to allow comparison of two variables (colour development time and reagent volume) simultaneously. The contour plots are presented as reagent volume versus time in the x-y plane and the contour lines represent absorbance or standard deviation values in the z direction. To determine the optimal colour development time and reagent volume from the contour plots in Figure 4-2, a reagent volume with a stable absorbance reading (Figure 4-2a) and low relative (%) standard deviation (Figure 4-2b) over time is prefered. Stable absorbance readings means the absorbance is not rapidly changing over time. Ideally a higher absorbance reading and therefore greater analytical sensitivity is preferred, however stablility and reproducibility are of primary importance. The dotted line at 1.6 mL indicates the reagent volume suggested by the Standard Method. The solid black lines represent an interpolated surface through the measured data points to help visualize the trends. The contour lines show that absorbance is not stable around the Standard Method conditions (1.6 mL and colour development time less than 0.5 hours). At 0.5 mL mixed reagent (for a 10 mL sample) and a colour development time of 1-3 hours a stable absorbance reading around 0.4 absorbance units is observed which suggests that the molybdenum blue complex is stable. The relative (or percent) standard deviation plot (Figure 4-2b) supports this, as the values that correspond to the points at 0.5 mL reagent after 1 hr are 1% or lower. In addition, the measured absorbance increased by 13% relative to Standard Method conditions, when using a volume of 0.5 mL.

4.4.2 Optimization of Ascorbic Acid Method: 1 m Light Path

In the 1 m light path of the ascorbic acid method, the volume of the mixed reagent was again varied as well as colour development time. A 10 mL standard with a concentration of 0.008 mg P/L was used for all these measurements. A contour plot similar to the 10 cm one shown in Figure 4-2 is shown in Figure 4-3a. Figure 4-3b shows a 2D plot of absorbance versus time, including error bars, to illustrate the stable absorbance after 16 hours and up to 75 hours.

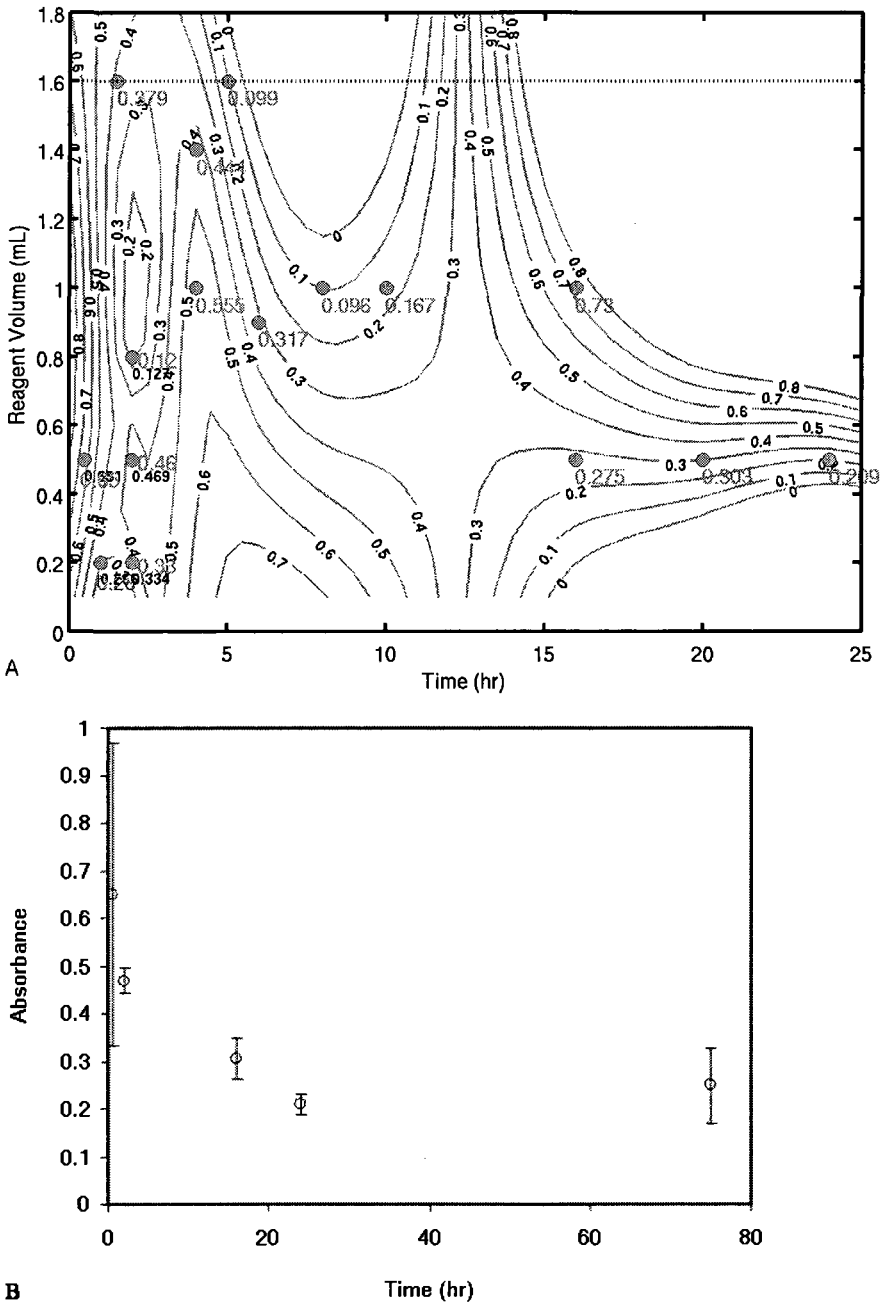

Figure 4-3: Results of the optimization with a 1 m light path. A) Contour plot of absorbance from ascorbic acid method with 1m light path. The dotted line at 1.6 mL is the Standard Method reagent volume. B) Time dependence of colour development using 0.5 mL of mixed reagent for a 10 mL sample.

0.5 mL of mixed reagent for a 10 mL sample was chosen for the 1m light path to be consistent with the modified method for the 10 cm light path, and also because a stable

region of absorbance at 0.5 mL can be seen in Figure 4-3a. Figure 4-3b is a plot of absorbance versus time when 0.5 mL of mixed reagent is used. There is variability in the absorbance numbers at the Standard Method time of 0.5 hours, but a stable region develops after 16 hours of colour development and 0.5 mL of mixed reagent. The error bars in Figure 4-3b illustrate the lack of stability and large error associated with short colour development times as suggested in the Standard Method.

4.4.3 Optimization of Stannous Chloride Method: 10 cm Light Path

In the stannous chloride method, the volume of the ammonium molybdate reagent was varied. The volume of the stannous chloride reagent was kept constant because its high viscosity made it difficult to vary in a precise manner. The time for colour development was also varied. The concentration of the 10 mL standard used for measurements was 0.05 mg P/L. The results of these measurements can be seen in Figure 4-4; the dotted line on the contour plots show the volume of ammonium molybdate reagent suggested in the Standard Method (0.4 mL and colour development time of 0.17 hours.

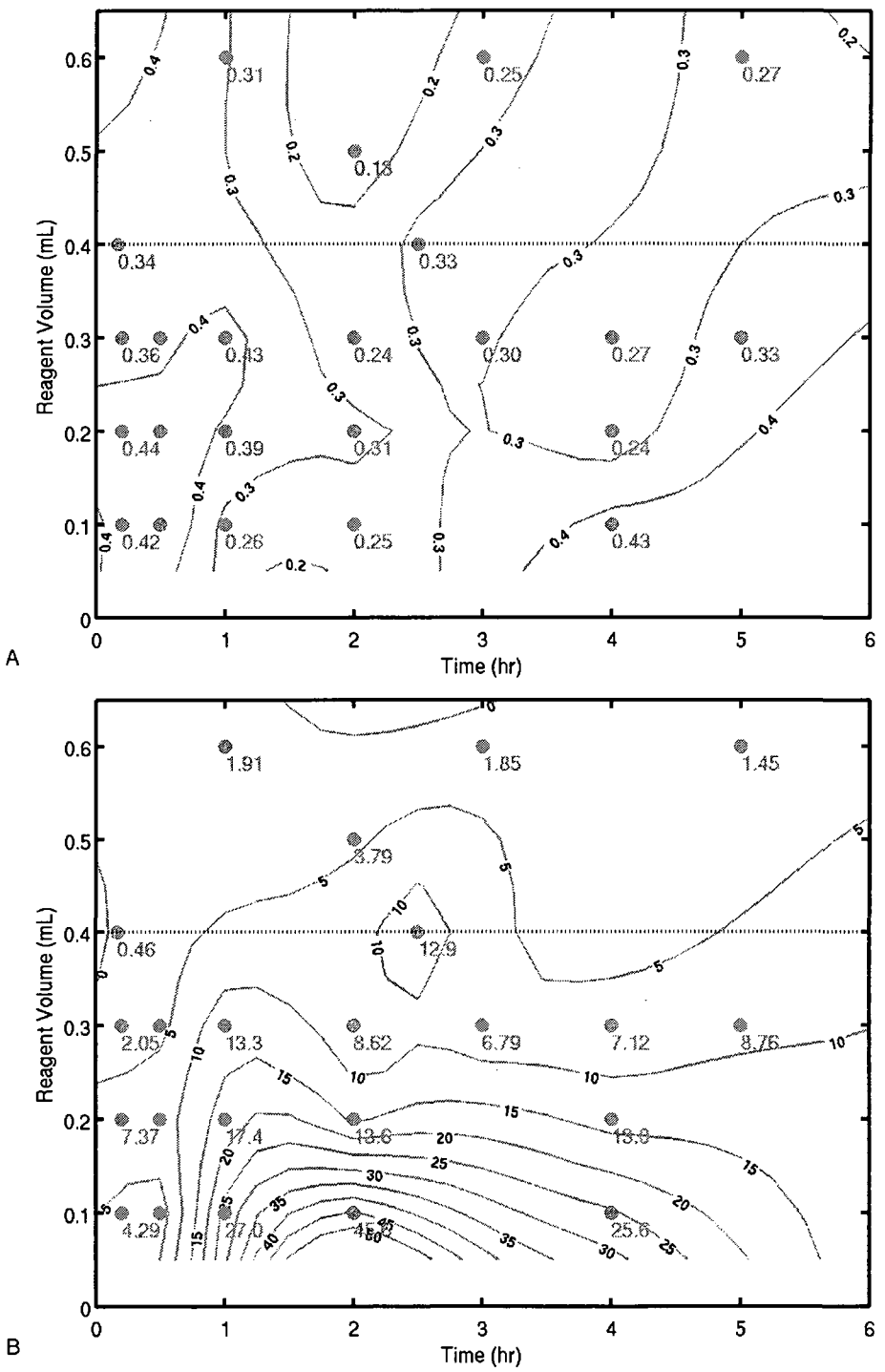

Figure 4-4: Contour plot of absorbance (A) and relative (%) standard deviation (B) from stannous chloride method with 10 cm light path. The dotted line at 0.4 mL is the volume of the ammonium molybdate reagent stated in the standard method.

From the contour plots in Figure 4-4, it can be seen that the highest absorbance values were obtained with reagent volumes below 0.3 mL in a 10 mL sample, and at colour development times of less than one hour. The most consistent results were obtained with a reagent volume of 0.2 mL. This is in agreement with the corresponding relative standard deviation plot (Figure 4-4b). Using a reagent volume of 0.2 mL and a colour development time of 0.25 hours, a 29% increase in sensitivity was achieved compared to the Standard Method conditions.

A comparison of the two method, ascorbic acid and stannous chloride, is shown in Figure 4-5

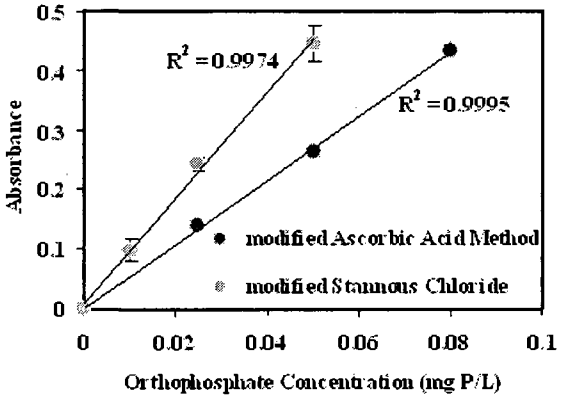

Figure 4-5: Comparison of a calibration curve prepared with stannous chloride vs. ascorbic acid methods at 10 cm path length.

Comparing the calibration curves with a 10 cm light path for both methods (Figure 4-5), it can be seen that although the stannous chloride method is more sensitive (steeper slope), the ascorbic acid method is more reproducible. Reproducibility is the more important factor for obtaining precise measurements.

4.4.4 Optimization of Stannous Chloride Method: 1 m Light Path

As with the 10 cm light path in the stannous chloride method, for the 1 m light path, the colour development time and the volume of the ammonium molybdate reagent were varied while the volume of the stannous chloride reagent was kept constant. The concentration of the 10 mL standard used for measurements was 0.005 mg P/L. These results can be seen in Figure 4-6.

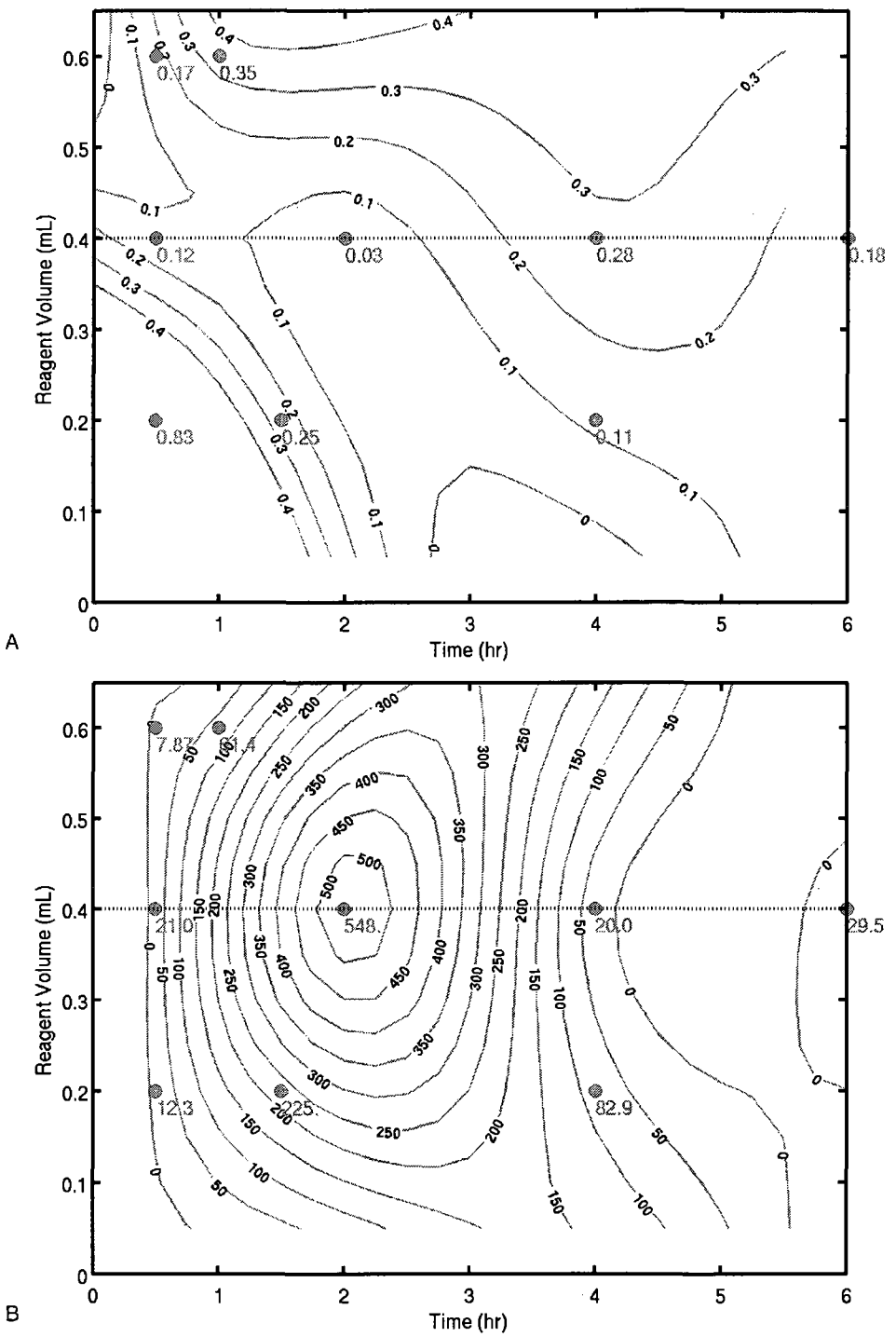

Figure 4-6: Contour plot of absorbance (A) and relative (%) standard deviation (B) from stannous chloride method with 1 m path length.

Measurements for the 1 m light path (Figure 4-6) do not show a region of stable absorbance. Additionally, in Figure 4-6b it can be seen that the relative standard deviations for the absorbance measurements were very high (up to 500%), and so the measurements themselves are not reproducible. From these results, it can be concluded that the stannous chloride method should not be used for low (0.1 μg P/L) concentration phosphate determination.

4.5 Confirming the Modified Methods

To test the methods developed for low level orthophosphate determination, natural samples were collected and measured. The actual detection limit for the 10 cm and 1 m path lengths is also determined. Assuming the detection limit is 10 and 100 times lower for the 10 cm and 1 m light path than for the 1cm light path a sample was prepared with concentrations five times the expected detection limit concentration (0.005 mg P/L and 0.0005 mg P/L were used for the 10 cm and 1 m detection limit determination respectively). Seven sample and seven blanks were prepared, and measured. The standard deviation (s) for the seven sample measurements was computed as well as the average of the seven blank measurements (y_{blank}). The signal detection limit is determined following Equation (29).

$$y_{dl} = y_{blank} + t \cdot s \tag{29}$$

where y_{dl} is the signal detection limit, y_{blank} is the mean of the blank measurements and t is a tabulated t value with n-1 degrees of freedom and 98% confidence. The concentration detection limit is then determined with a calibration curve where *m* is the slope of the curve. The concentration detection limit is calculated as shown in Equation (30).

$$Minimum\ detectable\ concentration = \frac{t \cdot s}{m} \tag{30}$$

Natural samples are measured using an external calibration and also by standard additions to identify matrix effects. Standard additions are performed where a calibration is created by preparing calibration standards using the natural water samples. By comparing the orthophosphate concentration determined using the standard addition

calibration curve compared to using the external calibration curve (standards prepared with Milli-Q water) the interference of matrix effects can be identified. Matrix effects result from more complex water chemistry (compared to ultrapure water) and have an unknown effect, either positive or negative interference.

The calculated concentration detection limit of the 10 cm path length was 0.0013 mg P/L, which is comparable to the expected limit of 0.001 mg P/L based on Beer's law (10 times longer path length can measure concentration 10 times lower) and knowing the detection limit for a 1 cm path length is 0.01 mg P/L. Using samples collected from the Grand River, in Cambridge, Ontario, Canada, two methods were used to determine the concentration of orthophosphate in the sample. An external calibration curve and standard additions to check for matrix effects are shown in Figure 4-7.

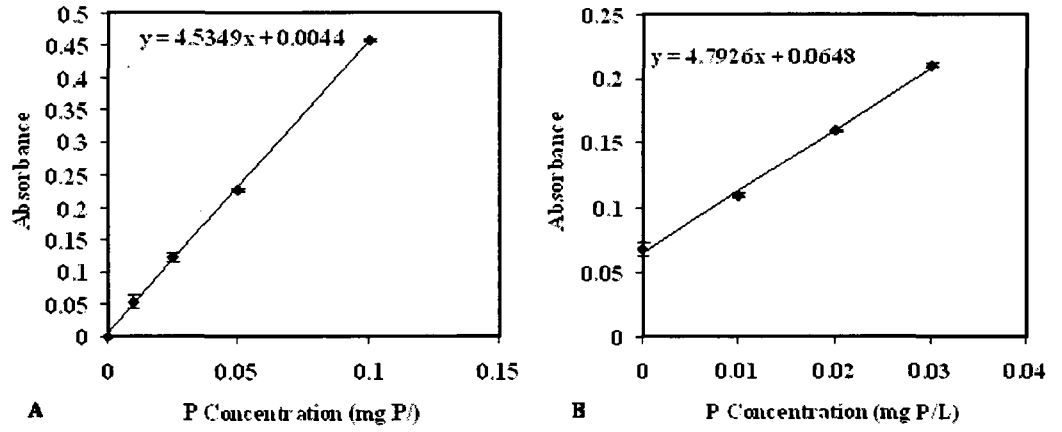

Figure 4-7: A) External calibration used to determine orthophosphate concentration in natural water sample using 10 cm path length. B) Average standard addition curve used to compare the concentration of orthophosphate in natural sample to external calibration using 10 cm path length.

The orthophosphate concentration was measured to be 0.150 mg P/L, with a 95 % confidence interval of 0.014 mg P/L using the external calibration. From the standard addition curve (Figure 4-7b) the orthophosphate concentration was calculated to be 0.136 mg P/L with a confidence interval of 0.014 at 95 %. Based on a t-test, the values determined from the external calibration and standard addition curve are the same with 95% confidence (P=0.05). The values are comparable, giving confidence to the concentration of orthophosphate measured through the reproducibility.

The reproducibility of the 1 m path length analysis was calculated using tap water samples. The water sample was acidified as to maintain the orthophosphate concentrate over a number of days while the experiments were being conducted. The concentration detection limit was 0.00021 mg P/L determined using Equation (30). As with the 10 cm path length, an external calibration was compared to a standard addition to determine if the orthophosphate concentrations were equivalent. The external calibration curve and standard addition are shown in Figure 4-8.

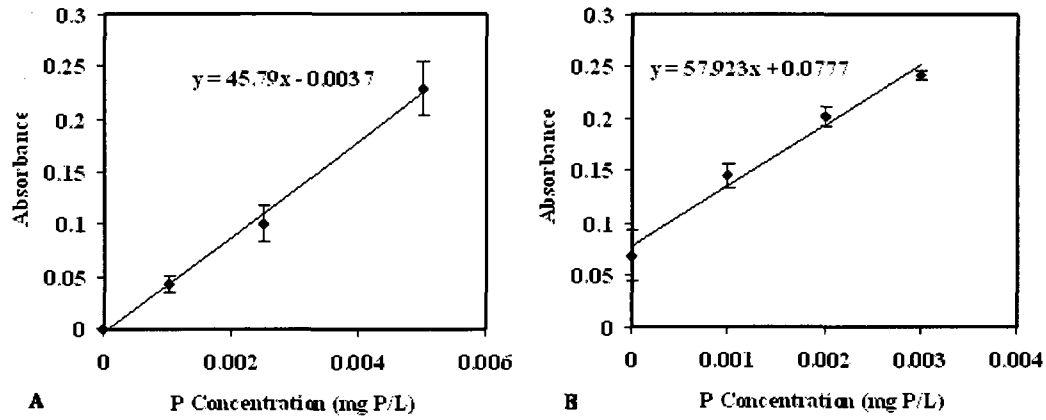

Figure 4-8: A) Calibration curve used to determine orthophosphate concentration in tap water sample using 1 m path length. B) Average standard addition curve used to compare concentration of orthophosphate in tap water sample to value determined to external calibration using 1 m path length.

The concentration found with the external calibration was 0.0072 mg P/L. The confidence interval was 0.0054 mg P/L at 95%. The standard addition concentration for the same sample was 0.0147 mg P/L, with a confidence interval at 95% of 0.0082 mg P/L. A comparison for the P values determined from the external calibration and standard addition curve for both the 10 cm and 1 m path lengths is shown in Table 4-1.

Table 4-1: Comparison of the external calibration to the standard addition for both the 10cm and 1m path lengths (± confidence intervals)

	External Calibration	Standard Additions
10 cm	0.150 ± 0.014 mg P/L	0.136 ± 0.014 mg P/L
1 m	0.0072 ± 0.0054 mg P/L	0.0147 ± 0.0082 mg P/L

The values determined for orthoP concentration in tap water using the 1 m light path are the same within the confidence interval for the external calibration and the standard addition curve. Based on t-test, the values are the same with 95% confidence. This indicates that the interference from matrix effects are negligible for both the 10 cm and 1 m path lengths for the samples tested.

The 10 cm path length gave very reproducible results, whereas the 1 m, although having the intervals overlap, was not reproducible. With the 1m path length the confidence intervals were large relative to measured amount.

4.6 Conclusions

The Standard Method for the determination of phosphate was optimized for path lengths longer than 1 cm. In the ascorbic acid method, the amount of colour-forming reagent was decreased from 1.6 mL to 0.5 mL for a 10 mL sample and the time allotted for colour development increased for both path lengths (10 cm and 1 m) tested, which increased sensitivity and reproducibility, compared to the Standard Method. The colour development time for the 10 cm path length was optimized at 1-3 hours, whereas the 1 m light path requires 24 hour colour development. For the stannous chloride method using a 10 cm path length, the amount of colour-forming reagent was decreased and the time allotted for colour development increased for an optimization of sensitivity compared to the Standard Method. Optimization of the stannous chloride method using a 1 m path length was not achieved because reproducible data could not be measured.

In comparing the ascorbic acid method to the stannous chloride method, it seems that the ascorbic acid method is better for determining phosphate at low concentrations. For instance, this method has a larger region of absorbance stability in the 10 cm light path than the stannous chloride method in the same path length. No stable region was achieved using the stannous chloride method and 1 m path length. Therefore, it has been determined that ascorbic acid results are more reproducible and have a clearer region of absorbance stability with respect to reagent volume and colour development time. It should be used preferentially over the stannous chloride method for determination of low-level phosphate.

Chapter 5

Designing a Filtration Protocol to Separate Dissolved Particulate Fractions for Orthophosphate Determination

5.1 Introduction

Chemical phosphorus (P) removal is achieved with the addition of metal (Fe and Al) salts, which precipitate, co-precipitate or adsorb the soluble phosphates to be removed with sludge. Although chemical phosphorus removal is widely used, the mechanism of removal is poorly understood. To improve the understanding of this process, batch tests in clean water have been performed. Solutions of phosphate and iron were mixed in polypropylene containers overnight, and filtered and measured for orthophosphate after 24 hours. Tests were performed varying pH and iron dose, to observe the phosphorus removal across a range of pH. Measured data shows poor reproducibility, particularly at low pH.

Determining the residual orthophosphate and therefore effective P removal, involves filtering samples through a 0.45μm filter and measuring orthophosphate colorimetrically in the filtrate. This is the standard (operational) definition in aquatic science for separating dissolved and particulate fractions. However, filtering these batch samples prepared in clean water, showed volume dependence with respect to orthophosphate in the filtrate. Inconsistencies in filtration have been reported by other researchers as well (Horowitz et al., 1992; 1996; Hall et al., 1996; Shiller, 2003; Morrison and Benoit, 2001). Horowitz et al., (1992) studied the effect of filtration on dissolved trace element concentrations in natural systems and concluded that additional factors to the filtration process, more than just pore size, need to be considered when

"dissolved" concentrations of Fe, and Al are being studied. Factors such as the volume of sample processed, amount of suspended sediment, and type of filter will all affect the dissolved fraction in the filtrate (Horowitz, 1992).

The volume dependence observed with filtration is the result of "filtration artifacts". This term is used to describe the effect of a build-up of colloids and colloidally associated material. The colloids are generally less than 450 nm in size, but the build up of material blocks the pores of the filter. A build-up of colloidal hydrous ferric oxide (HFO) on the filter will aid in removing phosphate from the sample during the filtration step. Phosphate associated with those colloids initially passing through the membrane will be interpreted as soluble phosphate. Although the particles are nanometer size (approximately 50 nm as determined from SEM images), a "mat" of these particles could block the 450 nm pores. Layers of HFO colloids on the surface of the filter continue to bind P to reduce the amount passing through the filter. Nutrients (including ortho- and total phosphate) alone have been tested separately from samples containing aluminum or iron and it was concluded they are unaffected by filtration artifacts (Horowitz et al., 1996).

In the synthetic samples, where the volume dependence with filtration is observed, the iron dose is typically high; 10mg Fe/L for 1 mg P/L (molar dose of 5). Moreover, low pH solutions compared to neutral or high pH, showed more variability with filtration. These conditions likely provided the most significant artifacts for filtration. To overcome the filtration artifacts associated with the specific synthetic samples, the separation of dissolved and particulate fractions is examined.

Syringe filtration is not the only method to separate the dissolved fraction. Suction filtration, vacuum filtration, and centrifugation are a few examples of other separation techniques. Variations of the traditional membrane filtration have also been studied in an effort to reduce membrane clogging. Hollow-fiber filters, commonly used in biotechnology, have been used to separate lake water with high particulate content. This technique is beneficial to ensure unchanging lake water composition with filtration and is gentle on fragile organisms (Jüttner et al., 1997). Tangential flow ultrafiltration (Morrison and Benoit, 2004) and electrofiltration using cross-flow filtration (Lin et al., 2007) minimize solid membrane contact to reduce clogging. These techniques are

beneficial for size separation and fractionation of colloids. However, for quick and easy on site sample filtration the ease and speed of syringe filtration is preferred. This is essential for wastewater plant operators to check regulations are being met and treatment is functioning properly. Also, aquatic scientists performing in-field measurements or dealing with time sensitive samples can quickly filter and process their data. Syringe filtration is the method of choice for researchers and wastewater engineers due to the ease of use and efficiency in dealing with large numbers of samples.

Due to the widespread use of syringe filtration, filters come in a variety of types and sizes. Focusing only on 0.45 μm pore size for separating dissolved fractions, filter diameter and thickness vary. The two basic types of membrane filters are sieve and tortuous path. Sieve membranes are extremely thin (10-15 μm thick) and as a result, only trap particles on the surface of the filter. Tortuous path membrane filters are thicker (100-150μm thick) and sponge-like therefore able to trap particles within the filter as well as on the surface (Horowitz, 1992). Tortuous path filters, such as Millipore and Sartorius filters are available in 0.45 μm pore size, and the sieve filters, such as Nuclepore and Poretics filters are 0.40 μm which is the real pore size, not woven like the tortuous path filters (Horowitz, 1992). Filter diameters range in size from 13 mm to as large as 142 mm. The large filter diameters are designed to filter larger sample volumes and are more expensive than the smaller diameter filters. The hypothesis, based on previous studies (Morrison and Benoit, 2001) is that tortuous path will be more consistent than sieve membranes since the sieve membranes clog more easily.

In addition to the type of membrane, the flow rate of sample across the membrane can affect the filtration results. According to Leppard (1992), the flow rate for filtration can provoke colloid aggregation. By reducing the flow rate in a series of experiments, filter-provoked aggregates should be reduced (in size and frequency) whereas natural aggregates will be unaffected.

Considering factors known to affect filtration, especially of samples containing colloidal iron, a protocol to separate dissolved and particulate fractions will be developed. The protocol will be designed to isolate the dissolved fraction of a sample in order to reproducibly measure orthophosphate in jar tests designed to mimic chemically mediated phosphorus removal in clean, pure water. The focus is on capturing the dissolved

fraction as anything that cannot be removed as a solid. The protocol will be developed based on syringe filtration and ensure it is applicable to a variety of samples. Key variables such as type and diameter of the filter, flow rate of sample and volume processed will be considered.

5.2 Experimental

5.2.1 Experimental Design

A protocol was determined by selecting the filtration variables that displayed the lowest reproducible residual phosphate concentration. The phosphate that was detectable in the filtrate was therefore classified as dissolved because it could not be separated from particulate matter. The variables that were considered in designing the protocol were volume of sample filtered, flow rate of filtration, type and diameter of the filter.

5.2.2 Sample Preparation

All samples were prepared by mixing 1 mg P/L from stock tribasic sodium phosphate (Fischer Scientific, New Jersey, USA) and 10 mg Fe/L from $FeCl_3 \cdot 6H_2O$ (Fluka, Switzerland) with Milli-Q water in a Teflon jug with a propeller mixer set at 350 rpm. The pH was adjusted to with 0.1 M NaOH (Sigma Aldrich, St. Louis, MO, USA) while mixing then set to mix overnight at 20 rpm. Unless otherwise specified, all samples prepared to test filter variables were ~pH 4 since variable data from previous studies (Smith et al., 2008a) predominates at low pH. They were filtered within four days since tests have shown the composition of the sample and iron colloids changes after this period of time. No filter pretreatments were performed as previous tests and work from Horowitz et al. (1996) and Hall et al. (1996) indicate there is no interference from filter material associated with the artifacts.

5.2.3 Filters

A combination of 25 mm and 47 mm diameter filters from Whatman and Millipore with a 0.45 μm and 0.40 μm pore sizes were used. The filters studied are summarized in Table 5-1.

Table 5-1: Summary of the filters tested

Filter	Filter Type	Pore size (µm)	Diameter (mm)	Note*
Whatman GMF GD/X	tortuous path	0.45	13	For volumes <10mL
		0.45	25	For volumes >10mL
Whatman Nuclepore	sieve	0.40	25	Smooth flat surface for viewing particles
		0.40	47	
Millipore	tortuous path	0.45	25	
		0.45	47	
Whatman Purabind	tortuous path	0.45	47	Diagnostic membrane. Product De-Activated

*Information from the manufacturer (Whatman)

The GMF GD/X filters are syringe filters designed for routine analysis of environmental samples. The filter includes a polypropylene housing and a pre-filtration stack and GF/F glass microfiber media made of Borosilicate Glass Fiber. The pre-filtration stack is designed to provide ease of filtration, and prevent clogging. The filters are available in 13 mm and 25 mm diameter; with the 13 mm intended for filtering samples less than 10 mL and the 25 mm used for samples greater than 10 mL. The other types are considered membrane filters and do not include a casing for syringe filtration. To house these membrane filters a "pop-top and swin-lok" plastic filter holder for 25 mm and 47 mm is used. The holders are made of polycarbonate or polypropylene and included a pre-filtration area before the membrane. The pre-filtration area is upstream of the membrane filter to reduce the particulate load on the filter and increase operating efficiency (Whatman, 2008).

The only sieve filter type tested is the nuclepore membrane filter, 25 mm and 47 mm, which was also used by Horowitz et al. (1996) and Hall et al. (1996). It is a polycarbonate membrane filter with high chemical resistance; high flow rates and is suitable for environmental samples. For tortuous path filters the Millipore membrane filters, 25 mm and 47 mm were tested and also used by Hall et al. (1996). The filters are made of cellulose acetate/nitrate, similar to Sartorius filters used by Horowitz et al. (1996) and Szabó et al. (2008).

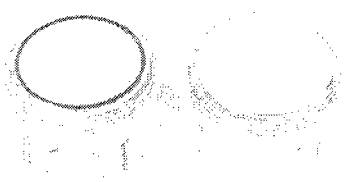

Figure 5-1: Sieve filter (Nuclepore) and tortuous path filter (Millipore) on the bottom half on the reusable filter casing

Figure 5-1 shows the Nuclepore (sieve) filter and the Millipore (tortuous path) filter moistened with water on the bottom half of the filter casing. The image illustrates the difference in thickness, as the thinner sieve filter is transparent compared to the thicker tortuous path filter.

Purabind membrane filters, 47mm, were the final type of filter tested. They are a high sterile diagnostic membrane filter, designed for lateral flow separations. Whatman has since modified these filters, and the Purabind filters used in this study are no longer available.

5.2.4 Filtration Set-up

Samples were drawn into a syringe (50 mL or 20 mL sterile syringe from NORM-JECT®, Germany) then mounted on a syringe pump. The syringe pump (KD Scientific 100, USA) was used to control the rate of filtration. The syringe pump was calibrated for accurate volume outputs, so the filtrate could be collected in small vials used for colorimetric orthophosphate determination. Consecutive aliquots of the filtrate were collected and reported as the volume through the filter (volume out). The first few aliquots (i.e. first mL and fifth mL) was collected in a volumetric flask (1 mL, 5 mL or 10 mL) and diluted to a volume of 10 mL for colorimetric orthophosphate analysis (minimum sample required for analysis).

5.2.5 Sample Analysis

After the samples were filtered, the filtrate was analyzed for orthophosphate colorimetrically. The modified Standard Method for ascorbic acid (4500-P. E.) as described in Chapter 4 and published in the Water Environment Federation Technical Conference and Exhibition proceedings 2008 (see Gilmore et al., 2008) was used for colorimetric phosphate determination. For determination of orthophosphate at concentrations greater than 0.01 mg P/L Standard Method 4500 P.E is followed using a

1 cm path length. For samples with lower concentrations of orthophosphate (0.001 to 0.01 mg P/L) a modified method was used with a 10 cm light path (see Chapter 4). Absorbance measurements were performed with an Ocean Optics (Sarasota, FL, USA) fiber optic spectrometer and the absorbance was measured at 650 nm. Light was passed from a tungsten halogen light source (Ocean Optics LS-1) through an optical fiber to a cuvette (1 cm or 10 cm) containing the sample. A second optical fiber transmitted the light signal to the detector (Ocean Optics QE5000).

Total iron was measured with a Perkin Elmer atomic absorption spectrometer (3100). The wavelength was set to 248.3 nm (recommended analytical line for Fe).

5.3 Results

By testing flow rate, type of membrane, filter diameter, and volume filtered, the goal was to design a protocol for separating dissolved and particulate fractions in the synthetic phosphorus and iron systems used to mimic very simple chemically mediated phosphorus removal in clean water. It is with these synthetic samples that the artifacts due to filtration clogging are most prominent. The lowest achievable orthophosphate concentration in the resulting filtrate is taken as the best representation of the dissolved fraction because it cannot be separated using filtration.

5.3.1 Flow Rate

Flow rate tests were performed using the 13 mm GMF GD/X filters. The hypothesis was that the residual phosphate concentration would be higher at slower flow rates since there would be fewer iron colloids blocking the filtered pores, therefore further binding phosphate on the surface of the filter. The fastest flow rate used in these tests, 500 mL/hour, is about half as fast as can be filtered by hand (without the syringe pump). Three flow rates, 500 mL/hour, 250 mL/hour, 50 mL/hour are compared in Figure 5-2, with residual orthophosphate concentration versus volume filtered.

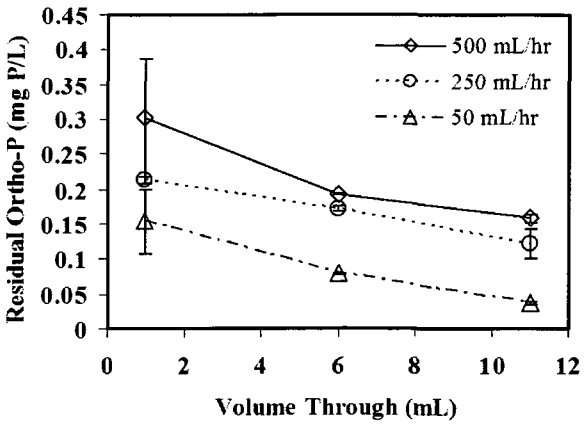

Figure 5-2: Flow rate comparison using 13 mm GMF GD/X filters. Syringe pump was used to control the rate.

In Figure 5-2, the volume dependence associated with filtering the synthetic samples of P is evident. Only volumes up to ~10 mL are reported for these filters, since that is all they are designed to filter (see Table 5-1). Examining the three flow rates tested, low flow rates tend to give lower residual phosphate concentrations and higher flow rates allow more phosphorus through the filter. The difference between filterable orthophosphate at 50 mL/hr compared to 500 mL/hour flow rates using these filters is almost doubled at each of the volumes reported in Figure 5-2 (1 mL, 6 mL, and 11 mL). At 11 mL there is almost an order of magnitude difference from 50 mL/hour where ortho-P is ~0.04 mg P/L to 500 mL/hour where ortho-P is ~0.2 mg P/L.

The result of this flow rate test differs from the expected results based on the report by Leppard (1992). Leppard (1992) suggested that filter-provoked aggregates would diminish with reduced flow rate. The observed trend of lower phosphate at low flow rate can be rationalized if the phosphate in the filtrate is predominantly associated with colloidal iron. Slow flow rates allow these tiny iron hydroxide particles to associate with the filter, but the kinetic energy at faster flow rates prevents the colloid-filtrate interactions and the colloid, along with associated phosphorus, passes through the filter.

Since the 13 mm GMF GD/X filters used for the flow rate test are only suitable for sample volumes less than 10 mL, the filters are not further considered. It is assumed that the same or similar trend of decreasing P concentration with decreasing flow rate, based on the mechanism above, is observed with the other filters described in Table 5-1.

To determine which flow rate is suitable for the filtration protocol, speed and efficiency were considered. At 50 mL/h, not even three replicates of a 10 mL sample can be filtered in an hour, and analysts would likely have multiple samples to filter and measure. The slower flow rates are not practical or efficient for daily experimentation because they are too time consuming. The flow rate selected for the filtration protocol presented here is 250 mL/hour since this rate produces reproducible low phosphate concentrations with reasonable efficiency. Larger sample volumes (>10 mL) will reach same residual P concentration as discussed in section 5.3.3.

5.3.1.1 Breakthrough of Filtrant

For all seven filters examined in this study, a breakthrough is seen after a certain volume of sample has been pushed through the filter. For initial aliquots of filtrate, the concentration of phosphate and iron in the filtrate decrease with volume filtered as is seen in Figure 5-2. However, after a volume of sample has been filtered (~30 mL for some filters, less for other) the residual orthophosphate and iron concentrations jump almost to the original starting concentration. This breakthrough is visible in plots discussed in the next section (Figure 5-3, Figure 5-4, and Figure 5-5) and can also been seen with the 13 mm GMF GD/X filters used for the flow rate tests show in Figure 5-2, when more than 10 mL are pushed through the filter (data not shown).

Breakthrough is a common phenomenon in filtration and has been illustrated recently by Kumar et al. (2008) for arsenate associated with iron oxide coated fibrous sorbents. Arsenate is very similar chemically to phosphate. The possibility that the filter is literally breaking is being ruled out since the trend happens in the various filters tested and consistently occurs at the same volume (for the filter being tested).

Eliminating the 13 mm GMF GD/X filter (because the volume capability is too small) from the seven initially compared in Table 5-1, there are six types of filters left to consider in developing a protocol. These six filters were used to filter synthetic samples at 250 mL/hr taking consecutive aliquots. The results are shown in Figure 5-3, with their respective breakthrough volumes clearly visible.

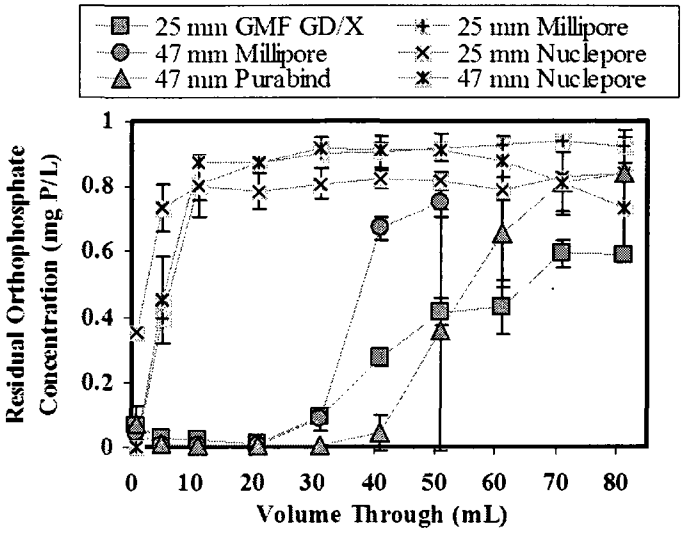

Figure 5-3: Comparison of all six filters tested plotted with residual phosphate versus volume filtered (volume through). Sample prepared with propeller mixer, pH 4

The filters shown in Figure 5-3 show two separate filter behaviors with respect to breakthrough. Three filters, two sieve filters (nuclepore) and the 25mm Millipore filter, show breakthrough after less than 10 mL is filtered (rapid breakthrough). The three other filters generate low orthophosphate concentrations in the filtrate before the breakthrough (high volume breakthrough). These are the 25 mm GMF GD/X syringe filters, 47 mm Millipore membrane filters and the 47 mm Purabind membrane filters, up to 30 mL filtered. Two filter behaviors, rapid breakthrough and high volume breakthrough will be considered separately.

5.3.2 Type of Filter

Each of the six filters shown in Figure 5-3 is considered in the following sections. Figure 5-4 shows the phosphate and total iron concentrations in the filtrate of samples filtered using 25 mm Millipore, 25 mm Nuclepore and 47 mm Nuclepore filters respectively. These three filter types give the highest concentrations passing through the filter.

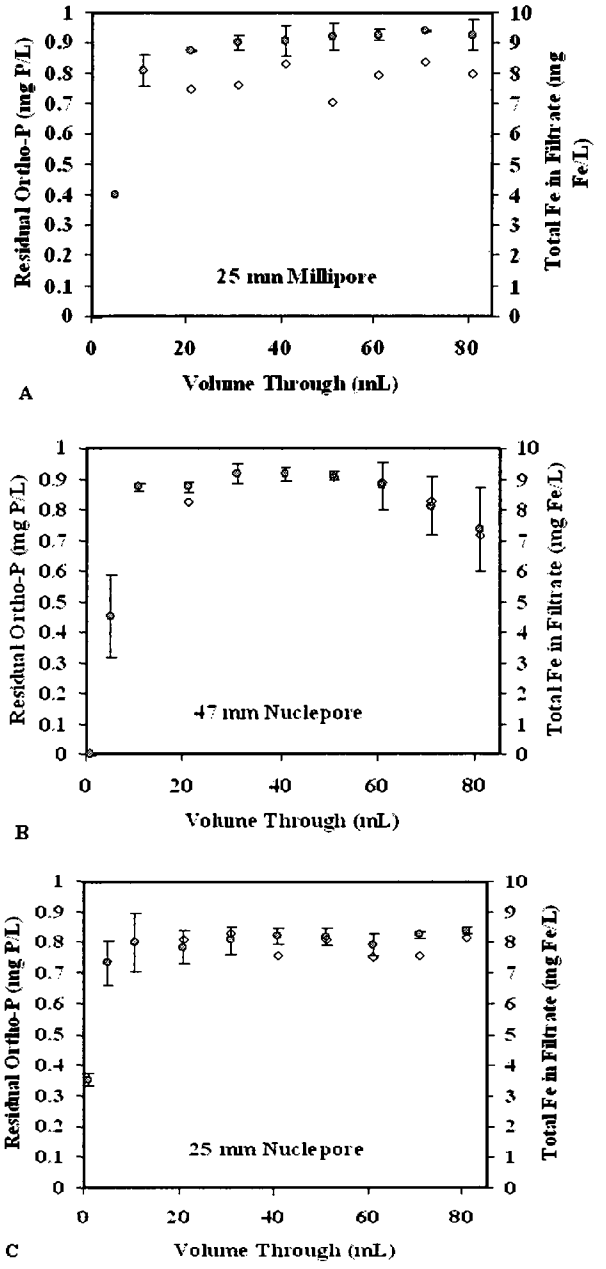

Figure 5-4: Residual orthophosphate (•) and total iron concentration (◊) in the filtrate using three different filters; A) 25 mm Millipore filters (tortuous path) and B) 25 mm and C) 47 mm Nuclepore sieve filters. The breakthrough happens for all three filters when less than 10mL has passed through the filter. Including the iron concentration in the filtrate in these plots, illustrates that the breakthrough allows both phosphorus and iron to pass through the filter almost to their original Fe, P concentrations (1 mg P/L and 10 mg Fe/L respectively).

In Figure 5-4, the three filters (two sieve filters) show breakthrough when less than 10 mL has passed through the filter. Showing the iron concentration across the range of volumes, illustrates that the breakthrough allows both phosphorus and iron to pass through the filter, such that the concentrations in the filtrate jump almost to the starting concentrations (1 mg P/L and 10 mg Fe/L) likely since P is associated with Fe colloids. It was expected that the sieve filters would clog faster than the tortuous path filters, which likely explains why the breakthrough happens quickly with the sieve filters. The tortuous path gives lower phosphate and iron concentrations in the filtrate, since more particulate matter is held up in the thicker filter, similar to results observed by Horowitz et al. (1992). The three filters (25 mm Millipore, 25 mm Nuclepore and 47 mm Nuclepore) shown in Figure 5-4 are not suitable for residual P determination because the aim is to estimate optimal separation of dissolved and particulate fractions.

Using the filters described in Figure 5-4 to achieve low phosphate concentrations, for example less than 0.5 mg P/L (50% removal), would require volumes less than 10 mL. The filters used to generate the data in Figure 5-5 are more suitable filters since they provide a larger window of sample volumes that reach low residual concentrations.

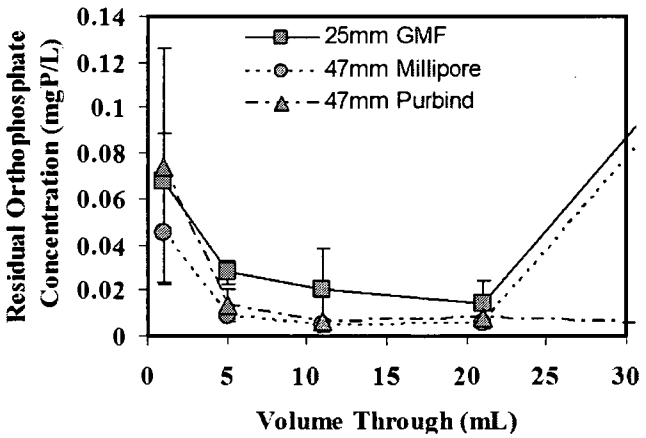

Figure 5-5: Residual orthophosphate concentration with volume filtered for the 25 mm GMF GD/X, 47 mm Millipore, and 47 mm Purabind filters. These filters do not show the breakthrough trend until after 20 or 30 mL of sample has been filtered.

The three filters shown in Figure 5-5 are considered tortuous path filters, and do not show breakthrough until ~30 mL has passed through the filter. Observing lower

concentrations in the filtrate when larger diameter (47mm versus 25mm) tortuous path filters are used is consistent with the trends observed by Hall et al. (1996).

Examining the results for the three filters plotted in Figure 5-5, the 47 mm Millipore filters vary the least in residual orthophosphate concentration with volume filtered, and are more reproducible, compared to the 25 mm GMF GD/X or 47 mm Purabind filters trial after trial. Although the 47 mm Purabind filter was able to give reproducibly low results, it did not stay intact when disassembling the filter holder, which is undesirable if it is of interest to examine the filter and associate particulate matter. Additionally, the Purabind filters have been modified since the start of the study, and the exact filters used here are no longer available.

5.3.3 Volume of Sample Filtered

Both the 25 mm GMF GD/X filter and the 47 mm Millipore filter are further considered in determining an appropriate volume to filter in establishing a filtration protocol. Setting a flow rate and type of filter to use will reduce the inconsistency due to filtration, but even from Figure 5-5 it is clear there is still some volume dependence when the flow rate is controlled and the large tortuous path filters are used. To further increase reproducibility in filtering the synthetic clean water samples (the special systems that show the most inconsistencies in filtration), a single volume of filtrate collected per filter is suggested. An appropriate volume of filtrate for colorimetric orthophosphate determination is 10 mL. At the chosen flow rate of 250 mL/hr, 10 mL of sample is reasonable. Moreover, approaching a volume near the breakthrough point is not desirable since standard deviations (error) would be large if repeated measurements show occasional breakthrough.

In a solution of pH~4 mixed in an Eberbach reciprocal shaker (Eberbach 6000, USA) for 24 hours, 10mL filtrate from the 25 mm GMF GD/X is 0.07±0.02 mg P/L (± standard error) after three replicates and 0.0036±0.005 mg P/L is achieved with the 47 mm Millipore filter. Similarly, a solution at pH ~6 shows less variability between the filters and excellent reproducibility when triplicates of 10 mL of filtrate are collected and measured. 0.051±0.002 and 0.047±0.002 mg P/L were recorded with the GMF GD/X and Millipore filters respectively. Since each of these measurements shows low standard

deviation, a sample volume of 10 mL (filtrate) is therefore suitable to increase reproducibility when filtering.

The replicate measures at 10 mL (filtrate) also showed lower orthophosphate concentration, and standard deviation is achievable with 47 mm Millipore filter over the 25 mm GMF GD/X filter. This agrees with the results presented in Figure 5-5, where over a range of volumes, the Millipore filter reaches lower orthophosphate concentration and has slightly smaller standard deviation than the GMF GD/X filers. The 47 mm Millipore membrane filters are therefore the filters of choice for simple, reproducible dissolved-particulate separations to achieve low phosphorus concentrations.

5.4 The Protocol

After testing the flow rate, volume of sample filtered and a variety of filters, a protocol for reproducible filtration of synthetic samples of phosphorus and iron has been created. The protocol is as follows

- 47 mm Millipore filter
- 250 mL/hr flow rate
- 10 mL of filtrate (volume out)

The protocol has been developed using synthetic samples prepared in ultra pure water at pH 4. Testing the protocol on natural water and wastewater samples will confirm if the protocol is widely applicable for reproducible dissolved-particulate separations and orthophosphate determination.

5.5 Testing the Protocol with Natural Water and Wastewater Samples

The "clean" water samples (synthetic samples prepared with ultrapure water) are the worst-case scenario for filtration because the smallest iron colloids are expected. Natural samples will have a more complicated matrix and the presence of inorganic and organic colloids help stabilize the colloids and allow large particles to form or aggregate (Pizarro et al. 1995). A protocol developed for filtration of the synthetic worst-case samples should be suitable for all samples. To test this, natural samples were collected and filtered across a range of volumes, but the flow rate was held constant (250mL/hr) and the 47 mm Millipore filter was used for all.

The first test was performed on river water samples taken near an effluent stream from the Preston Wastewater Treatment Plant in Cambridge, Ontario, Canada. The location of the sampling site is shown in Figure 3-3 (Chapter 3) along with the location of the three sample locations. The results are shown in Figure 5-6.

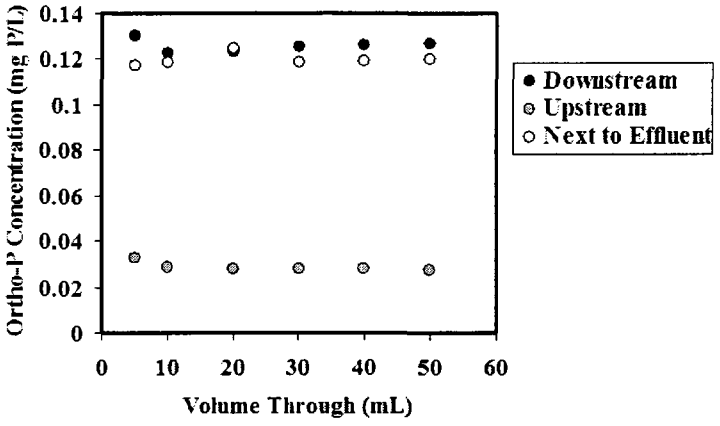

Figure 5-6: Samples from the Grand River, near a wastewater effluent stream, filtered following the filtration protocol. Three samples were collected, one upstream from where the effluent meets the Grand River, one downstream and one sample from the storm ditch the effluent flows directly into ("Next to Effluent"). Replicate measurements were not made.

The orthophosphate concentration is very constant across the range of volumes for all three samples collected. Replicate measurements of the orthophosphate concentration in the Grand River are compared with replicate measures of synthetic samples in Table 5-2.

Table 5-2: Comparison of replicate orthophosphate measurements in synthetic samples and natural river water sample

	Orthophosphate Concentration (mg P/L)	Standard Deviation (mg P/L)
Synthetic sample, pH~4	0.124	0.002
Synthetic sample, pH~6	0.0036	0.005
Grand River	0.047	0.002

Triplicate measures of orthophosphate concentration were made in the filtrate of synthetic Fe and P samples at pH 4 and 6 as well as a water sample from the Grand River,

downstream from a wastewater effluent. The results in Table 5-2 show the average orthophosphate concentration and the standard deviation associated with the measurement. The standard deviation is low for all three samples, indicating the filtration protocol is appropriate for synthetic pure water samples as well as natural water samples.

Groundwater and raw wastewater samples were obtained. The groundwater is from a shallow well in the riparian zone of the Beverly Swamp, at the John Mount field site, near Valens, Ontario. The raw wastewater is from a pilot plant at the New Hamburg water treatment plant in the Township of Wilmot. The result of filtering these samples is shown in Figure 5-7.

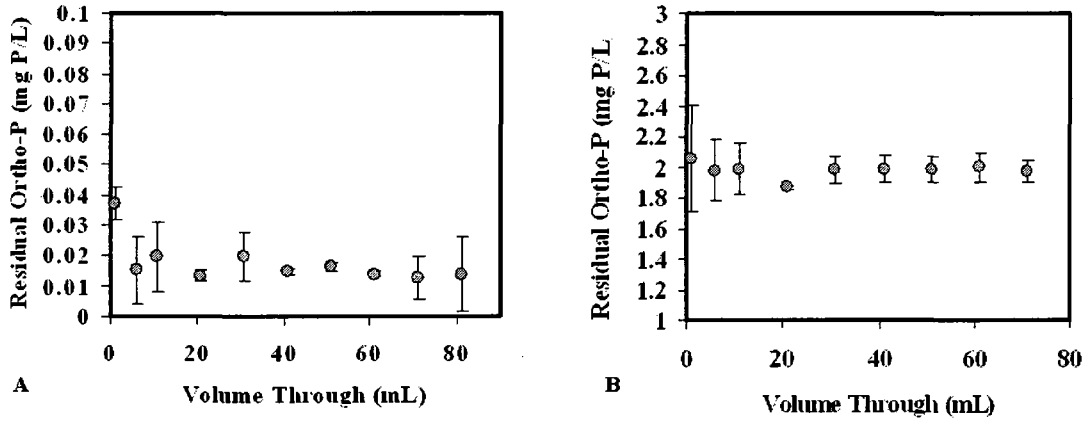

Figure 5-7: Testing the protocol in natural and wastewater samples. A) Groundwater sample B) Mixed Liquor from pilot treatment plant

Plot A in Figure 5-7 is the groundwater sample. The orthophosphate concentration is around 0.15 mg P/L. Plot B in Figure 5-7 is the sample of raw wastewater (mixed liquor). The orthophosphate in this untreated wastewater is much higher than in the groundwater or river water samples. The average orthophosphate concentration in this sample was around 2 mg P/L. The plots show almost no volume dependence across the range of 1 mL filtered to 80 mL filtered. Due to the dilution error associated with diluting the 1 mL and 5 mL samples to 10 mL for orthophosphate analysis, the error is slightly larger. Overall these plots indicate reproducibility in filtration and orthophosphate determination.

The reproducibility in filtering and measuring these natural samples illustrates that the filtration issues that have been presented here are a special case for the specific samples of phosphate, iron and Milli-Q water. It also demonstrates that the protocol designed to reduce the error associated with filtration of synthetic lab samples, is applicable in natural samples as well. The final test of the protocol was to see if the revised method improves lab-based sorption tests. Therefore, jar tests were designed to generate residual orthophosphate data across a range of pH, to compare with previously generated data. Figure 5-8 shows this comparison.

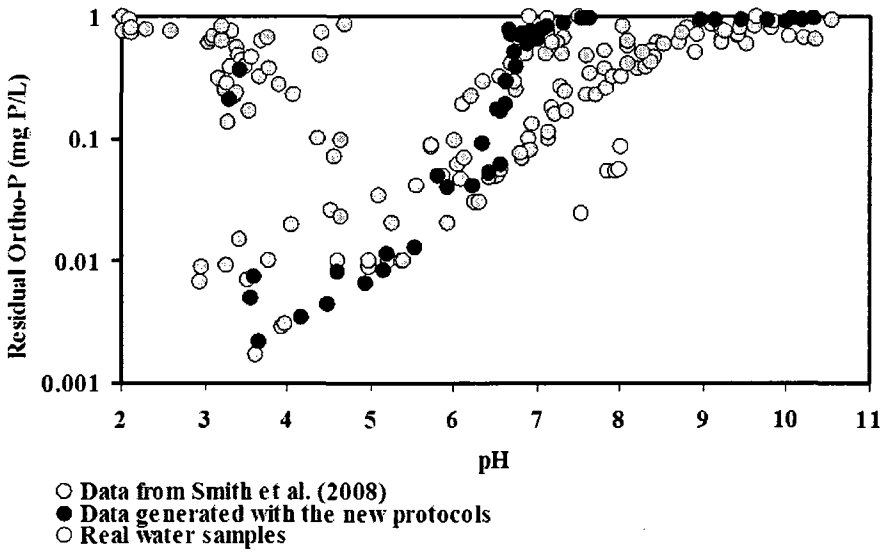

Figure 5-8: A comparison of data generated following the filtration protocol and the optimized method for low level orthophosphate analysis to data that was previously generated. The data generated before the development of these new protocols is shown in grey, and the new data generated with the filtration protocol and optimized colorimetric methods are shown in black. The samples were prepared with Milli-Q water, 1 mg P/L and 10 mg Fe/L, pH adjusted with 0.1M NaOH and shaken on a reciprocal shaker overnight (as described in Chapter 3). The data shown in open circles represent effluent collected from Cambridge, Ontario, Canada, treated in the same fashion as the laboratory created samples (i.e spiked to 1mg P/L and 10 mg Fe/L).

The data shown in grey in Figure 5-8 was measured before the filtration protocol was designed and also before the low level orthophosphate determination method was optimized (Chapter 4). The data above pH 5 has been published before by Smith et al. (2008) and illustrates a proof of principle of surface complexation modeling being used to explain chemically mediated phosphorus removal. The scatter in the data, especially

below pH 5 was suspected to be the result of inconsistent filtration and poor low level orthophosphate analysis. The data in black was generated following these new protocols and demonstrates that reproducible and consistent data can now be obtained for jar tests simulating chemical phosphorus removal. In particular, the reproducibility at low pH has been dramatically improved. The revised protocol gave reproducible data at higher pH values as well, but showing higher than expected residual phosphate. The residual phosphate measured at these circumneutral pH values do not agree with other experiments (Szabó et al., 2008) which were performed in tap water and raw effluent. It can be reasonably concluded that ultra pure water is not a good model media for wastewater.

To test more reasonable, wastewater-like media, open circles in Figure 5-8 represent measurements of water samples collected in Cambridge, Ontario, Canada. Phosphate was added so the final phosphate concentration was 1 mg P/L, and iron added to 10 mg Fe/L. These points show that lower phosphorus concentrations are achievable when more complex water chemistry is considered. Further consideration of water chemistry including water hardness is discussed in Chapter 6.

5.6 Conclusions

A filtration protocol for achieving reproducible low residual phosphate concentrations separating dissolved and particulate fractions was outlined. The suggested filtration rate is 250 mL/hour since reproducible residual concentrations are achieved in a reasonable amount of time. Faster rates result in higher residual orthophosphate concentrations and slower flow rates are inefficient (see Figure 5-2). The 47 mm Millipore membrane filter was determined to be the most reproducible in terms of residual orthophosphate concentrations resulting in the most consistent concentrations with varying sample volumes between 5 and 30 mL (see Figure 5-5). Testing the protocol on natural samples, with a more complicated matrix than the synthetic samples, indicates the volume dependence observed in the synthetic samples is less evident in the natural samples. Moreover, the protocol designed to overcome the inconsistent filtration of the synthetic lab samples is applicable to natural samples to obtain reproducible orthophosphate concentrations.

5.7 Acknowledgements

Thank you to all who helped collect samples. Sarah DePalma, Monique Robichaud, Rachael Diamond, Miranda Lewis, Merrin Macrae, Andrew Higgins, Wayne Parker.

Chapter 6

Application of a Factorial Design to Study Chemically Mediated Phosphorus Removal

6.1 Introduction

Chemically mediated phosphorus (P) removal, during wastewater treatment, is an effective means of reducing nutrients reaching sensitive environments. The addition of metal salts, typically iron or aluminum, results in coagulation reactions that remove soluble phosphorus. Although this method of treatment is widely used, the mechanism of removal is poorly understood.

Understanding the mechanism of removal is the first step to improving the treatment process, however being able to model the system is beneficial from an engineering perspective. With a model and detailed understanding of the chemical phosphorus removal mechanism, interactions with other areas of the treatment process can be studied. For example, treatment plants are moving towards using biological and chemical phosphorus removal in combination (de Haas et al., 2000), and in order to optimize this practice a detailed understanding and optimization of each process is needed.

The focus of this research is using iron (Fe(III)) for phosphorus removal, although aluminum interactions are thought to be similar (WEF, 1998; Szabó et al., 2008). Hydrous ferric oxides (HFO) are formed from the rapid hydrolysis of ferric iron (Dzombak and Morel, 1990), such as the addition of ferric chloride to wastewater. Phosphate is adsorbed to the surface of hydrated (Fe(III)) oxide (HFO) and also co-precipitates (Hammer and Hammer, 2001; Smith et al., 2008a). Co-precipitation is thought to be the predominant mechanism initially, responsible for initial rapid removal upon addition of the metal salt. Adsorption continues to bind phosphate for longer

periods of time (hours or days) (Szabó et al., 2008; Li and Stanforth, 2000). Further investigation on the kinetics of removal is still needed, including how the ratio of Fe/P and mixing intensity affects removal rates and final (equilibrium) values.

In wastewater treatment utilizing chemical P removal the iron dose is determined partly by the phosphorus in the influent and the regulations on effluent (required total phosphorus in effluent). The ratio of metal dosed to initial P (Me:P) is usually 1.5-2 to achieve 80-98% removal, but a molar dose closer to 5 is needed to get down to 0.01 mg P/L as total phosphorus (Szabó et al., 2008). Other factors such as mixing, affect the required dose. Ideally, the system is well mixed at the dosing point, however, mixing intensity is usually low (G = 20-100 s^{-1}) in treatment plants. Lab-scale experiments often employ a much higher mixing intensity, G = 300 to 1000 s^{-1} (Szabó et al., 2008). Szabó et al. (2008) varied mixing intensity in jar tests with tap water and found faster mixing, especially initially in the coagulation process, results in lower residual phosphorus concentrations. They report an equation (Equation (31)) relating residual phosphorus concentration to mixing intensity (G) at a given Fe: P molar ration based on their results.

$$P = 0.805e^{-0.006G} \tag{31}$$

In Equation (31) from Szabó et al. (2008) for an Fe:P molar ration of 1.8, P is residual soluble orthophosphate concentration in mg P/L and G is mixing intensity in s^{-1}.

The pH dependence of phosphorus removal is well studied, but remains an important consideration for further research since the process is very pH dependent. The optimal range for removal, as predicted by a semi-empirical equilibrium based model is pH 6.2-7 (Takács et al., 2006a). However, excellent removal (down to 1% of input phosphorus) is possible according to chemical equilibrium, surface complexation modeling and experimental observation at very low pH (between pH 4 and 6) (Smith et al., 2008b). Laboratory measurements and equilibrium based modeling by Smith et al. (2008a) confirm that phosphorus removal with iron is better at lower pH as shown in Figure 6-1.

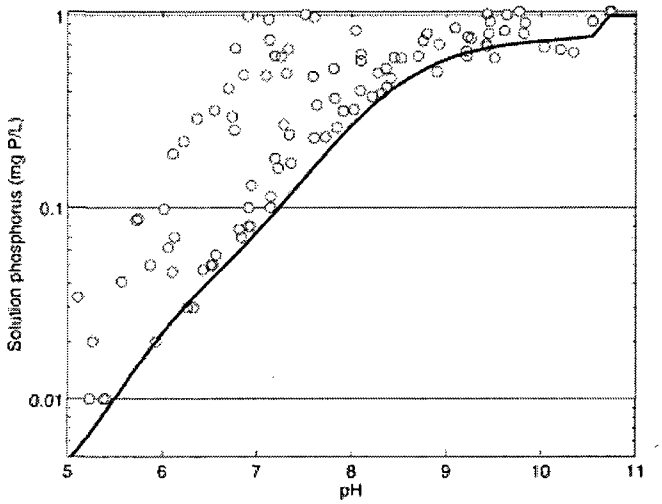

Figure 6-1: Residual phosphorus (orthophosphate) versus pH for experiments performed with 1 mg P/L initially and an iron dose of 10 mg Fe/L. Open circles are experimental results and the line is model predicted results from the Surface Complexation Model for phosphorus removal developed by Smith et al. (2008a).

The jar test used to generate the data in Figure 6-1 (open circles) were performed with 1 mg P/L and an iron dose of 10 mg Fe/L, in ultra pure water. It can be seen that the residual phosphorus after shaking the samples for 24 hours and measuring the orthophosphate concentration (after filtration) changes significantly with pH, where lower pH achieves better removal than high pH. Compare the difference in residual phosphorus at pH 6 and 8 for example; there is an order of magnitude difference; ~0.01mg P/L at pH 6 and ~0.3 mg P/L at pH 8.

At basic pH, the iron phosphate interactions are affected by the point of zero net charge. HFO has a point of zero charge in the range of 7.9-8.2 (Dzombak and Morel, 1990). Above the point of zero net charge adsorption is reduced due to electrostatic repulsion (negative solid and negatively charged phosphate) (Daou et al., 2007), however, adsorption interactions are present since the covalent bond between phosphate and the HFO surface forms inner sphere complexes. Inner sphere complexes, unlike outer sphere complexes, are not directly pH dependent. These surface electrostatic interactions will also play a significant role in the binding of other anions and cations to the surface of HFO (Stumm, 1992).

The wastewater matrix can also affect chemical P removal. Calcium and magnesium are examples of cations that are present in wastewater that could interact with HFO or phosphate. At high pH (>10), calcium in the form of lime, can be added for phosphorus removal. This technique is not typically employed at treatment plants due to the high dose required and the high pH (WEF, 1998). However, a study on using combinations of metal salt for P removal found that when a small amount of calcium (2 mmol/L) is added to chemical precipitation with aluminum or iron, a broader pH range of optimal removal is achieved (Hsu, 1973). Fettig et al. (1990) found similar results where below pH 5 a mixed phosphate, Fe(III) and calcium precipitate forms, and above pH 6.8 calcium phosphate alone precipitates (when ortho-P concentrations are greater than
0.5 mol/L). For wastewater treatment this indicates the presence of calcium could aid in achieving lower residual phosphorus in the effluent.

Magnesium in wastewater can also precipitate phosphate as struvite ($MgHN_4PO_4 \cdot 6H_2O$) when ammonium ions are also present in reducing conditions (WEF, 1998). Magnesium forms stronger phosphate complexes than calcium; however iron (III) complexes are stronger than both calcium and magnesium (Jenkins et al., 1971). The presence of magnesium also affects calcium phosphate precipitations such that beta-tricalcium phosphate will precipitate instead of apatite (Jenkins et al., 1971). Peng et al. (2007) also concluded that magnesium and organic acids may inhibit Ca-P precipitation due to the insignificant Ca-P precipitation they observed at high pH.

Modelling of chemically mediated phosphorus removal is currently based on equilibrium chemistry. Without a kinetic portion to describe P removal, the current model does not accurately simulate reality. Wastewater treatment is a dynamic, multi-step process and needs to take reaction rates into account when simulating the process. Aside from observing an initial rapid removal likely due to co-precipitation and a slower removal for hours for days, likely due to adsorption, very little is known about the kinetics of these processes. Kinetic experiments and modeling have been performed for other areas of the wastewater treatment process. The kinetics of struvite precipitation and biological P removal has been examined. Researchers (Quintana et al. (2005); Rahaman

et al., 2008; Ohlinger, 2000) have been able to determine rate constants for the removal of phosphorus by struvite precipitation following first order kinetics.

The current equilibrium based model needs to consider kinetic factors. Additionally, mixing intensity and a more realistic wastewater matrix including alkalinity, calcium and magnesium, needs to be considered. To improve our understanding of chemically mediated phosphorus removal and prepare to model the process for integration into whole plant modeling software a factorial design is used to study the relationship between factors likely to affect P removal. A 2^4 factorial design will allow two reasonable extremes of four major factors to be studied simultaneously. Statistical analysis will give insight into the process of chemical P removal and point to areas of focus needed to better model the process.

The objectives of the following study are to therefore improve the understanding of chemically mediated phosphorus removal with respect to iron dose, pH, mixing intensity and water hardness. The knowledge gained from this lab scale study will provide necessary knowledge to improve the modeling of this nutrient removal process and direct future experimental studies.

6.2 Experimental

6.2.1 Experimental Set up

Laboratory experiments were set up to control the pH of a 3L solution of simple synthetic wastewater spiked with 1 mg P/L. The solution was mixed with a propeller mixer (three paddles) connected to a motor (Talboys Instruments Corp., BODINE motor, model 102), such that the rotation of the paddle was at 75 or 500 rpm (see calculation of mixing intensity section 6.2.4). The solution was dosed with iron ($FeCl_3$) which signified the start of the experiment (time zero). Samples were drawn, using a syringe, from the 3L solution to be filtered immediately and measured for orthophosphate. The total volume of sub-samples removed did not exceed 10% of the total solution volume. An average of ten samples were taken between 1 min and 6 hours after starting (dosing the iron), and three more samples around 24 hrs of mixing.

6.2.2 Orthophosphate Analysis

Orthophosphate was measured in the filtrate of the sub-samples. The details on a filtration protocol designed for filtration of these specific sample types is outlined in the WEFTEC 2008 Conference proceedings (see Gilmore et al., 2008) and also in Chapter 5 of this thesis. Essentially, syringe filtration using a 0.45 μm filter from Millipore, where only the first 10mL of filtrate is considered and the flow rate of filtration is controlled at 250 mL/hour. Orthophosphate is determined colorimetrically following the Standard Method 4500-P. E. (Standard Method, 1998) with a 1 cm path length or the modified colorimetric method for low level analysis using a 10 cm path length (Gilmore et al., 2008).

6.2.3 Equipment and Materials

Phosphate was spiked from a stock solution (1000 mg P/L) prepared from $Na_3PO_4 \cdot 12H_2O$, from Fischer Scientific, New Jersey, USA. The stock solution for dosing iron was prepared from ferric chloride salt ($FeCl_3 \cdot 6H_2O$ Fluka, Switzerland). The pH was adjusted with 0.1 M NaOH (Sigma Aldrich, St. Louis, NJ, USA) and 0.2 M H_2SO_4 (95-98% pure, Sigma Aldrich, St. Louis, MO, USA).

The pH of the solution was held constant (±0.1) using an automatic titrator system with half cell pH electrodes from Thermo Scientific. The pH meter, a Dual pH meter and Titrimeter (model 9501) and buret (dispenser 8901-5/16a mod. 93) are from Tanager Scientific Systems Inc.

6.2.3.1 Synthetic Hard and Soft Water

Synthetic fresh water was prepared following guidelines from Environment Canada (1990). The hard water is intended to have a final hardness between 160 and 180 mg/L as $CaCO_3$ and the soft water between 40-48 mg/L as $CaCO_3$. Sodium Bicarbonate, $NaHCO_3$ was obtained from EMD Chemicals Inc., Gibbstown, N.J. USA and calcium sulfate dehydrate, $CaSO_4 \cdot 2H_2O$, magnesium sulfate heptahydrate, $MgSO_4 \cdot 7H_2O$ and potassium chloride, KCl were obtained from Sigma Aldrich, St. Louis Mo., USA. 1000 mg/L stocks solutions of each of the four reagents were prepared by dissolving appropriate quantities of the salt in Milli-Q water (18.2 MΩ, Milli-Q).

6.2.4 Calculating Mixing Intensity

The mean velocity gradient (G) was calculated following equation by Camp and Stein (1943)

$$G = \sqrt{\frac{P}{V \cdot \mu}} \tag{32}$$

where P is power dissipated in the water, V is the volume of the suspension and μ is the dynamic viscosity. The calculation for P is adapted from Svarovsky (2000) and shown as an expanded expression for mean velocity gradient in Equation (33).

$$G = \sqrt{\frac{C_D A_p \rho (V_p - V)^3}{2V\mu}} \tag{33}$$

In this expression (Equation (33)), C_D is a drag coefficient, A_p is the projected area of the paddles, ρ is density, $(V_p\text{-}V)$ is the relative velocity between the paddle (V_p) and the fluid. C_D is assumed to be 1.2 and viscosity and density of pure water were used (detailed calculations are shown in the Appendix).

6.2.5 Experimental Design

A 2^4 factorial design was used in this study. Experiments were performed in random order, only once. The four factors are iron dose, pH, mixing and water hardness. Reasonable values corresponding to high (+) and low (-) points for each factor were chosen based on the literature reviewed and previous experiments. The high and low values are listed for each factor in Table 6-1.

Table 6-1: Factors and levels used in the factorial design

Factor	Low (-)	High (+)
Iron dose (mg Fe/L)	5	10
pH	6	8
Mixing intensity, G (s^{-1})	23.5	376.0
Water Hardness (mg/L as $CaCO_3$)	~44	~170

6.2.6 Qualitative Comparisons

The data collected from 16 experiments can be presented in numerous ways. The following sections review qualitative comparisons of the data over the 24 hour period each experiment was performed.

6.2.6.1 Iron Dose

A visual comparison of the effect of dose is shown in Figure 6-2. In each of the graphs, two experiments are plotted, where only the dosing differs; all other experimental conditions are constant. A variety of experimental conditions are covered with the four plots in Figure 6-2. The four plots illustrate that the experiments performed with a higher dose of iron (10 mg Fe/L in black squares) reach a lower orthophosphate concentration in the filtrate. As expected, a higher dose removes more phosphate. After 24 hours, the low dose (5 mg Fe/L for 1 mg P/L), shown in open squares in Figure 6-2, still removes between 70% and 90% of the phosphorus depending on the other experimental conditions. It is interesting also to note that the relationship between iron dosed and phosphorus removed is not linear. Twice the dose (5 mg Fe/L to 10 mg Fe/L) results in an order of magnitude difference in residual phosphorus, both initially and after the equilibration period (24 hours).

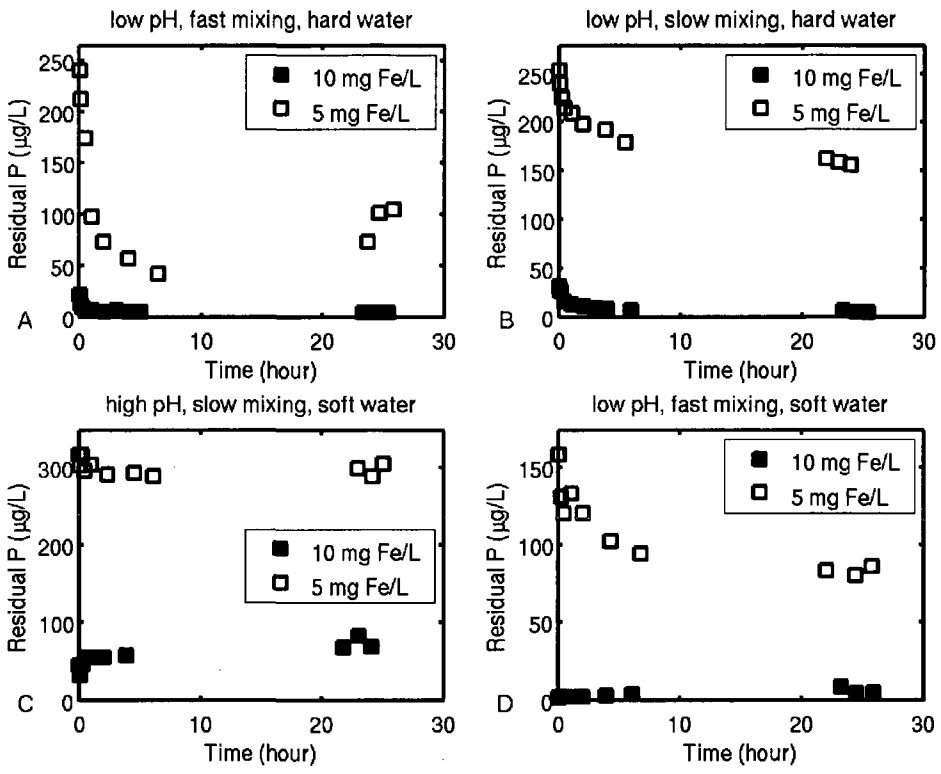

Figure 6-2: Comparing the effect of dose on residual phosphorus. Initial phosphorus was 1 mg P/L. An iron dose of 10 mg Fe/L is shown in black squares and a dose of 5 mg Fe/L is shown with open squares.

6.2.6.2 Solution pH

The comparison of the effect of high (pH 8) and low (pH 6) pH, shown in Figure 6-3 shows that low pH is able to reach a lower residual phosphorus level than high pH. This was expected from previous experiments as shown in Figure 6-1, due to the nature of the phosphorus and iron species at acidic pH, there is an attraction between the positive iron species and the negatively charged solution phosphorus species.

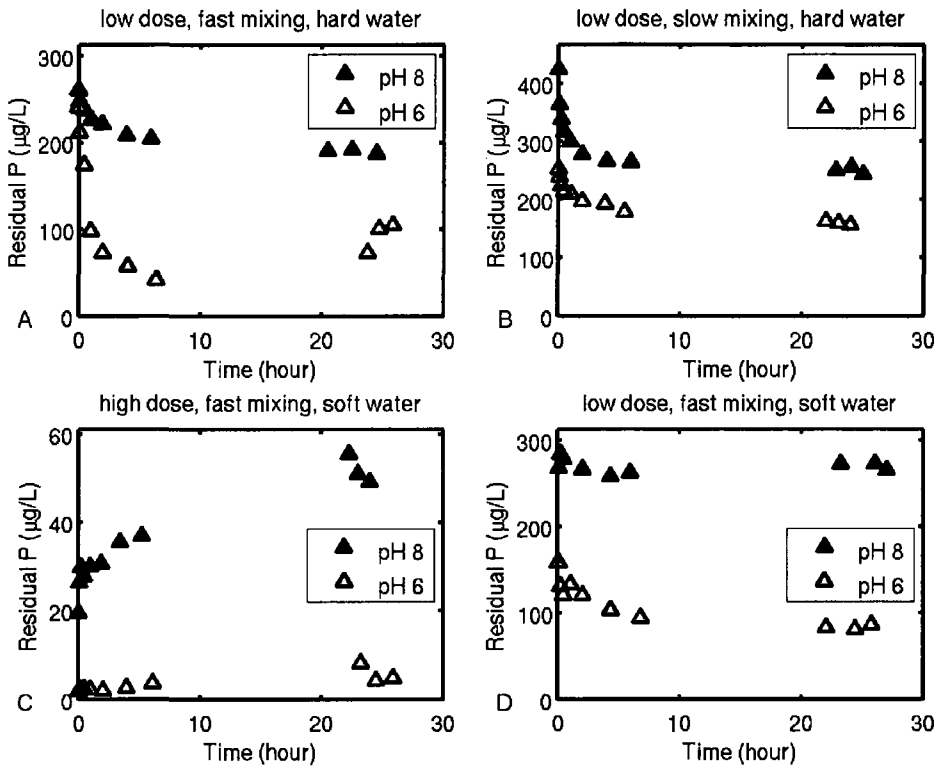

Figure 6-3: Comparison of the effect of pH. High pH experiments were performed at pH 8 (shown in black triangles) and low pH experiments were performed at pH 6 (open triangles).

In Figure 6-3-A initially, the residual phosphorus level is similar for the experiments performed at pH 8 and pH 6. However, after the 24 hour equilibration period, the residual P concentration stabilizes at different levels, lower for the experiments performed at pH 6. The other three plots in Figure 6-3 (B-D) do not show this trend. After the initial rapid removal, likely due to co-precipitation of the phosphorus and iron, the experiments performed and pH 6 and pH 8 are at different residual phosphorus levels.

6.2.6.3 Mixing Intensity

The initial hypothesis in terms of mixing intensity was that faster mixing will result in better phosphorus removal because it keeps the iron colloids sufficiently small to allow more surface area for P sorption. The data comparing the effect of mixing intensity, shown in the four plots in Figure 6-4, does support this hypothesis. The plots (A-D)

demonstrate that faster mixing gets to lower residual phosphorus concentrations than slower mixing.

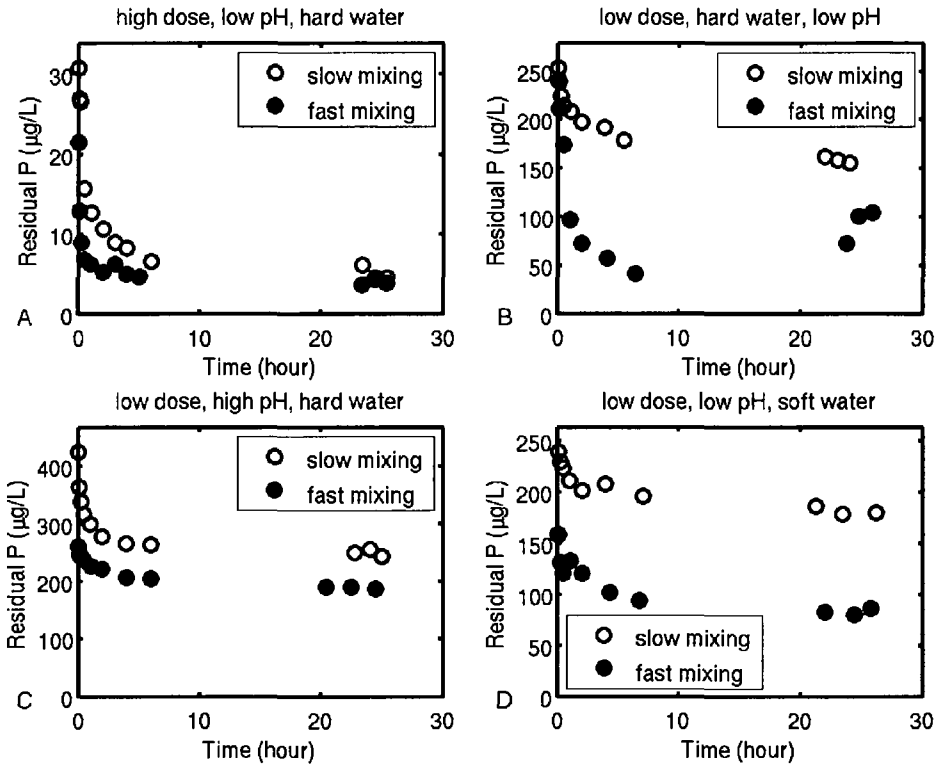

Figure 6-4: Comparison of the effect of mixing intensity on residual phosphorus removal. Each plot (A-D) compares two experiments where all variables are the same except mixing intensity. High mixing intensity or "fast mixing" (G=376 s^{-1}) is shown in black dots and low mixing intensity of "slow mixing" (G=23.5 s^{-1}) is shown in open circles.

In plots A and B of Figure 6-4, it is evident that the difference in residual P as a result of mixing intensity is more pronounced after a period of a few hours. Initially, the removal that is likely due to co-precipitation results in similar residual P concentration regardless of mixing intensity. However, after the samples have been mixing for a few hours, the difference in residual P, as a result of mixing intensity, increases. The mechanism of removal after a few hours (up to days according to Szabó et al. (2008)) of mixing is likely due to adsorption, and as a result, mixing plays an instrumental role. More intense mixing will keep the iron flocs small and provide more surface area for P to adsorb. Although this is an interesting observation, it is inconsistent between all mixing

experiments. In plots C and D of Figure 6-4, for example, the different mixing intensity result in different residual phosphorus levels both initially and over time.

The results for mixing intensity can also be compared to the work done by Szabó et al. (2008) through the equation (Equation (31)) developed relating mixing intensity (G) to residual P based on their jar test data (shown in Chapter 2, Figure 2-9). The predicted residual P based on Equation (31) using the fast mixing intensity from this project is 80 μg P/L. The data in Figure 6-4, plot B shows this residual P (80 μg P/L) from fast mixing (black circles) within the first few hours of mixing (~2-3 hours). In plot D, the residual P concentration from fast mixing is around 80 μg P/L after 24 hours. The predicted residual P from Equation (31) at fast mixing is 700 μgP/L. From the plots in Figure 6-4, residual P is never recorded to be this high. The first sample measured is around 1 minute after the addition of iron, where P concentration are around 30-450 μg P/L. Therefore in this project, a residual P of 700 μgP/L could only be observed less than a minute after the addition of iron.

The experiments performed by Szabó et al. (2008) to derive Equation (31) were performed at lower doses than are used in this project. As a molar dose, Szabó used 1.8 (Fe/P) and the low dose in this project is a molar dose of 2.5 (Fe/P). Additionally, the water hardness and exact pH of the experiments Szabó et al. (2008) performed is not reported. This could explain why there is only a weak correlation between the equation-predicted P based on the work Szabó et al. (2008) and the residual P concentration observed in this project.

6.2.6.4 Water Hardness

The effect of hard and soft water (presence of calcium and magnesium) on P removal is not as significant as the other factors tested, but it is clear water hardness affects P removal. A comparison of experiments done in hard water versus soft water is made in four plots shown in Figure 6-5

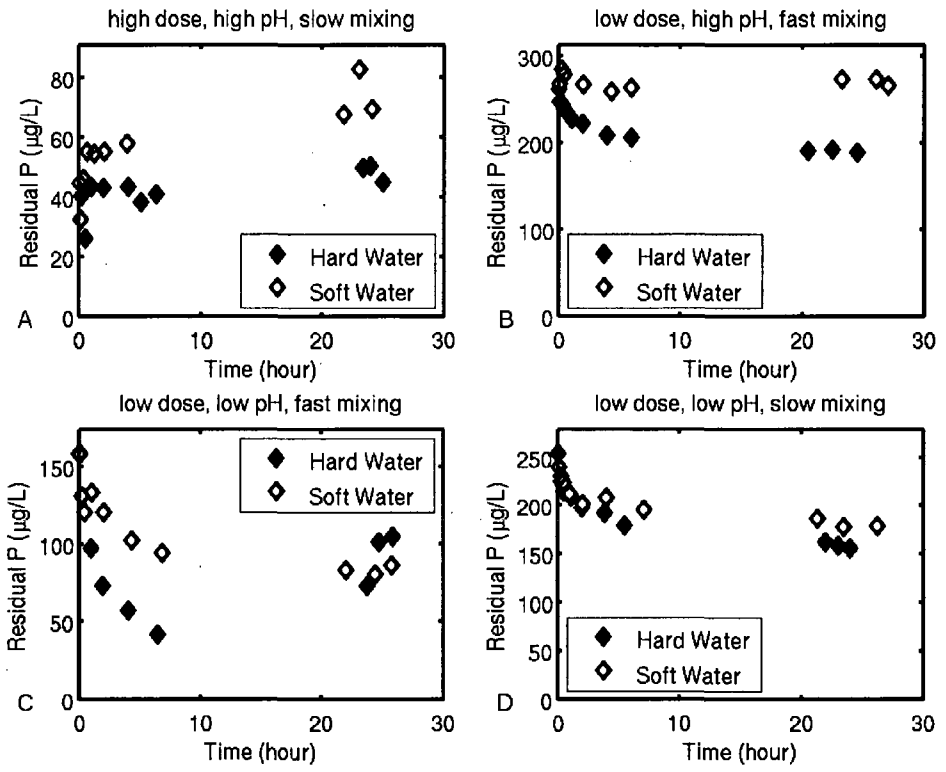

Figure 6-5: Comparison of the effect of water hardness. Experiments performed in hard water (~170 mg/L as $CaCO_3$) are shown in black diamonds and experiments performed in soft water (~44 mg/L as $CaCO_3$) are shown in open diamonds.

The four plots (Figure 6-5) show that experiments performed in hard water reach a lower residual orthophosphate concentration than experiments performed in soft water. This indicates that calcium and magnesium ions, present in higher concentration in hard water, aid in the removal process. Similar to the comparisons on the effect of mixing, the difference in residual P due to water hardness is more prominent after a few hours of mixing. Initially the residual P is at a similar concentration for experiments performed in either hard or soft water. The interpretation from this is that the interaction of calcium and magnesium ions is more significant during the adsorption processes than during the co-precipitation process that observed initially. This could be a result of calcium phosphate precipitations aiding to remove phosphate from solution (Rietra et al., 2001; Carlson et al., 1997) as a mixed calcium phosphate precipitate forming above pH 6.8 (Fettig et al., 1990). But that could only describe the mechanism at high pH. Another

possible mechanism for the presence of calcium aiding in P removal during adsorption is the formation of calcium carbonate to act as a seed for HFO formation and nucleation (Fettig et al., 1990). With increased amounts of HFO, P can adsorb to the surface to be removed as a precipitate.

The effect of water hardness is further observed when all the factors are plotted simultaneously, as is done in Figure 6-6.

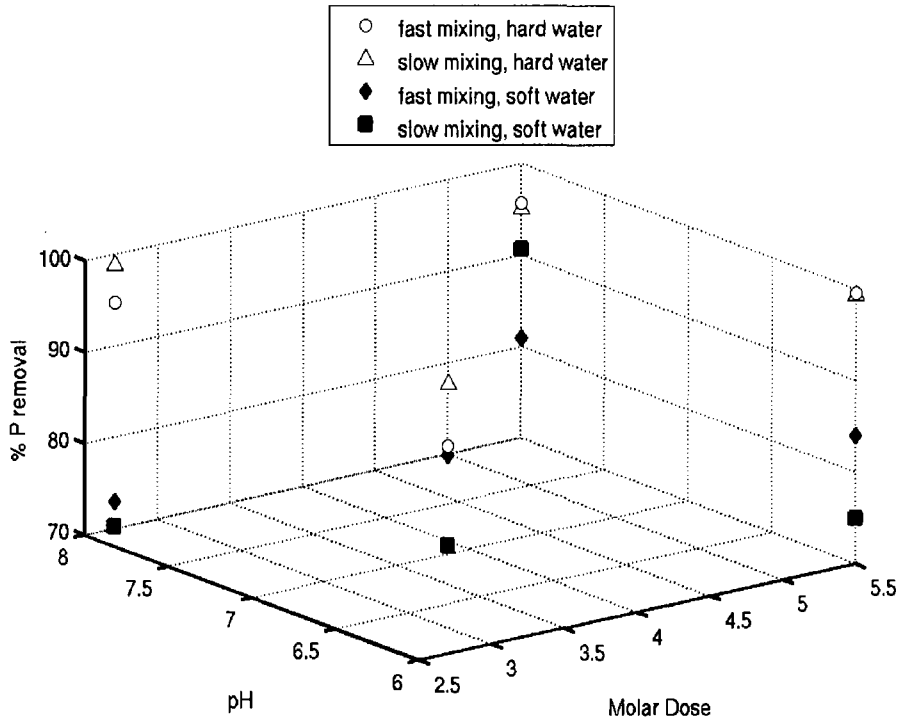

Figure 6-6: All four factors represented in one plot. The analytical response is expressed as percent P removed (on the z-axis). The average of the 'equilibrium P numbers' was used here (22-26 hours of mixing). pH and molar dose are on the x- and y-axis respectively, and mixing intensity and water hardness are expressed with various data points. The black points are soft water experiments and the open points are hard water experiments.

To plot all four factors simultaneously, the analytical response is simply the average of the equilibrium P concentration (average P after 22-26 hours of mixing). In Figure 6-6, this is represented as percent P removed (on the z-axis). pH and molar dose are on the x- and y-axis and mixing intensity and water hardness are represented with the various data points. The hard water experiments are shown in open symbols in Figure 6-6, while the soft water experiments are shown with black symbols. Because there are only two

variables for each factor, for example only two options for molar dose and two options for pH, the data points are stacked in four locations on the plot. The information this plot presents is that all the experiments performed in hard water (open points) are above (higher % P removal) than all the experiments done in soft water (black points). This further illustrates that although the effect of water hardness on P removal is less significant than the other effects, experiments performed in hard water remove more phosphorus than experiments performed in soft water.

6.2.7 Statistical Analysis

The factorial design used to understand chemically mediated phosphorus removal in a lab setting, considered four factors, dose, pH, mixing intensity and water chemistry, with residual orthophosphate concentration as the analytical response. Statistical analysis was performed, in Statistical Analysis Systems software (SAS Institute Inc., Cary, NC, USA), using the average orthophosphate concentration after mixing for 22-26 hours (after 24 hours the system is assumed to be in equilibrium). This data is shown in Table 6-2.

Table 6-2: Summary of the equilibrium P values for each of the 16 experiments. The average is taken from the three or four orthophosphate concentrations (± standard error) determined around 24hrs. The last column is the average time corresponding to the average P concentration.

Experiment #	Average "equilibrium" P (mg P/L)	Average Time (hrs)
1	0.0424 ± 0.0005	21.45
2	0.048 ± 0.001	24.14
3	0.0051 ± 0.0003	24.42
4	0.004 ± 0.002	24.42
5	0.1900 ± 0.0006	22.50
6	0.093 ± 0.006	24.79
7	0.250 ± 0.002	23.96
8	0.159 ± 0.001	23.00
9	0.052 ± 0.001	23.11
10	0.073 ± 0.003	23.03
11	0.011 ± 0.004	22.85
12	0.0044 ± 0.0002	25.24
13	0.2699 ± 0.001	25.46
14	0.0832 ± 0.0009	24.08
15	0.298 ± 0.003	24.10
16	0.181 ± 0.001	23.69

The standard error in Table 6-2, is determined from the average of the three or four equilibrium values used to calculate the average equilibrium P. Replicate experiments were not performed. Due to the lack of replicate experiments, standard error for the factorial analysis was calculated using the three and four-way interactions. The three and four way interactions were determined to be insignificant, since plots for three-way interactions show no obvious interaction, which validates the assumption for the error calculation. The main effects and the two-way interacting effects are shown in Table 6-3

Table 6-3: Main effects and two way interactions of the factorial design

Effect	*F* ratio	*p* value
Dose	321.71	<0.0001*
pH	90.86	0.0002*
Mixing	16.07	0.0102*
Water Hardness	6.46	0.0517
Dose and pH	17.49	0.0086*
Dose and Mixing	9.18	0.0291*
Dose and Water Hardness	1.93	0.2229
pH and Mixing	0.65	0.4565
pH and Water Hardness	4.03	0.1008
Mixing and Water Hardness	0.09	0.7775

*values are significant at $p<0.05$

Dose, pH, and mixing are significant parameters, and water hardness did not show a significant effect (at $p<0.05$) under the conditions tested. This correlates with the visual analyses done in section 6.2.6. Visually there appeared to be an effect of water hardness, although not as significant as the other factors. Statistically, the effect of water hardness is not significant at a 95% confidence interval (see Table 6-3), but would be considered significant at a 94% confidence interval, for example.

Significant two-way interactions are also highlighted in Table 6-3. Two factor interactions between dose and pH as well as dose and mixing are significant (at $p<0.05$). Plots of the significant two way interactions are shown in Figure 6-7.

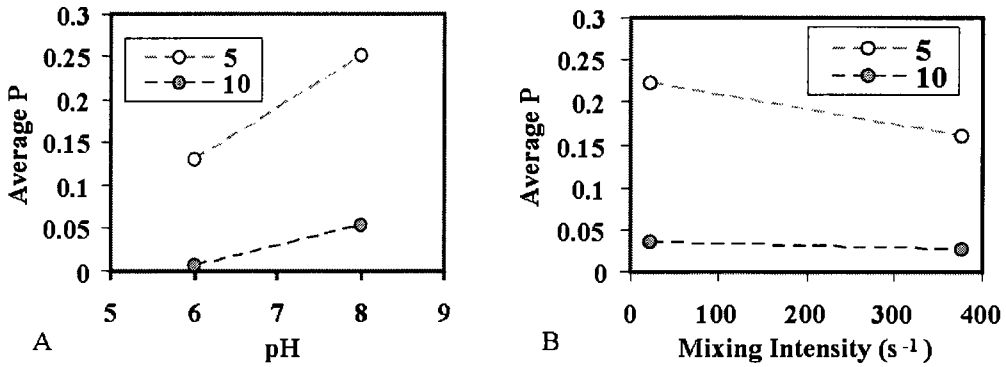

Figure 6-7: Significant two way interactions. A) Dose by pH. B) Dose by mixing intensity. A dose of 5 mg Fe/L is shown in open circles and a dose of 10 mg Fe/L is shown in shaded circles

Plotting the data this way better illustrates the interactions. For example, in Figure 6-7-A, it is clear that at a lower dose, pH has a greater effect. Similarly, in Figure 6-7-B at the lower dose, mixing has a greater effect.

Since the statistical analysis has identified significant two way interaction, studying the main effect alone becomes irrelevant. This has implications for modeling, such that variables will need to be considered together.

6.2.8 Kinetics

Since very little is actually known about the kinetics of chemically mediated phosphorus removal, determining rates of reactions and rate constants would be greatly beneficial from a modeling perspective. Research on struvite precipitation kinetics found the reactions fit a first order model, however kinetic constants appear to be higher in real wastewater compared to synthetic liquor (Rahaman et al., 2008). Moreover, the reaction rate constant that were determined for struvite precipitation changed with mixing intensity (Rahaman et al., 2008). It is expected that modeling chemical phosphorus removal with iron would show similar trends.

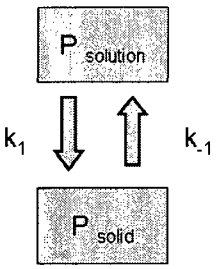

Figure 6-8: Representation of the forward and reverse reactions to P precipitation and dissolution

The residual orthophosphate concentration over time provides the foundation for determining rate constants. Since the system is approaching equilibrium, both the forward and reverse reactions need to be considered (Morel and Herring, 1993). Figure 6-8 shows a visual representation of the forward and reverse reactions for P removal. A first order reaction with respect to phosphorus removed (forward reaction) and phosphorus back into solution (reverse reaction) was assumed.

Rate constants were determined using non-linear regression analysis. The initial rapid P removal due to co-precipitation was assumed to be instantaneous. A P_o value (initial P) was determined as the P concentration after co-precipitation. Figure 6-9 shows two examples of the curves that were fit to data.

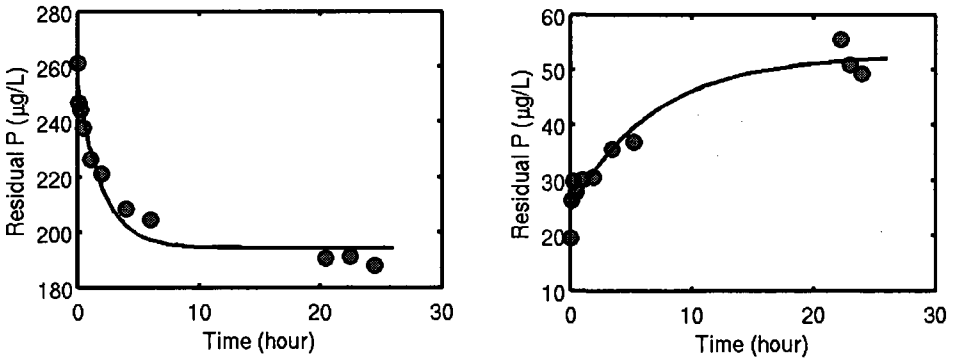

Figure 6-9: An example of the curves fit to the data to determine rate constants for the reaction.

From the curves fit to the data (as shown in Figure 6-9) and the initial phosphorus concentration, P_o (after co-precipitation) and rate constants were determined for a forward (k_1) and reverse reaction (k_{-1}) assuming a first order reaction. The forward reaction is solution phosphate to solid phosphate (k_1) and the reverse reaction is solid phosphate to solution phosphate (k_{-1}) (see Figure 6-8). A first order rate matrix can be

created to represented the kinetic equations and allow integration of the rate equations to obtain rate expressions for the reacting species (Pogliani et al., 1996). The reaction represented in Figure 6-8 can be expressed simply with A as the reactant ($P_{solution}$) and B as the products (P_{solid}).

$$A \underset{k_{21}}{\overset{k_{12}}{\rightleftharpoons}} B \tag{34}$$

The rate matrix (**K**) will be a 2x2 matrix as shown below:

$$\begin{bmatrix} -k_{12} & k_{21} \\ k_{12} & -k_{21} \end{bmatrix} = K \tag{35}$$

The eigenvalues (λ) and eigenvectors (ψ) are determined using Matlab (see script in Appendix). The diagonal matrix, exp(Λt), can be defined as follows (Equation (36)):

$$\exp(\Lambda t) = \begin{bmatrix} \exp(\lambda_1)t & 0 \\ 0 & \exp(\lambda_2)t \end{bmatrix} \tag{36}$$

At each time (t), concentrations of A and B can be determined using Equation ((37)).

$$\begin{aligned} A(t) &= \psi \exp(\Lambda t)\psi^{-1} A_0 \\ B(t) &= \psi \exp(\Lambda t)\psi^{-1} B_0 \end{aligned} \tag{37}$$

Alternatively, the integrated rate laws as written in Equations (38) and (39) (Pogliani et al., 1996) relate concentrations of A and B to initial concentration (A_0 and B_0) and the rate constants (k).

$$A = \frac{A_o}{k}\left[k_{21} + k_{12}\exp(-kt)\right] + B_o \frac{k_{21}}{k}[1 - \exp(-kt)] \tag{38}$$

$$B = \frac{B_0}{k}[k_{12} + k_{21}\exp(-kt)] + A_0 \frac{k_{12}}{k}[1 - \exp(-kt)] \tag{39}$$

where t is time and k is k_1/k_2. A_0 is the initial concentration, expressed at P_0 for the amount of phosphorus in solution after the initial rapid removal due to co-precipitation. B_0 would be the initial amount of precipitate which is assumed to be zero.

Rates of the forward (k_1) and reverse reactions (k_{-1}) were determined for all 16 experiments. The rates for the forward reaction ($P_{solution} \rightarrow P_{solid}$) ranged from 45.75 µg/L·hr to 1375.92 µg/L·hr. The rates for the reverse reaction ($P_{solid} \rightarrow P_{solution}$) were all significantly less than the forward reactions, as expected. The rates for the reverse reaction ranged from 0.5 µg/L·hr to 459.71 µg/L·hr. The rate of the reverse reactions are

all less than 40% of the rate of the forward reactions and 10 of the 16 experiments showed the reverse rate less than 10% of the forward rate.

The large range of rate constants determined for the 16 different experiments performed indicates that modeling the kinetics of the process of chemical phosphorus removal will not be straight forward. Had one rate constant been determined, or there was a visible trend in the rate constants compared to the variables tested, modeling the process would be significantly simpler than what these results suggest. No conclusions could be made about trends in the rate constants determined with respect to the factors tested. Further investigation of the kinetics of chemically mediated phosphorus removal with iron is still needed.

6.2.9 Comparison to the Surface Complexation Model

The surface complexation model for chemical phosphorus removal developed by Smith et al. (2008a) predicts residual phosphorus based inputs of iron dose, pH and an active site factor (ASF). The active site factor is the key modelling parameter that will be used to varying mixing intensity to compare to the data from this project. The model and the ASF are described in more detail in Chapter 2 (section 2.4.3.3). Smith et al. (2008a) describe the derivation of reasonable ASF values for the Fe-O-P system, where a value of 1.18 would be suitable for a well mixed system and 0.31 for a poorly mixed system. The theoretical limit is 6, since ASF is describing oxygen sites available for binding and the chemical structure iron hexahydrate (see Figure 2.8 in Chapter 2) would theoretically have 6 oxygen sites available for binding (although this is not realistically possible).

Table 6-4 shows measured residual P concentrations and surface complexation model predicted P concentrations for various ASF values. The SCM does not consider water hardness, therefore there are two values (a hard and soft water result) for each dose and pH combination. The P values are again the average of the equilibrium values.

Table 6-4: Measured residual P concentration and surface complexation model predicted P concentration for various ASF values. The model uses iron dose, pH and ASF values as inputs.

Dose (mgP/L)	pH	Slow Mixing		Fast Mixing			
		Measured P (mgP/L)	Model Predicted ASF=0.31	Measured P (mgP/L)	Model Predicted ASF=1.18	Model Predicted ASF=2	Model Predicted ASF=3
10	8	0.0482	0.7853	0.0424	0.2572	0.1015	0.0447
		0.0733		0.0520			
10	6	0.0051	0.4806	0.0039	0.0206	0.0053	0.0021
		0.0111		0.0044			
5	8	0.2496	0.9124	0.1900	0.5609	0.3255	0.1735
		0.2978		0.2699			
5	6	0.1592	0.7552	0.0929	0.1508	0.0328	0.0109
		0.1814		0.0832			

Comparing the data from measured P values to the expected residual P concentration from the SCM model, it is clear the SCM predicts higher residual P values than are observed. For fast mixing experimental data compared to model prediction with an ASF of 1.18 (well mixed) the model predicts a residual P concentration on average six times higher than is observed for the high dose experiments and about 2 times higher than is observed in the low dose experiments. A visual comparison of the experimental results to model predicted residual P is shown in the 1:1 plots in Figure 6-10. The plot on the left shows slow mixing data compared to model predicted results with an ASF of 0.31 (poorly mixed system) and fast mixing data to model predicted results with an ASF of 1.18 (well mixed system).

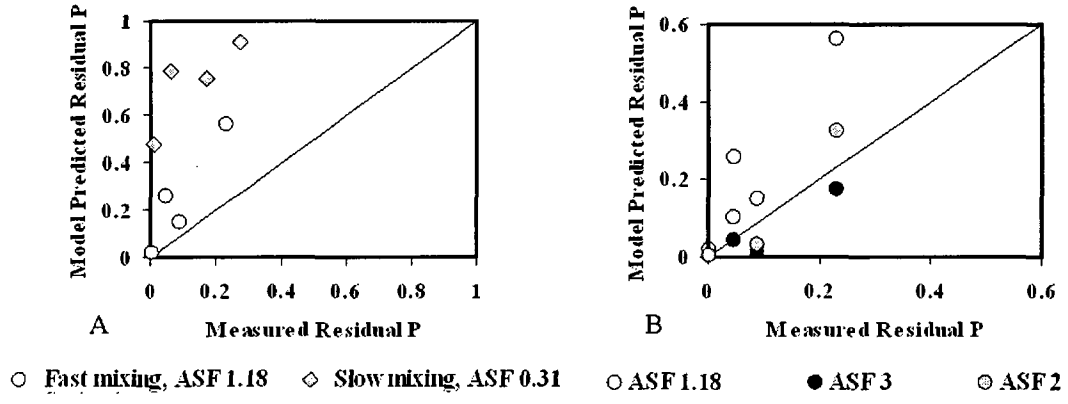

Figure 6-10: A 1:1 plot comparing SCM predicted residual P to experimentally measured residual P. A) compares slow mixing with an ASF input of 0.31 and fast mixing experiments to the model output with an ASF of 1.18. B) shows only fast mixing experimental data with three different ASF inputs: 1.18, 2 and 3.

The data in Figure 6-10 A) falls above the 1:1 line indicating the model predicts higher residual P than is experimentally observed. Figure 6-10 B) shows only the fast mixing experimental data compared to three model predicted results with increasingly higher ASF values. When an ASF value of 1.18 in used in the SCM the residual P is over predicted (open circles fall above 1:1 line). When a value of 3 is used (black circles) the model under-predicts residual P values, and when an ASF of 2 is used in the model (grey circles), the points straddle the 1:1 line. Therefore, the appropriate ASF value to model fast mixing as was used in the experiments described here is around 2. For the experiments described here, four factors were varied to observe the change in residual P concentration, however the SCM does not consider all these factors. Variable water chemistry for example (hard and soft water) is not currently considered in the SCM, this likely affects how the model predicted results compared to experimentally observed results. Moreover, the SCM also does not consider factors simultaneously, such as dose and mixing and dose and pH, as is discussed in section 6.2.7 on two-way interactions.

6.3 Conclusions

A 2^4 factorial design was used to study four factors thought to be significant in chemically mediated phosphorus removal in wastewater. By comparing two extremes of four factors simultaneously, it was found that solution pH, iron dose and mixing intensity

are statistically significant, at a 95% confidence interval, in removing phosphate from solution by precipitation with iron. Water hardness showed an effect on P removal, but not as significant as the other factors.

A high dose of iron (10 mg Fe/L for 1 mg P/L) is orders of magnitude better at removing phosphate compared to a low dose (5 mg Fe/L). As expected from previous lab studies, low pH (pH 6) reached a lower residual P concentration than high pH (pH 8), since pH 8 is approaching the pH_{pzc} and the attractions between the negatively charged P species and positively charged Fe species would be reduced. High mixing intensity (376 s^{-1}) achieves lower residual P concentrations compared to low mixing intensity (23.5 s^{-1}) since at high mixing intensity the iron flocs are kept small, providing more surface area for P to adsorb. Finally, the presence of calcium and magnesium in hard water, aid in removing soluble P, more so than in soft water (where Ca and Mg concentrations are lower). The experiments performed in hard water were able to remove more P than the experiments performed in soft water.

Significant two-way interaction between dose and pH as well as dose and mixing, indicate these variables need to be considered simultaneously when describing or modeling chemically mediated phosphorus removal with iron. Rate constants for the adsorption reactions to remove P from solution (k_1) and the reverse reaction ($P_{solid} \rightarrow P_{solution}$, k_{-1}) were determined for the 16 experiments performed. It was found that a first order reaction fits well with the adsorption process and initial removal by co-precipitation is assumed to be instantaneous. The wide range of rate constants indicates that modeling the kinetic processes of chemically mediated P removal will potentially involve changing rate constants but, more work needs to be performed.

Comparing the residual orthophosphate concentrations observed for the 16 experiments to surface complexation model showed the model predicted high residual orthophosphate concentrations when an ASF value of 1.18 or 0.31 are used for a well mixed and poorly mixed system, respectively. If the ASF value is increased to ~2 in the model, the model more accurately predicts residual P results observed from the fast mixing experiments.

Chapter 7
Conclusions and Future Work

To protect sensitive aquatic environments from eutrophication by effectively reducing the nutrient load from wastewater effluents, a detailed understanding of chemically mediated phosphorus removal is needed. Additionally, as regulations on phosphorus in wastewater effluents move to lower levels, the analytical methods for phosphorus determination needs to be optimized to measure these low levels. The goals of this research project were to optimize the Standard Method for low level orthophosphate determination and minimize the interference of filter clogging artifacts by designing a filtration protocol acceptable for dissolved particulate separations. With the analytical methods optimized for low P levels, lab scale experiments were designed to further the understanding of factors affecting chemically mediated P removal from a modelling perspective.

Optimization of the Standard Method for low level orthophosphate determination was achieved in Chapter 4 of this thesis. It was found that by reducing the volume of mixed reagent added to a sample containing phosphate and increasing the colour development time, concentrations approaching 0.1 μg P/L can be measured. For orthophosphate concentrations between 1 mg P/L and 0.1 mg P/L a 1cm path length is used (as described in the Standard Method). For concentrations between 0.1 mg P/L and 0.01 mg P/L a 10 cm path length of absorbance is employed. The mixed reagent is reduced to 0.5 mL from Standard Methods for a 10 mL sample and the colour is allowed to develop for 1 to 3 hours. Similarly for concentrations below 0.01 mg P/L a 1 m light path can be used. A mixed reagent volume of 0.5 mL for a 10 mL sample is again suggested and colour development should be 24 hours. Following these guidelines, accurate and reliable orthophosphate determinations can be achieved at low levels.

The error associated with separating dissolved and particulate fractions in the synthetic jar tests used to mimic chemically mediated phosphorus removal showed significant volume dependence. Filter clogging artifacts are caused by colloidal iron aggregating on the surface of the filter to reduce the orthophosphate passing through to be measured as dissolved. This phenomenon is particularly significant in the synthetic samples of P and Fe prepared in Milli-Q water at low pH. The error associated with these artifacts is less significant in natural water samples and a neutral or high pH. To reduce the error in the synthetic samples, different filters, flow rates and sample volumes were tested to develop a protocol for dissolved particulate separations that reduces the error from filter clogging artifacts. A 47 mm Millipore filter is suggested with a flow rate of filtration of 250 mL/hr and 10 mL of filtrate collected. This protocol was confirmed on natural samples of river water, ground water and raw wastewater, and proves to be an efficient and reliable way to separate dissolved and particulate fractions for orthophosphate analysis.

Finally, to continue understanding and modelling chemically mediated phosphorus removal, factorial designed experiments were employed to consider four significant factors simultaneously. Reasonable high and low values were chosen for iron dose, solution pH, mixing intensity and water hardness to create a 2^4 factorial design. 16 experiments were performed where sub-samples of the reacting solution were removed over a 24 hour period and analyzed for orthophosphate. The results revealed that iron dose, solution pH, and mixing intensity are significant factors to phosphorus with iron at a 95% confidence interval. Also, significant two-way interactions between dose and pH and dose and mixing were identified. These two-way interactions indicate that future modeling efforts need to consider these variables simultaneously, instead of creating a model with separate dose, pH and mixing codes. Attempts to determine rate constants for the rate of phosphorus removal from solution (and the reverse reaction) were calculated with the data from 16 experiments over a 24 hour period. The initial removal due to co-precipitation of phosphate and iron was assumed to be instantaneous, and a rate for the remainder of the process (predominantly adsorption) was calculated. There appears to be no trend in the rate constants determined, which has implications for future modelling efforts.

The results gathered from the factorial experiments are just the beginning of a much larger project to model chemically mediated phosphorus removal and incorporate this model into whole plant modeling software such as BioWin™. Future work will involve incorporating the findings of this research, particularly the two-way interactions between dose and mixing and dose and pH, into the current Surface Complexation Model. Additionally, incorporating kinetic factors into the currently equilibrium based model is needed. More research and testing will be needed to understand the kinetics of chemically mediated phosphorus removal. From this project, it is clear there is variation in the rate constants for the removal of phosphorus, and future work should establish more closely what causes the variations in rate. For example, do iron dose, pH, mixing or water hardness directly affect the rates of removal or rates of dissolution (reverse reaction)? Are there other factors that more strongly affect the rate of removal?

Future work in the laboratory is also needed to incorporate a more complicated matrix more closely resembling the wastewater matrix. For example, incorporating organic matter would likely be the next step. As was outlined in the literature review, organic matter may have the ability to aid in removing phosphorus or interfere with chemical phosphorus removal. Perhaps similar experiments to the ones described in Chapter 6 could be repeated with the addition of tannic acid, a surrogate for natural organic matter, as part of the water chemistry.

Chapter 8

Appendix

A Additional Data from Filtration Experiments (Chapter 5)

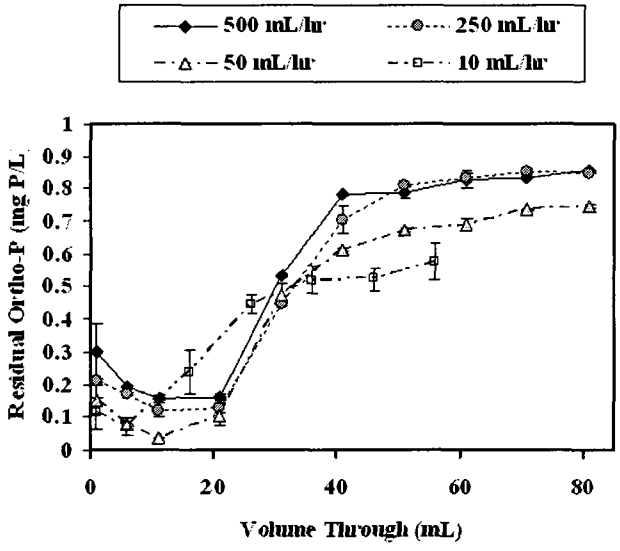

Figure A-1: Flow rate comparison using 13 mm GMF GD/X filters. 500 mL/hr, 250 mL/hr, 50 mL/hr and 10 mL/hr were tested using a syringe pump to control the flow rate. Volumes up to 80 mL through the filter were measured. The breakthrough is evident at all flow rates to occur around 20 mL of sample through the filter.

Table A-1: Comparison of repeat orthophosphate measurements (± standard error) for the 25 mm GMF GD/X filter and the 47 mm Millipore filter at three pH values. At pH 4 both 10 mL filtered and 25 mL filtered were considered. Samples were prepared as described in the methods (Chapter 3) but were shaken on an Eberbach reciprocal shaker (Eberbach 6000, USA), overnight instead of with a propeller mixer. The decision to use the 47 mm Millipore filters and 10 mL sample volume considered these concentrations and standard deviations in addition to other factors discussed in the text of Chapter 5.

	pH 4		pH 6		pH 8	
	GD/X	Millipore	GD/X	Millipore	GD/X	Millipore
10mL	0.07±0.02 mg P/L	0.0036±0.0005 mg P/L	0.051±0.002 mg P/L	0.047±0.002 mg P/L	0.96±0.03 mg P/L	0.8±0.2 mg P/L
25mL	0.014±0.001 mg P/L	0.007±0.006 mg P/L				

B Calculating G for the System at 75 rpm and 500 rpm

Adapted from Svarovsky (2000)

$$G = \sqrt{\frac{C_D A_p \rho (V_p - V)^3}{2V\mu}}$$

$C_D = 1.2$

$\rho = 1 \times 10^3 kg/m^3$

$V = 0.003 m^3$

$\mu = 1.0 \times 10^{-3} kg/m \cdot s$

$A_p = 3 \times 0.015 m \times 0.015 m$

$= 6.75 \times 10^{-4} m^2$

$V_p = r(2\pi)(rpm)(\frac{\min}{s})$

$= (0.025m)(2\pi)(75 \min^{-1})(\frac{1\min}{60s})$

$= 0.196 m/s$

$(V_p - V) = 0.8V_p$

$= (0.8)(0.196 m/s)$

$= 0.16\ m/s$

- C_D, drag coefficient, is assumed to be 1.2 based on the length to width ratio of the paddle (Svarovsky, 2000)
- G_{75rpm} changes to 19 s^{-1} if C_D is assumed to be 0.8 and 26 s^{-1} if C_D is 1.5. The high a low mixing intensity values (G) are still appropriate for the factorial design with any of these CD values.
- μ, viscosity of liquid, is assumed to be 1.0 x 10^{-3} kg/m·s, the viscosity of water at 20°C.

$$G_{75rpm} = \sqrt{\frac{(1.2)(6.75 \times 10^{-4} m^2)(1 \times 10^3 kg \cdot m^{-3})(0.16 m \cdot s^{-1})^3}{2(0.003 m^3)(1.0 \times 10^{-3} kg \cdot m^{-1} \cdot s^{-1})}}$$

$= 23.5 s^{-1}$

$V_p = r(2\pi)(rpm)(\frac{\min}{s})$

$= (0.025m)(2\pi)(500 \min^{-1})(\frac{1\min}{60s})$

$= 1.309 m/s$

$(V_p - V) = 0.8V_p$

$= (0.8)(1.309 m/s)$

$= 1.047 m/s$

$$G_{500rpm} = \sqrt{\frac{(1.2)(6.75 \times 10^{-4} m^2)(1 \times 10^3 kg \cdot m^{-3})(1.047 m \cdot s^{-1})^3}{2(0.003 m^3)(1.0 \times 10^{-3} kg \cdot m^{-1} \cdot s^{-1})}}$$

$= 376.0 s^{-1}$

C Factorial Design

Table C-2: Factorial design, with 'highs' and 'lows' for each of 16 experiments

Experiment #	Dose 5mg Fe/L (-) 10mg Fe/L (+)	pH pH 6 (-) pH 8 (+)	Mixing Intensity Slow (23.5 s^{-1}) (-) Fast (376.0 s^{-1}) (+)	Water Hardness Soft (-) Hard (+)
1	+	+	+	+
2	+	+	-	+
3	+	-	-	+
4	+	-	+	+
5	-	+	+	+
6	-	-	+	+
7	-	+	-	+
8	-	-	-	+
9	+	+	+	-
10	+	+	-	-
11	+	-	-	-
12	+	-	+	-
13	-	+	+	-
14	-	-	+	-
15	-	+	-	-
16	-	-	-	-

D Complete set of Results for Factorial Experiments

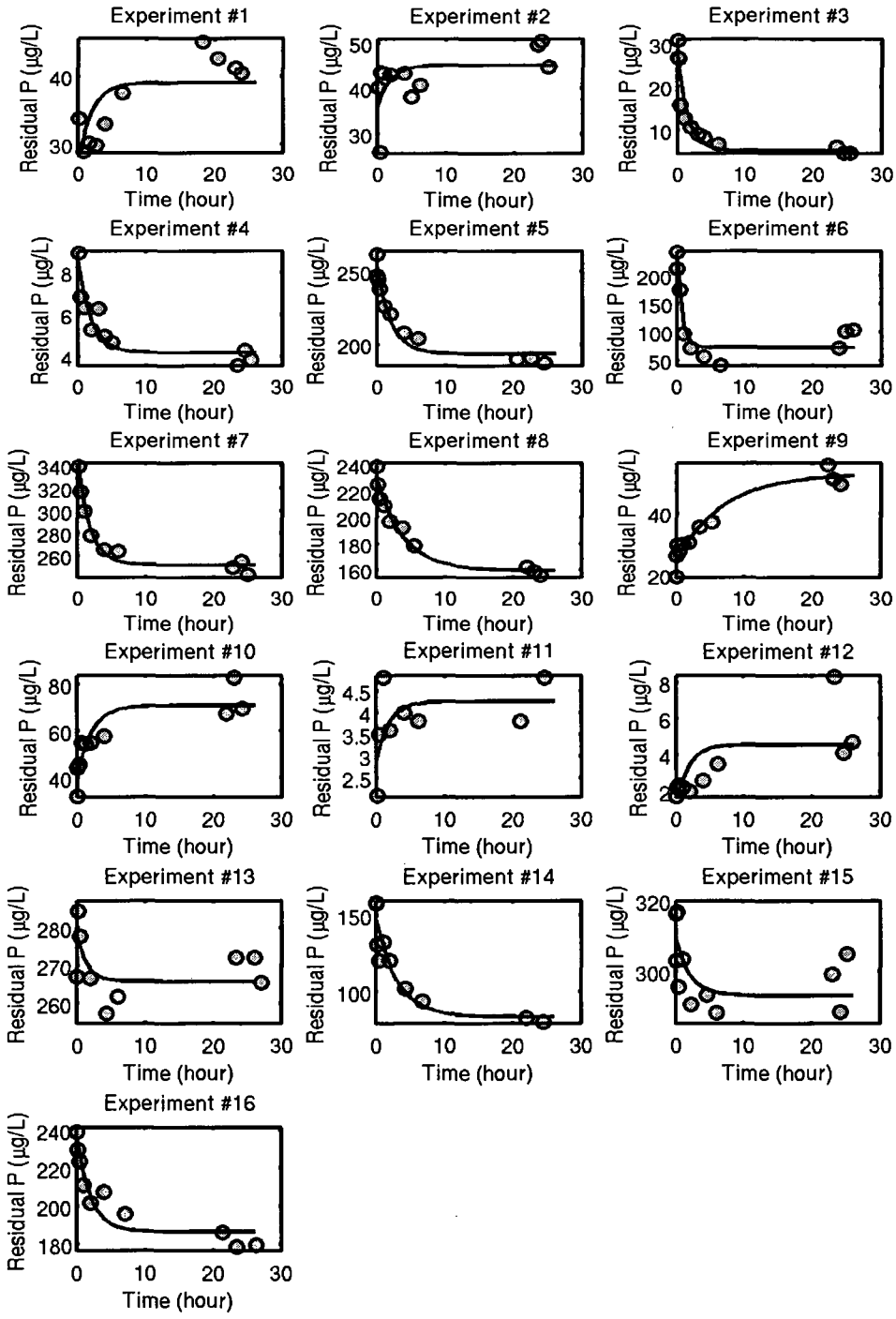

Figure D-2: Data from all 16 experiments in factorial design. Dots are data points and the line is fit to the points to determine rates of P removal. Experiment numbers (1-16) correspond with experiment numbers in Table C-2.

E Matlab Script to Process Kinetic Data

```
% file to process kinetic data
% start by loading the data
% k12 is ppte rate constant
% k21 is dissolution rate constant
% A0 is the amount of P in solution after the rapid removal is done

function ll=Rate_data_summary
warning('off'); figure(1); clf
options=optimset('lsqcurvefit');

names=strvcat(...
'01',...
'02',...
'03',...
'04',...
'05',...
'06',...
'07',...
'08',...
'09',...
'10',...
'11',...
'12',...
'13',...
'14',...
'15',...
'16'...);

namesx={'01','02','03','04','05','06','07','08','09','10','11','12','13','14','15','16'}

for i=1:size(names,1)
 data=returndata(names(i,:));
t=data(:,1)';
P=data(:,2);

% intial guess
k12=0.35; k21=0.125; A0=0.4; p=[A0 k12 k21]; %model=returnmodel(p,t)
lb=[0 0 0]; ub=[1 10000000 10000000];
%params=lsqcurvefit(@returnmodel,p,t,P',lb,ub)
params=lsqcurvefit(@returnmodel,p,t,P');

A0=(params(1));
k12=(params(2));
k21=(params(3));

time=0:1:26; model=returnmodel(params,time);

subplot(221); h=plot(t,P*1000,'ko',time,model*1000,'k');
set(h,'linewidth',2); set(h,'markersize',8); set(h,'markerfacecolor','b')
set(gca,'fontsize',14); set(gca,'linewidth',2)
h=xlabel('Time (hour)'); set(h,'fontsize',14)
h=ylabel('Residual P (\mug/L)'); set(h,'fontsize',14)
```

```
txt=['print fig',names(i,:),' -dpng']; eval(txt)

paramsummary(i,:)=[A0*1000 k12*1000 k21*1000]

end

rowLabels = namesx;
columnLabels = {'$A0 (\mu g P/L)$', '$k_{12} (\mu g L^{-1} hr^{-1})$','$k_{21} (\mu g L^{-1} hr^{-1}) $'};
matrix2latex(paramsummary, 'paramsummary.tex', 'rowLabels', rowLabels, 'columnLabels', columnLabels, 'alignment', 'c', 'format', '%-6.2f');

end
```

F Rate Constants

Table F-3: Rate constants (forward and reverse reactions) and initial P concentration (P_o) determined from the curves fit to the data for the 16 experiments

Experiment #	P_o (µg P/L)	k_1 (µg/L·hr)	k_{-1}(µg/L·hr)
1	29.69	71.25	3.39
2	38.37	45.75	2.54
3	30.62	1351.38	9.11
4	8.36	407.77	1.65
5	251.39	284.76	67.39
6	240.77	1378.92	109.32
7	347.05	467.71	158.51
8	230.03	212.90	40.39
9	25.24	114.49	6.48
10	42.10	259.30	20.42
11	2.65	747.05	3.21
12	1.77	78.83	0.50
13	277.68	570.38	206.65
14	147.65	275.03	24.92
15	313.90	1101.02	459.71
16	231.76	222.10	49.71

Chapter 9
References

Altundoğan, S. H., & Tümen, F. (2001). Removal of phosphates from aqueous solutions by using bauxite. 1: Effect of pH on the adsorption of various phosphates. *Journal of Chemical Technology and Biotechnology, 77*, 77-85.

Blaney, L. M., Cinar, S., & SenGupta, A. K. (2007). Hybrid anion exchanger for trace phosphate removal from water and wastewater. *Water Research, 41*, 1603-1613.

Bradford, M. E., & Peters, R. H. (1987). The relationship between chemically analyzed phosphorus fractions and bioavailable phosphorus. *Limnology and Oceanography, 32*(5), 1124-1137.

Briggs, T. A. (1996). Dynamic modeling of chemical phosphorus removal in the activated sludge process. (M. Eng, McMaster University, Hamilton, Ontario, Canada).

Camp, T. R., & Stein, P. C. (1943). Velocity gradient and internal work in fluid motion. *Journal of Boston Social Civil Engineers, 30*, 219-237.

Carlsson, H., Aspegren, H., Lee, N., & Hilmer, A. (1997). Calcium phosphate precipitation in biological phosphorus removal systems. *Water Research, 31*(5), 1047-1055.

Carpenter, S. R., & Lathrop, R. C. (2008). Probabilistic estimate of a threshold for eutrophication. *Ecosystems, 11*(4), 601-613.

Clancy, W. J. (1985). *Heuristic classification* No. STAN-CS-85-1066 Stanford University.

Daou, T. J., Begin-Colin, S., Grenèche, J. M., Thomas, F., Derory, A., Bernhardt, P., Legaré, P., and Pourroy, G. (2007). Phosphate adsorption properties of magnetite-based nanoparticles. *Chemistry of Materials, 19*, 4494-4505.

de Haas, D. W., Wentzel, M. C., & Ekama, G. A. (2000). The use of simultaneous chemical precipitation in modified activated sludge systems exhibiting biological excess phosphate removal. Part 1: Literature review. *Water SA, 26*(4), 439-452.

de Haas, D. W., Wentzel, M. C., & Ekama, G. A. (2001). The use of simultaneous chemical precipitation in modified activated sludge systems exhibiting biological excess phosphate removal. Part 6: Modeling of simultaneous chemical-biological P removal-review of existing models. *Water SA, 27*(2), 135-150.

Diamadopoulos, E., & Benedek, A. (1984). The precipitation of phosphorus from wastewater through pH variation in the presence and absence of coagulants. *Water Research, 18*, 1175-1179.

Dzombak, D. A., & Morel, F. M. M. (1990). *Surface complexation modeling, hydrous ferric oxide.* New York, NY: Wiley-Interscience.

Earth Tech Canada Inc. (2007). *Wastewater Treatment Master Plan Tech Memo#7 East Side Community Servicing.* Retrieved 02/09, 09, from <http://www.region.waterloo.on.ca/web/region.nsf/0/3D1D45AD4AF6B9E885256FFE00672B4F/$file/Appendix%20F.pdf?openelement>

Elliott, H. A., O'Connor, G. A., Lu, P., & Brinton, S. (2002). Influence of water treatment residuals on phosphorus solubility and leaching. *Journal of Environmental Quality, 31*, 1362-1369.

Environment Canada. (1990). *Environmental protection series. Biological test method: Acute lethality test using daphnia spp.* Retrieved 11/12, 2008, from <http://www.etc-cte.ec.gc.ca/organization/bmd/pubs/pubs_en/1RM11EnglishFinal.pdf>

Environmental Protection Agency. (1978). *EPA method 365.3 phosphorus, all forms (colorimetric, ascorbic acid, two reagents)*

Fettig, J., Ratnaweera, H. C., & Ødegaard, H. (1990). Simultaneous phosphate precipitation and particle destabilization using aluminum coagulants of different basicity. *Proceedings of the 4th Gothenbug Symposium October 1-3, 1990 Madrid, Spain,* 221-242.

Froelich, P. N. (1988). Kinetic control of dissolved phosphate in natural rivers and estuaries: A primer on the phosphate buffer mechanism. *Limnology and Oceanography, 33*, 649-668.

Geelhoed, J. S., Himestra, T., & Riemsdijk, W. H. V. (1997). Phosphate and sulfate adsorption on goethite: Single anion and competitive adsorption. *Geochimica Et Cosmochimica Acta, 61*, 2389-2396.

Gilmore, R. L., Goertzen, S., Murthy, S., Takács, I., & Smith, D. S. (2008). Chemically mediated phosphorus removal: Optimization of analytical methods. *Proceedings of the 81st Annual Water Environmental Federation Technical Exhibition and Conference. October 18-22,* Chicago, IL. , *Session 49* 3756-3774.

Gunnars, A., Blomqvist, S., Johansson, P., & Andersson, C. (2002). Formation of Fe(III) oxyhydroxide colloids in freshwater and brackish seawater, with incorporation of phosphate and calcium. *Geochimica et Cosmochimica Acta, 66*, 745-758.

Hall, G. E. M., Bonham-Carter, G. F., Horowitz, A. J., Lum, K., Lemieux, C., Quemerais, B., and Garbarino, J. R. (1996). The effect of using 0.45 μm filter membranes on 'dissolved' element concentrations in natural waters. *Applied Geochemistry, 11*, 243-249.

Hammer, M. J. L., & Hammer, Mark J. Jr. (2001). *Water and wastewater technology.* (4th ed.). Upper Saddle River, New Jersey: Prentice Hall.

Hiemstra, T., & Van Reimsdijk, W. H. (1996). A surface structural approach to ion adsorption: The charge distribution (CD) model. *Journal of Colloid and Interface Science, 179*, 488-508.

Holliday, V. T., & Gartner, W. G. (2007). Methods of soil P analysis in archaeology. *Journal of Archaeological Science, 34*, 301-333.

Horowitz, A. J., Elrick, K. A., & Colberg, M. R. (1992). The effect of membrane filtration artifacts on dissolved trace element concentrations. *Water Research, 26,* 753-763.

Horowitz, A. J., Lum, K. R., Garbarino, J. R., Hall, G. E. M., Lemieux, C., & Demas, C. R. (1996). Problems associated with using filtration to define dissolved trace element concentrations in natural water samples. *Environmental Science and Technology, 30*(3), 954-963.

Hsu, P. H. (1973). Complementary role of iron(II), sulphate and calcium in precipitation of phosphate from solution. *Environmental Letters, 5*, 115.

Jenkins, D., Ferguson, J. F., & Menar, A. B. (1971). Chemical processes for phosphate removal. *Water Research, 5*, 369-389.

Jüttner, F., Meon, B., & Köster, O. (1997). Quasi *in situ* separation of particulate matter from lake water by hollow-fiber filters to overcome errors caused by short turnover times of dissolved compounds. *Water Research, 31*, 1637-1642.

Kreller, D. I., Gibson, G., vanLoon, G. W., & Horton, J. H. (2002). Chemical force microscopy investigation of phosphate adsorption on the surfaces of iron(III) oxyhydroxide particles. *Journal of Colloid and Interface Science, 254*, 205-213.

Kumar, A., Gurian, P. L., Bucciarelli-Tieger, R. H., & Mitchell-Blackwood, J. (2008). Iron oxide-coated fibrous sorbents for arsenic removal. *Journal American Water Works Association, 100*(4), 151-164.

Leckie, J., & Stumm, W. (1970). *Water quality improvements by physical and chemical processes* Univ. Texas, Austin.237.

Leppard, G. G. (1992). Size, morphology and composition of particulates in aquatic ecosystems: Solving speciation problems by correlative electron microscopy. *Analyst, 117*, 595-603.

Li, L., & Stanforth, R. (2000). Distinguishing adsorption and surface precipitation on phosphate and goethite (α-FeOOH). *Journal of Colloid and Interface Science, 230,* 12-21.

Lijklema, L. (1980). Interaction of orthophosphate with iron(III) and aluminum hydroxides. *Environmental Science & Technology, 14*, 537-541.

Lin, Y., Sung, M., Sanders, P. F., Marinucci, A., & Huang, C. P. (2007). Separation of nano-sized colloidal particles using cross-flow ultrafiltration. *Separation and Purification Technology, 58*, 138-147.

Lytle, D. A., & Snoeyink, V. L. (2002). Effect of ortho- and polyphosphates on the properties of iron particles and suspensions. *Journal American Water Works Association,* , 87-99.

Magnuson, M. L., Lytle, D. A., Frietch, C. M., & Kelty, C. A. (2001). Characterization of submicrometer aqueous iron(III) colloids formed in the presence of phosphate by sedimentation field flow fractionation with multiangle laser light scattering detection. *Analytical Chemistry, 73*, 4815-4820.

Maher, W., & Woo, L. (1998). Procedures for the storage and digestion of natural waters for the determination of filterable reactive phosphorus, total filterable phosphorus and total phosphorus. *Analytical Chimica Acta, 375*, 5-47.

Marbek Resource Consultants. (2005). *Review of existing Municipal Wastewater Effluent (MWWE) regulatory structures in Canada.* Retrieved 03/30, 08, from <http://www.ccme.ca/assets/pdf/mwwe_cnsltn_hrf_conrpt_e.pdf>

McNaught, A. D., & Wilkinson, A. (1997). *IUPAC Compendium of Chemical Technology*. Oxford, United Kingdom: Blackwell Science.

Mikutta, C., Krüger, J., Lang, F., & Kaupenjohann, M. (2006). Acid polysaccharide coatings on microporous goethites: Controls of slow phosphate sorption. *Soil Science Society of America Journal, 70*, 1547-1555.

Mino, T., Van Loosdrecht, M. C. M., & Heijnen, J. J. (1998). Microbiological and biochemistry of the enhanced biological phosphate removal process. *Water Research, 32*(11), 3193-3207.

Morel, F. M. M., & Hering, J. G. (1993). *Principles and applications of aquatic chemistry*. New York, NY: John Wiley and Sons, Inc.

Morgan, S. L., & Deming, S. N. (1974). Simplex optimization of analytical chemical methods. *Analytical Chemistry, 71*(11), 1170-1181.

Morrison, M. A., & Benoit, G. (2004). Investigation of conventional membrane and tangential flow ultra-filtration artifacts and their application to the characterization of freshwater colloids. *Environmental Science and Technology, 38*, 6817-6823.

Murthy, S., Takács, I., Dold, P., & Al-Omari, A. (2005). Examining the bioavailability of chemically removed phosphorus at the Blue Plains Advanced Wastewater Treatment Plant. *Conference Proceedings. 78th Annual Water Environmental Federation Technical Exhibition and Conference. October 29-November 2. Washington, D.C, USA*

National Institute of Standards and Technology (2001). *NIST Standard Reference Database 46.* Gaithersburg, MS., USA

Neethling, J., Benisch, M., Dave, C., Fisher, D., & Gu, A. Z. (2007). Phosphorus speciation provides direction to produce 10 µg/L. *Conference Proceedings. 80th Annual Water Environmental Federation Technical Exhibition and Conference. October 12-17th, San Diago California,*

Oğuz, E. (2004). Removal of phosphate from aqueous solution with blast furnace slag. *Journal of Hazardous Materials, B114*, 131-137.

Oğuz, E., Gürses, A., & Canpolat, N. (2003). Removal of phosphate from wastewaters. *Cement and Concrete Research, 33*, 1109-1112.

Ohlinger, K. N., Young, T. M., & Schroeder, E. D. (2000). Postdigestion struvite precipitation using a fluidized bed reactor. *Journal of Environmental Engineering, 126*, 361-368.

Peng, J., Wang, B., Song, Y., Yuan, P., & Liu, Z. (2007). Adsorption and release of phosphorus in the surface sediment of a wastewater stabilization pond. *Ecological Engineering, 31*, 92-97.

Pizarro, J., Belzile, N., Filella, M., & Leppard, G. G. (1995). Coagulation/Sedimentation of submicron iron particles in a eutrophic lake. *Water Research, 29*(2), 617-632.

Pogliani, L., Berberan-Santos, M. N., & Martinho, J. M. G. (1996). Matrix convolution methods in chemical kinetics. *Journal of Mathematical Chemistry, 20*, 193-210.

Quintana, M., Sánchez, E., Colmenarejo, M. F., Barrera, J., García, G., & Borja, R. (2005). Kinetics of phosphorus removal and struvite formation by the utilization of by-product of magnesium oxide production. *Chemical Engineering Journal, 111*, 45-52.

Rahaman, M. S., Ellis, N., & Mavinic, D. S. (2008). Effects of various process parameters on struvite precipitation kinetics and subsequent determination of rate constants. *Water Science and Technology, 57.5*, 647-654.

Raichenko, A. I., Grigor'ev, V. I., Mai, V. K., Petrina, N. D., & Sleptsova, N. P. (1969). Forced filtration of a liquid alloy in a porous material under the influence of electromagnetic forces. *Poroshkovaya Metallurgiya, 11*(83), 40-44.

Richardson, C. J. (1985). Mechanisms controlling phosphorous retention capacity in freshwater wetlands. *Science, 228*, 1424-1427.

Rietra, R. P. J. J., Hiemstra, T., & Riemsdijk, W. H. V. (2001). Interaction between calcium and phosphate adsorption on goethite. *Environmental Science Technology, 35*, 3369-3374.

Sedlak, R. I. (1991). *Phosphorus and nitrogen removal from municipal wastewater. principles and practice* (2nd ed.). New York: Lewis Publishers.

Shiller, A. M. (2003). Syringe filtration methods for examining dissolved and colloidal trace element distributions in remote field locations. *Environmental Science and Technology, 37*, 3953-3957.

Smeck, N. E. (1985). Phosphorus dynamics in soils and landscapes. *Geoderma, 36*, 185-199.

Smith, D. S., Gilmore, R. L., Szabó, A., Takács, I., Murthy, S., & Diagger, G. (2008b). Chemically mediated phosphorus removal to low levels: Analysis and interpretation of data. *Proceedings of the 81st Annual Water Environment Federation Technical Exhibition and Conference. October 18-22, Chicago, IL, , session 47* 3558-3574.

Smith, D. S., & Ferris, F. G. (2001). Proton binding by hydrous ferric oxide and aluminum oxide surfaces interpreted using fully optimized continuous pK_a spectra. *Environmental Science and Technology, 35*, 4637-4642.

Smith, D. S., Takács, I., Murthy, S., Diagger, G., & Szabó, A. (2008a). Phosphate complexation model and its implications for chemical phosphorus removal. *Water Environment Research, 80*(5), 428-438.

Spivakov, B. Y., Maryutina, T. A., & Muntau, H. (1999). Phosphorus speciation in water and sediments. *International Union of Pure and Applied Chemistry, 71*, 2161-2176.

Standard Methods for Examination of Water and Wastewater. (1998). (20th ed.). American Public Health Association (APHA) and American Water Works Association (AWWA) and Water Environment Federation (WEF); Washington DC, USA

Stumm, W. (1992). *Chemistry of the solid-water interface*. New York, NY: John Wiley and Sons, Inc.

Stumm, W., & Morgan, J. J. (1996). *Aquatic chemistry*. New York, NY: Wiley.

Svarovsky, L. (2000). *Solid-liquid separation* (Fourth ed.). London UK: Butterworth-Heinemann.

Szabó, A., Takács, I., Murthy, S., Diagger, G., Licskó, I., & Smith, D. S. (2008). The significance of design and operational variables in chemical phosphorus removal. *Water Environment Research, 80*(5), 407-416.

Takács, I., Murthy, S., Smith, D. S., & McGrath, M. (2006a). Chemical phosphorus removal to extremely low levels: Experience of two plants in the Washington, DC area. *Water Science & Technology, 53*, 21-28.

Takács, I., Murthy, S., & Fairlamb, P. M. (2006b). Chemical phosphorus removal model based on equilibrium chemistry. *Water Science & Technology, 52*, 549-555.

Tongesayi, T., Byam, E. J., Keysper, S. B., & Crounce, M. J. (2008). Adsorption and desorption of phosphate on Fe_2O_3: Effect of fulvic acid and pH. *Environmental Chemistry, 5*, 161-168.

Towns, T. G. (1986). Determination of aqueous phosphate by ascorbic acid reduction of phosphomolybdic acid. *Analytical Chemistry, 58*, 223-229.

Tribe, L., & Barja, B. (2004). Adsorption of phosphate on goethite. *Journal of Chemical Education, 81*, 1624-1627.

vanLoon, G. W., & Duffy, S. J. (2000). *Environmental chemistry a global perspective*. New York, NY: Oxford University Press.

WEF. (1998). *Water environment federation: Biological and chemical systems for nutrient removal*. VA, USA: Water Environment Federation; WEF.

Whatman. (2008). *Complete component solutions for diagnostic manufactures.* Retrieved 04/11, 2008, from <http://www.pm.e-symposium.com/whatman/DiagnosticsSolutions.pdf>

Zanini, L., Robertson, W. D., Ptacek, C. J., Schiff, S. L., & Mayer, T. (1998). Phosphorus characterization in sediments impacted by septic effluent at four sites in central Canada. *Journal of Contaminant Hydrology, 33*, 405-429.